

STRUGGLE AT THE SITE OF NERVE INJURY

*A rat sciatic nerve study on fundamental
problems of peripheral nerve injury*

Xander Smit

STRUGGLE AT THE SITE OF NERVE INJURY

*A rat sciatic nerve study on fundamental problems
of peripheral nerve injury*

STRIJD TER PLAATSE VAN HET ZENUWLETSEL

*Een nervus ischiadicus ratten studie naar de fundamentele problematiek
omtrent het perifere zenuwletsel*

Proefschrift

ter verkrijging van de graad van doctor aan de
Erasmus Universiteit Rotterdam
op gezag van de rector magnificus
Prof.dr. S.W.J. Lamberts
en volgens besluit van het College voor Promoties.

De openbare verdediging zal plaatsvinden op
vrijdag 13 oktober 2006 om 11.00 uur

door

XANDER SMIT
geboren te Eindhoven

This thesis was financially supported by:

*J.E. Jurriaanse Stichting, Nederlandse Vereniging voor Plastische Chirurgie,
Nederlandse Vereniging voor Hand Chirurgie, the Esser Foundation, Stichting Anna Fonds,
AB Medical PRS, Ethicon Products, Carl Zeiss B.V., Harlan Nederland, Dermaprof B.V. / Bioprof B.V.,
Convatec (a Bristol-Meyers Squibb Company), Baxter*

ISBN-10: 90-9020531-4

ISBN-13: 978-90-9020531-1

© 2006 X. Smit, Rotterdam, The Netherlands

Cover photo by Ron Mulder, <http://www.stormfoto.nl>

Cover design by Rob de Widt jr.

Printed by City Print, Rotterdam, The Netherlands

Promotiecommissie

Promotor:

Prof.dr. S.E.R. Hovius

Overige leden:

Prof.dr. C.I. de Zeeuw

Prof.dr. C.J. Sijders

Prof.dr. R.T.W.M. Thomeer

Copromotor:

Dr. J.W. van Neck

Paranimfen:

Jean-Bart Jaquet

Hinne Rakhorst

Contents

Chapter 1

GENERAL INTRODUCTION:	9
1.1 PHYSIOLOGY	10
1.2 PATHOPHYSIOLOGY	12
1.3 EXPERIMENTAL RESEARCH	14
1.4 GENERAL AIM AND OUTLINE OF THE THESIS	25

Chapter 2

STATIC FOOTPRINT ANALYSIS: A TIME-SAVING FUNCTIONAL EVALUATION OF NERVE REPAIR IN RATS	33
<i>X. Smit, J.W. van Neck, M.J. Ebeli, S.E.R. Hovius</i> <i>Scand J Plast Reconstr Surg Hand Surg. 2004 Dec;38(6):321-5</i>	

Chapter 3

MAGNETONEUROGRAPHY: RECORDING BIOMAGNETIC FIELDS FOR QUANTITATIVE EVALUATION OF ISOLATED RAT SCIATIC NERVES	43
<i>X. Smit, B.S. de Kool, E.T. Walbeehm, E.B.M. Dudok van Heel, J.W. van Neck, S.E.R. Hovius</i> <i>J Neurosci Methods, 2003: 125; 59-63</i>	

Chapter 4

RECOVERY OF NEUROPHYSIOLOGICAL SIGNALS IN TIME AFTER RAT SCIATIC NERVE REPAIR: A MAGNETO-NEUROGRAPHIC STUDY	53
<i>X. Smit, B.S. de Kool, J.H. Blok, G.H. Visser, S.E.R. Hovius, J.W. van Neck</i> <i>Accepted J Peripher Nerv Syst</i>	

Chapter 5

PERIPHERAL NERVES IN THE RAT EXHIBIT LOCALIZED HETEROGENEITY OF TENSILE PROPERTIES DURING LIMB MOVEMENT	69
<i>J.B. Phillips, X. Smit, N. De Zoysa, A. Afoke, R.A. Brown</i> <i>J Physiol. 2004 Jun 15;557(Pt 3):879-87</i>	

Chapter 6

REDUCTION OF NEURAL ADHESIONS BY BIODEGRADABLE AUTOCROSSLINKED HYALURONIC ACID GEL AFTER INJURY OF PERIPHERAL NERVES: AN EXPERIMENTAL STUDY	83
<i>X. Smit, J.W. van Neck, A. Afoke, S.E.R. Hovius</i> <i>J Neurosurg. 2004 Oct;101(4):648-52 (new significant data were added to this chapter)</i>	

Chapter 7

RGTA, A HEPARAN SULFATE MIMETIC, SIGNIFICANTLY REDUCES NEURAL ADHESIONS AFTER PERIPHERAL NERVE INJURY IN RATS	97
<i>H.M. Zuidendorp, X. Smit, B.S. de Kool, J.H. Blok, D. Barritault, S.E.R. Hovius, J.W. van Neck</i> <i>To be submitted</i>	

Chapter 8

GENERAL DISCUSSION, CONCLUSIONS AND RESEARCH PERSPECTIVES	109
NEDERLANDSE SAMENVATTING	122
LIST OF PUBLICATIONS	128
DANKWOORD	130
CURRICULUM VITAE	134

1

General Introduction

Introduction

The clinical outcome after nerve injury is not satisfactory and nerve injuries of the upper extremity cause long lasting disabilities. Loss of sensory and motor function, accompanied by pain and discomfort not only have functional consequences but also have major social and psychological impact³⁹.

Over the last decades clinical and experimental research have achieved a remarkable progress in the understanding of neurobiology involved in nerve injury and in developing concepts to promote recovery of function. However, Lundborg emphasized that this progress does not correspond to clinically improved results after nerve injury and repair⁵⁴. This mismatch can be explained by different hypotheses, all of them probably contributing to reality:

- Erroneous conclusions can result from extrapolation from animal model to human conditions.
- Beneficial effects on the recovery process after nerve injury demonstrated in experimental studies are too subtle to cause an effect of clinical importance in human.
- Proving potential beneficial effects in randomized clinical outcome studies after nerve injury is rarely feasible. Patients and injuries are too heterogeneous, consequently leading to statistical problems.

This last hypothesis stresses the significance of well-designed experimental research in the field of physiology and pathophysiology of peripheral nerves. Validated experimental methods providing quantifiable outcome data should provide a solid base for potential beneficial strategies promoting recovery after peripheral nerve injury in a clinical setting. The general aim of this thesis is to provide quantifiable experimental techniques to assess physiological and pathophysiological processes involved in peripheral nerve injury. The processes investigated in this thesis are focussed on the site of nerve injury. The studies in this thesis allow for a more critical appraisal of underlying fundamental problems causing clinical symptoms of peripheral nerve injury, such as decreased conduction capacity and extraneural scarring.

1.1 Physiology

Knowledge of physiology of the peripheral nervous system is vast, and extending every day. For this introduction, physiology is confined to a brief overview on the basic anatomy of the peripheral nervous system and to the way a peripheral nerve signals.

1.1.1 BASIC ANATOMY

Peripheral nerve fibers terminate in all tissue organs of the body. There are three major kinds of nerve fibers, (1) sensory, (2) motor and (3) sympathetic, arising from neurons of dorsal root ganglia, the ventral horn of the spinal cord, and the sympathetic

ganglia, respectively. Density of their innervation varies between organs. A nerve fiber is defined as the conducting or functional unit of the nerve cell and is formed by an axon enveloped by a single layer of Schwann cells with or without a myelin sheath (Figure 1). A nerve cell (neuron) consists of a cell body providing metabolic activity and a long axon connecting in the periphery. Each individual nerve fiber is surrounded by endoneurium, mainly composed of collagen fibers. Fascicles are formed by groups of fibers surrounded by the perineurium, which is formed by fibroblasts and collagen. An outer sheath of fibrocollagenous tissue, the epineurium, binds fascicles into a nerve trunk. Blood flow is important, of course, in maintenance of nerve structure and function. Peripheral nerves have a specialized circulation that is not extensively discussed here. The course of the blood vessels allow for stretching of the nerve, which occurs during normal movement of the body.

The anatomical course and properties of a peripheral nerve allow freedom of normal joint movement without disturbing neurological function. The exact mechanism of this phenomenon has been studied extensively but has not completely been revealed yet^{57,92,93}.

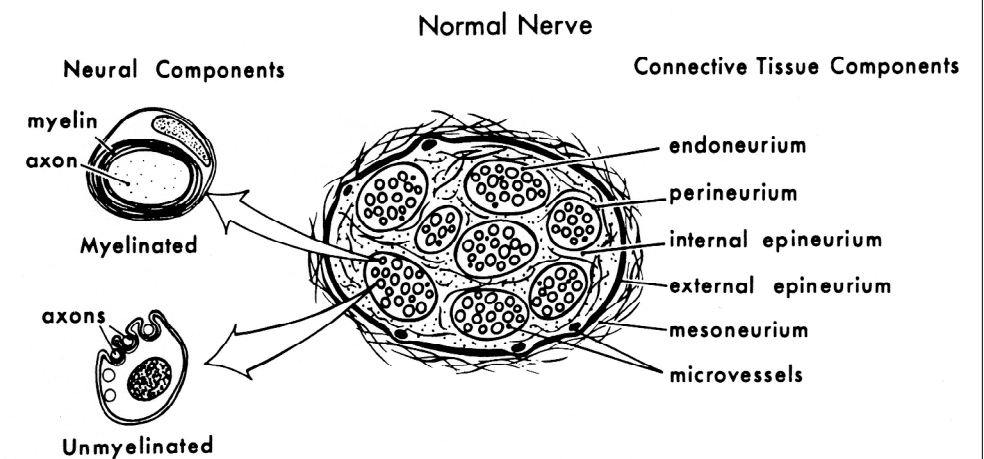


Figure 1. Schematic composition of a peripheral nerve⁵⁷.

1.1.2 NEURONAL SIGNALING

Neuronal signaling is controlled by electrical gradients across the membrane of the axon. In a resting axon, the membrane potential is approximately -70mV . This baseline electrical gradient is maintained by ion pumps in the cell membrane. Ion channel proteins can modify the electrochemical gradient across the axon by changing their permeability to ions in response to chemical transmitter substances (ligand-gated channels in synapses) and depolarization (voltage-gated channels along the length of the axon). If an axon membrane is depolarized by a large enough current (threshold), voltage-gated channels will open and lead to an explosive change in membrane potential (depolariza-

tion), immediately followed by a wave of repolarization, collectively called an action potential. Adjacent membrane sections will depolarize resulting in propagation of the action potential along the axon. Speed of conduction along the axon is limited by capacitance and resistance of the axon. Therefore, increasing axon diameter (low capacitance) will lead to an increase of speed of conduction. Conduction velocity can also be increased by minimizing leakage of current. Segmental insulation is created by Schwann cells forming a myelin sheath around the axon. Between each myelin segment there is a bare area termed the Node of Ranvier, containing a concentration of voltage-gated channels. Due to the insulation, depolarization jumps from node to node, greatly increasing the conduction velocity. Myelin sheaths also reduce the electrical capacitance (Figure 2). Single nerve fibers differ in diameter and degree of myelination^{57,92,93}.

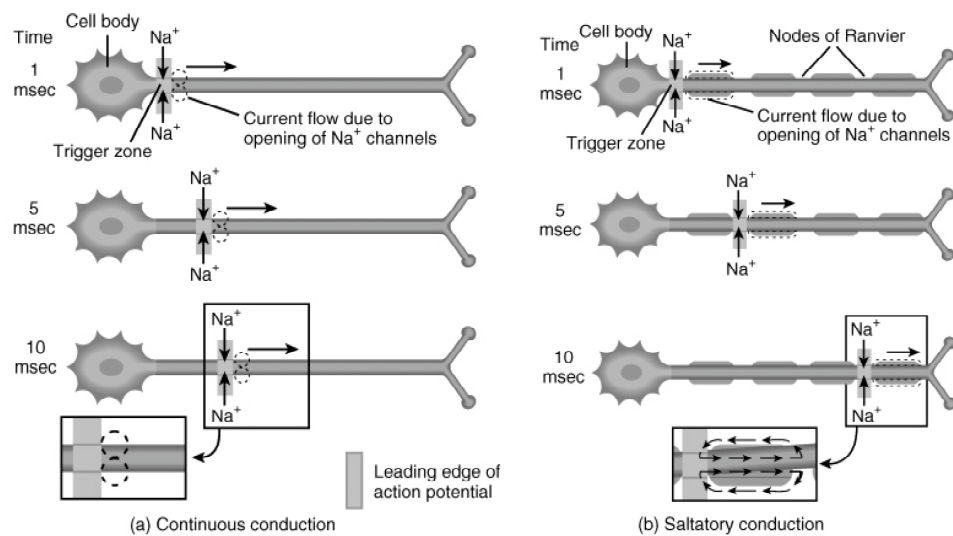


Figure 2. Neuronal signaling without myelin insulation (continuous conduction) and with myelin insulation (saltatory conduction).

1.2 Pathophysiology

1.2.1 NERVE INJURY

Peripheral nerves are not prone to solitary injury. The intimate relations that nerves establish with surrounding tissue like bone, tendon and / or blood vessels render them more susceptible to combined tissue damage⁹².

Seddon introduced a terminology for different forms of traumatic nerve injuries, which is widely adopted⁸⁵.

- **Neuropraxia.** Continuity of the axon is preserved, however temporarily and localised conduction block occurs.

- **Axontmesis.** Injury causes axonal disruption and degeneration distal to the lesion will occur. Axon regeneration is facilitated by preserved continuity of endoneurial sheath and basal lamina of the Schwann cell layer.
- **Neurontmesis.** It involves total loss of continuity of the nerve. Degeneration will only be followed by partial successful regeneration, under the condition that minimal dehiscence of the nerve stumps exists or that the nerve is repaired.

After axontmesis and neurontmesis axons in the distal segment begin to degenerate (Wallerian degeneration) as a result of separation from the metabolic resources of the cell bodies. Macrophages and Schwann cells clear myelin and axonal debris and produce cytokines to enhance nerve growth. The proximal end of the nerve stump only experiences minimal degradation. Nevertheless, many neurophysiological changes occur in the proximal segment¹⁰¹. Within 24 hours, new axonal sprouts will originate from the proximal axons and regenerate along the basal lamina of Schwann cells. Maturation of the regenerating nerve involves myelination of axons and increase of fiber diameter. Functional reinnervation requires axons to regenerate until they reach their target organ

^{57,92,93}

1.2.2 FUNDAMENTAL PROBLEMS AT THE SITE OF INJURY IN HUMANS

Multiple factors can be held responsible for poor functional outcome after nerve injury³⁹. Predicting factors can be traced back to different mechanisms involved in the process of recovery after nerve injury. Over the last decade, more is known about important mechanisms, which are not directly related to the peripheral nervous system but to the central nervous system. The plasticity of the brain can be defined as the capability of synapses to change, as circumstances require. Age, cooperation, motivation and cognitive capacity of the patient, sensory reeducation and hand therapy are predicting factors, which all involve remodeling of the brain⁵⁵.

A subdivision of predicting factors can be made by focusing on the site of injury. Here, some fundamental problems related to the site of injury are addressed.

Quantity of axon regeneration. Limited regeneration over the injured site and into the distal segment has a major negative effect on functional recovery. Large numbers of regenerating axons escape into intervening tissue as they emerge from the proximal segment. Furthermore, scarring between the proximal and distal nerve end and intraneural scarring in the distal segment will prevent axons to reach their target organ. The dying back phenomenon also contributes to a reduction of the number of axons regenerating into the distal segment. Promoting axon growth into the distal nerve segment will enhance the chance of successful contact with a distal end organ^{45,51,57,58,92}.

Speed of axon regeneration. The rate of axon regeneration varies. In humans, after axontmesis axons grow by 1-6 mm / day and after neurontmesis this growth is less (1-2 mm / day). The speed with which axons regenerate is dependent on multiple factors like age, severity and level of injury, co morbidity and species. Concentrating on the site of injury, actual speed is determined by time: (1) taken by the cell body to recover, and consequently for axons to start growing and reach the site of injury, (2) taken by regenerat-

ing axons to bridge the site of injury, (3) taken by regenerating axons to reach their end organ⁹².

A slow rate of axon regeneration will allow formation of scar tissue at the suture site and in the distal segment, constricting growing axons. Furthermore, prolonged denervation of target organs will not only negatively influence these target organs but also related structures like bone, joints and tendons^{17, 84, 92, 99}.

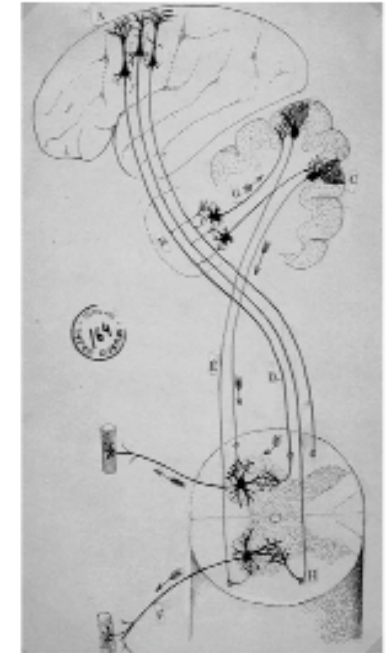
Bridging the gap. When a nerve segment is lost in peripheral nerve injury, the nerve gap dilemma arises. In optimal nerve repair, the suture line should be tension free. If “critical” tension of the suture line is reached, the nerve gap should be bridged by a nerve interponate. In literature however, no consensus exists on the definition “critical”. The disadvantage of an interponate (autologous nerve graft, degradable or non degradable tubes) are the two suture lines which are to be crossed by regenerating axons. An alternative for bridging a small gap is end-to-end repair under tension. The disadvantage of bringing nerve ends together under tension is the aggravating formation of fibrosis at the site of reconstruction. It is obvious that comprehension on tension of peripheral nerves is of paramount importance in bridging a nerve gap^{32, 59, 92, 94}.

Neural adhesions. Local tissue damage with or without nerve injury will effectuate migration and proliferation of fibroblasts and extraneural collagen deposition. Collagen fibers, enveloping the nerve, can contract, increasing the risk of compression neuropathies that can be accompanied by dysfunction and pain. Traction neuropathies arise during limb movement and muscle contractions, when nerves adhere to surrounding tissue and lose their mobility in its bed. Furthermore, when a nerve adheres to its surrounding tissue, limb movement and muscle contractions may cause painful traction neuropathies^{37, 92}.

1.3 Experimental research

Evaluation techniques in experimental research on nerve regeneration serve multiple purposes. Neuroscientists have been trying to gain insight in the fundamental organizational and functional principle of the nervous system and its process of regeneration for more than a century (*Figure 3*). When Santiago Ramón y Cajal (1852–1934) discovered the reduced silver nitrate method, he was able to reveal paramount knowledge on traumatic degeneration and regeneration of the nervous system⁷⁶. A second important objective of assessment techniques in nerve research is to discriminate between two experimental groups. In numerous studies, strategies are tested that may benefit recovery after a specific type of nerve injury^{1, 3, 6, 8, 9, 13, 88, 90}. It may be redundant to mention, but when formulating a specific hypothesis on a concept involved in nerve injury, one should carefully consider the choice of method for testing the hypothesis.

Figure 3. Diagram of Ramón y Cajal showing the dual motor pathway and direction of current flow (modified from the original).



Currently used techniques of assessment

1.3.1 HISTOLOGY

- Quantitative (morphological) analysis of nerve fibers
- Confocal laser scanning microscopy of regenerating axons
- Retrograde tracing of regenerating axons
- Morphological analysis of neural scarring

QUANTITATIVE (MORPHOLOGICAL) ANALYSIS OF NERVE FIBERS

(Immuno)histochemical samples from cross sectional nerve areas can be quantified for axon- and fiber diameter, myelin thickness and g-ratio (axon diameter / myelinated fiber diameter). It was found that when g-ratio equals 0.6, which approximates average values observed in most nerves, the relationship is theoretically optimal for the spread of current from one node of Ranvier to the next^{80, 87}. Although still being labor intensive, (semi) automated software has facilitated morphological analysis. The current digital technique allows image analysis software to count and measure myelinated fibers^{40, 90, 91, 102}. Histograms of myelinated fiber size and median fiber diameter provide quantitative data on the regeneration process.

Immunocytochemistry does not only facilitate morphological analysis. The combination of antibodies to S-100 (Schwann cells) and neurofilament (axons) is widely used to quantify the number of Schwann cells in the distal segment that are flanked by a regenerated axon^{34, 35, 52, 65, 110}. Immunocytochemistry can therefore be used to evaluate axon regeneration in the early phase after injury.

Compared to light microscopy, electron microscopic photographs give a more detailed view of cell organelles and laminar structure of myelin and also visualize small unmyelinated fibers. The main advantage of morphological analysis is that it allows for early assessment of regeneration, i.e. quantitative measure of axon sprouts. On the other hand, histology does not provide information on the nerve's fundamental function, i.e. conducting a signal. Other known disadvantages are: (1) measurement related bias, i.e. susceptibility of (semi) automated soft- and hardware to errors, (2) sampling related bias, i.e. obliquity of the plane of section and the shrinkage of fiber borders²³, (3) disputable time between injury and harvesting and disputable level of harvesting nerve samples which are both related to the dying back phenomenon and to the number of sprouts counted⁵⁸.

Outcome measures of (morphological) analysis of nerve fibers can be influenced by the abovementioned disadvantages, and may result in wrong conclusions. Quantitative (morphological) analysis of nerve fibers will not be used in this thesis.

CONFOCAL LASER SCANNING MICROSCOPY OF REGENERATING AXONS

Confocal laser scanning microscopy (CLSM or LSCM) is a valuable tool for obtaining high resolution images and 3-D reconstructions. The key feature of confocal microscopy is its ability to produce blur-free images of thick specimens at various depths. This imaging technique allows both *in vivo* (real-time)^{72,82} and *ex vivo*^{16,30,31,64} visualisation of (regenerating) nerve fibers. Besides (semi) quantitative assessment, three dimensional imaging of axon sprouting in longitudinal sections can be of great value in developing tubular strategies to bridge nerve gaps. Measurement- and sampling related bias can be reduced, but not totally excluded.

Confocal laser scanning microscopy is of great value when studying behavior patterns of regenerating axons. Up to now, there is no surplus value of confocal laser scanning microscopy over conventional morphological analysis of nerve fibers concerning quantitative outcome.

RETROGRADE TRACING OF REGENERATING AXONS

The ability of axons to transport various molecules retrogradely allows labeling of their specific nerve cell bodies in the anterior horn of spinal cord (motor) and in dorsal root ganglia (sensory). In theory, double labeling techniques are appropriate for quantitative analysis of axons regenerating over an injured region. In the double labeling technique all existing (motor and/or sensory) axons are labelled. After the experimental regeneration time only those cell bodies are labelled which have an axon that regenerates (with one or more sprouts). The outcome measure is the ratio between double and solitary labelled neurons. Different neuronal tracers, like horseradish peroxidase (HRP), fast blue (FB), true blue (TB), diamidino yellow (DY), Biotinylated dextran amines (BDA), Fluoro-Gold (FG) and cholera toxin B subunit (CTB) have been studied for their properties in various reports^{18,27,28,33,50,75,77,78,83}. Each type of tracer has a relative labeling efficiency depending on different factors: (1) type of nerve fiber applied to (sensory or motor), (2) combination of tracers used (3) type of tracer uptake and (4) dura-

tion of experiment. Administering neural tracers is of influence on reliability and practicability of the assessment technique. Uptake can take place by (micro) injection into nerve or muscle (only motor axons), and by application to a cut nerve end. For long-term experiments using double labeling it is necessary that at least one of the two tracers has a minimal surviving capacity lasting the experimental duration^{63,66}.

In preface to this thesis, pilot studies using retrograde tracers as quantitative outcome measure failed due to: (1) nerve injury caused by micro injection, (2) low number of neurons that were double labeled in control groups. The use of retrograde tracers as an quantitative measure is therefore not further explored in this thesis.

MORPHOLOGICAL ANALYSIS OF NEURAL SCARRING

Histological staining for collagen fibers (by Masson's trichrome) is often used to assess the formation of neural adhesions after nerve injury^{25,26,69-71,74}. Evaluation is performed by: (1) pure description of collagen tissue in relation to nerve tissue, (2) surface or thickness measurements of collagen layers, (3) grading the number of fibroblasts per microscopic field.

This technique does not allow assessment of collagen fiber architecture. Especially, this structural design of collagen is of paramount importance in developing adhesions. Therefore, evaluation of neural scarring should primarily not be achieved by histology. A biomechanical approach of scoring neural adhesions is further investigated in this thesis.

1.3.2 NEUROPHYSIOLOGY

- Electroneurography
- Electromyography
- Magnetoneurography

ELECTRONEUROGRAPHY (ENG)

Electroneurography measures the potential difference between two points on the surface of a nerve trunk. Two extracellular recording electrodes pick up the maximally evoked electrical activity of all active fibers, giving a summed potential called a compound nerve action potential (CNAP). The greater the number of active fibers the larger the CNAP amplitude. In other words, the amplitude of the CNAP depends on the properties of single nerve fibers within the whole nerve. Other indicators of CNAP are conduction velocity (CV) and area of CNAP. In recent literature, *in vivo* ENG is not frequently used as a measure of neural regeneration^{12,41,46}. ENG is an invasive method and therefore only suitable for longitudinal measurements using implanted recording equipment²⁰. Furthermore, *in vivo* neurophysiological measurements are heavily prone to errors, i.e. variation in recording distances and temperature that highly contribute to outcome variability. Recent studies showed that *ex vivo* nerve measurements, enabling high reproducibility and signal quantification, can be performed with ENG in (compartmental) bath solutions^{21,22,61,62,73,100}.

Thus, to produce quantifiable neurophysiological outcome measures, an ex vivo recording set up is preferable over in vivo recording, especially in smaller sized experimental animals. A remaining disadvantage of ENG is that electrically recorded CNAPs vary with the impedance of biological tissues surrounding the nerve, and by the position of the nerve in relation to the sensor. Therefore, an alternative ex vivo neurophysiological method, like magnetoneurography, should be explored.

ELECTROMYOGRAPHY (EMG)

In EMG, electrical activity is recorded in the muscle as an evoked response to stimulation. CV and amplitude of compound muscle action potential (CMAP) are used as indicators of neural regeneration^{44,98}. Because of the influence of the motor unit size after reinnervation, CMAP indirectly reflects the number of regenerated axons²⁴. Furthermore, motor unit numbers can be estimated by dividing the amplitude of EMG response to maximum stimulation of the muscle nerve by the average amplitude of the first (5-15) motor unit potentials^{15,24,45}. Percutaneous stimulation of the nerve and intramuscular recording does allow longitudinal measurements. However, CMAPs vary according to stimulation level, recording placement within the muscle and subsequent conduction distance in the recording setup.

In conclusion, EMG is less suitable to provide reproducible and quantifiable outcome measures in experimental animal studies and is not further explored in this thesis.

MAGNETONEUROGRAPHY (MNG)

Magnetic recording of neurophysiological signals has been introduced by Wikswo in 1980¹⁰⁷. Conducted action potentials through axons generate intracellular action currents, resulting in so called compound nerve action currents (CNAC's). These CNAC's produce magnetic fields outside the nerve, that are directly related to intra-axonal currents. In MNG, toroidal coil sensors record the changes in these biomagnetic fields. A major advantage of MNG is that the impedance of surrounding tissues hardly influences magnetic fields. A calibration pulse allows signal amplitude calibration, enabling signal quantification^{46, 104-106}. The MNG model is based on distal stimulation and proximal recording of an injured nerve (*Figure 4*). This way, only those axons with regenerating fibers are stimulated and recorded. In 'in vivo' rabbit studies, MNG has been used for quantification of peripheral nerve regeneration after microsurgical end-to-end repair^{47, 48, 102}. The outcome of MNG is directly related to the regenerated nerve's conduction capacity. A disadvantage of this toroidal MNG technique is that no longitudinal measurements can be made, in order to follow regeneration of a nerve. Furthermore, accurate in vivo MNG measurements of the small sized rat sciatic nerves were impeded due to an overlap of the stimulus artifact and the MNG signal.

MNG is a potential neurophysiological technique to provide quantitative outcome measures in an experimental rat model. The feasibility of ex vivo MNG measurements of the rat sciatic nerve should be further investigated.

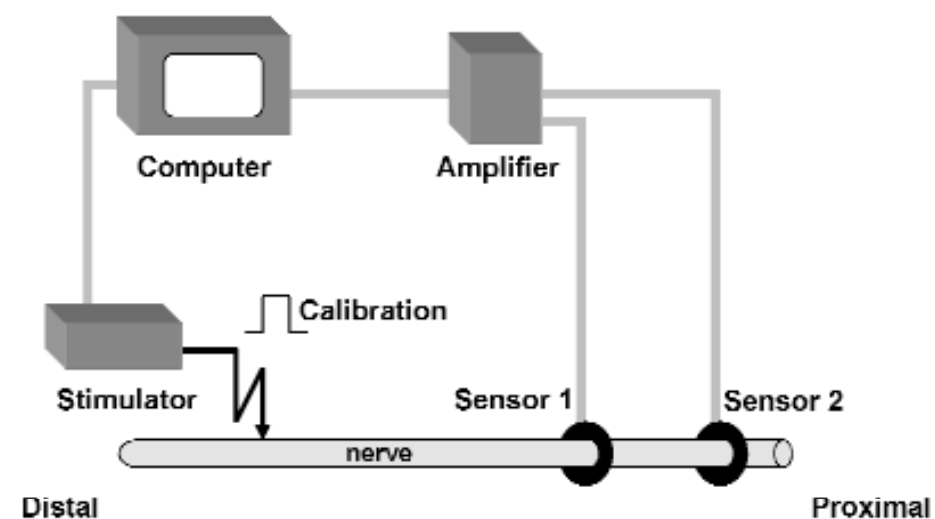


Figure 4. Distal stimulation and proximal recording are shown in a schematic representation of the MNG setup.

1.3.3 FUNCTION OF TARGET ORGANS

- Footprint / walking track analysis
- Muscle strength and weight analysis
- Sensory function evaluation
- Sweating quantification

FOOTPRINT / WALKING TRACK ANALYSIS

The most commonly used method of evaluation of function of target organs after nerve injury in the rat is walking track analysis. The sciatic function index (SFI), developed by de Medinaceli¹¹ and later adapted by Bain², is calculated using three measures of hind leg footprints acquired by walking track analysis (*Figure 5*): the 1-5 toe spread (TS), the 2-4 toe spread (ITS) and the print length (PL). Different techniques are used to obtain footprints for walking track analysis, ranging from visible footprints in a walkway^{11,53} to digitally recorded footprints⁹⁷. Static video footprint analysis (Static Sciatic Index and static TSF) has been reported as a reliable alternative increasing the speed of assessment⁴.

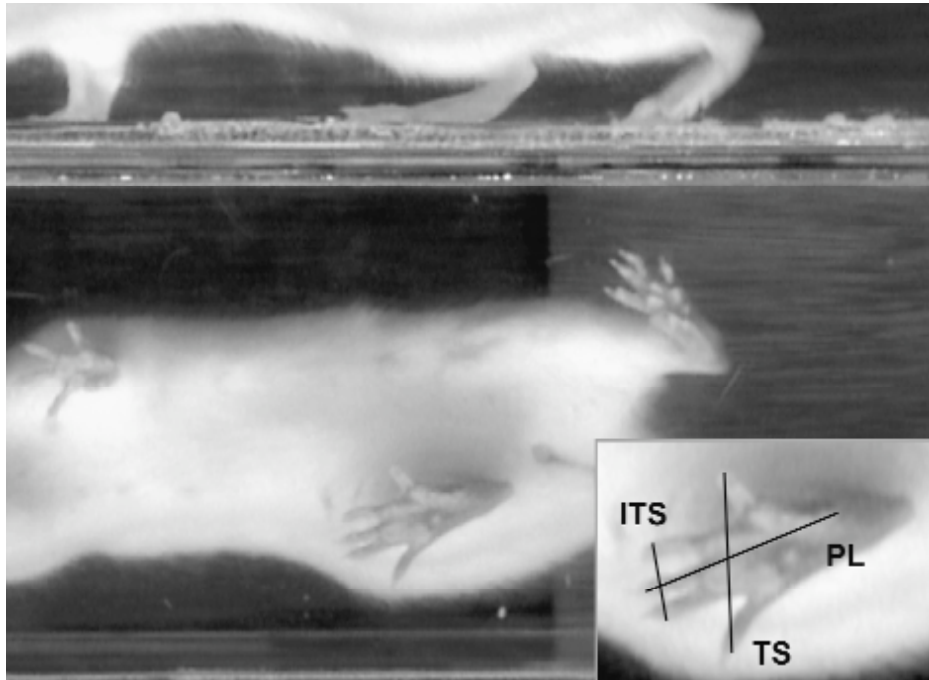


Figure 5. Footprint of an unoperated left hind paw. Note the mirror image in the plantar view. The maximal foot placing can be determined from the lateral view of the video screen. On the detailed footprint the whitened pressure points are visible, which are used to measure the toe spread (TS), intermediate toe spread (ITS), and print length (PL).

A disadvantage of any kind of footprint analysis is exclusion of animals because of autotomy and contractures of the hind paws after sciatic nerve injury. Strategies to reduce autotomy include use of anti-nail-bite lotion⁸⁹ and use of breeds less prone to autotomy such as Lewis rats⁵. However, there is no solid technique to prevent contracture of hind paws after sciatic nerve injury.

Digital recording of walking tracks allows for additional assessment of stance phase of a gait cycle (stance duration and ankle angle)^{95,96}. Furthermore, a scoring system of seven variables is described to evaluate the walking pattern of a rat⁶⁰. Functional gait analyses still enable partial functional evaluation in rats with autotomy or contractures. However, their discriminating power has not widely been confirmed yet.

As footprint or walking track analyses are non invasive techniques, they can be used as supplementary methods of evaluation of recovery pattern in time after nerve injury.

The extra value of walking track analysis over static footprint analysis is disputable, and subject of investigation in this thesis. Previous reports studying different measures of neural regeneration (including walking track analysis) lack the use of an accurate neurophysiological technique (as discussed earlier)^{19,41,86}. Therefore, the recovery patterns of functional and neurophysiological features are further examined using a newly developed ex vivo MNG method to provide neurophysiological outcome data.

MUSCLE STRENGTH AND WEIGHT EVALUATION

After stimulation of the nerve, a strain gauge can measure contraction force of the tendon/muscle itself or plantar flexion force of the hind paw^{41,44,108}. Measurement of muscle contraction force provides quantitative data on reinnervation of individual muscles.

Denervation of muscles causes atrophy and decrease in muscle weight (MW), followed by increase in MW when reinnervation occurs. MW should be expressed as a percentage of opposite limb controls and is subject to variations in: (1) accuracy of harvesting, (2) infiltration of connective tissue and fat, and (3) degree of hydration¹⁹. Obviously, MW is an end point measurement and often used in addition to other evaluation methods^{35,79,91,108}.

In this thesis, MW is used as an additional quantitative outcome measure and investigated for its relation to conduction capacity.

SENSORY FUNCTION EVALUATION

The withdrawal response after application of a pain stimulus can assess return of sensory function after nerve injury^{10,14,36,43,98}. Various techniques are reported, such as the time point of withdrawal after small electric current on the lateral foot sole innervated by the sural nerve (division of sciatic nerve). To exclude bias caused by collateral sprouting, it is necessary to transect nerves innervating surrounding skin¹⁰. As a consequence reliable longitudinal measurements are not feasible. In another technique withdrawal time of the paw from a heat source is determined as a marker of sensory function⁴³. However, adaptation of the animal to the pain stimulus cannot be excluded.

In preface to this thesis, a pilot study using a pain withdrawal test demonstrated a poor discriminating power between regenerating and non regenerating nerves. Therefore, sensory function will not be further assessed in this thesis.

SWEATING QUANTIFICATION

Sweating of paws reflects autonomic nerve activity. Reinnervation of mice hind paws sweat glands after peripheral nerve injury can be quantified by counting active sweat glands after induction by Pilocarpine^{42,64,98}.

The recovery of the autonomic nervous system is not further studied in this thesis.

GENERAL REMARK

When evaluating function of target organs it is of critical importance to understand the significance of the outcome measure. Target organ function after peripheral nerve injury is dependent on multiple factors: (1) number of regenerated axons into the distal segment, (2) appropriate reinnervation of original target organs, (3) relation between number of regenerated axons and function measured in target organ (4) compensation or correction of misdirected regenerated axons by cortical / central plasticity, (5) influence of denervation on target organ (atrophy, scar formation).

Therefore, when studying fundamental problems at the site of injury, the function of target organs is only of relative value.

1.3.4 BIOMECHANICS

- Neural tensile forces
- Neural adhesions

NEURAL TENSILE FORCES

Numerous experimental animal studies have focussed on the limits to which nerves can be stretched before their function is compromised. It is known that straining nerves beyond the physiological tension range can alter their conduction properties^{67, 103} and intraneural blood flow⁵⁶ and can result in permanent loss of function^{49, 81}. When considering the mechanical properties of neural tissue it is important to define and understand biomechanical terminology namely: elasticity, force, stress, strain, stiffness.

The simplest way to start is to consider an ideal elastic rod. Applying a tensile force to the rod will cause an increase in its length. That increase in length will depend on mainly two factors; its cross sectional area and the properties of the material the rod is made from. The rod is then said to be stressed. It is customary to define stress as the force per unit cross-sectional area, for example N/m². The material is said to be elastic if the rod returns to its original length when the force is removed.

To enable comparison between materials, the amount the rod extends under a given force is converted as a ratio of its length and that ratio is called strain. Since it is a ratio, it is unit-less. A given force will cause different materials to extend by a different amount (given the same cross sectional area). The amount of force required to extend the rod by one unit is a measure of stiffness for the material and has the unit N/m. Linear elastic material exhibits a straight line curve going through the origin in a force against extension graph (Figure 6).

It is known that peripheral nerves do not act like an ideal elastic rod. Nevertheless, experimental studies investigating actual mechanical properties within normal physiological conditions are rare. In this thesis, the distribution of strain and stiffness is examined along the length of healthy nerves.

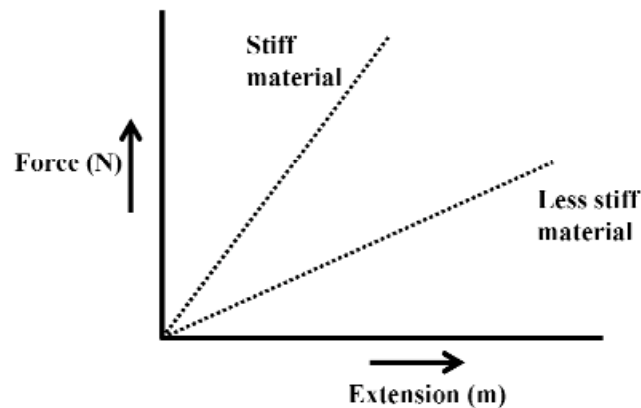


Figure 6. Graph demonstrating the principles of elastic material. Certain material is less stiff if less force is necessary to extend this material.

NEURAL ADHESIONS

The assessment of nerve adhesions in an experimental model is not straightforward. The most accepted method of assessing nerve adhesions is through surgical evaluation of the wound; that is, an investigator scores the adhesions according to the difficulty experienced during nerve dissection (Figure 7)^{1, 25, 71, 74}. Despite blindly randomised evaluation, the outcome measure of this scoring system is not completely objective and quantitative.

Tissue	Grade	Definition
Skin and muscle fascia	1	skin or muscle fascia entirely closed
	2	skin and muscle fascia partially open
	3	skin and muscle fascia completely open
Nerve adherence and nerve separability	1	no dissection or mild blunt dissection
	2	some vigorous blunt dissection required
	3	sharp dissection required

Figure 7 Grading scale introduced by Petersen⁷⁴ in which the investigator has to give a score to the difficulty of dissection.

The extent of scar formation adhering two gliding layers is related to the force necessary to break adhesions between these layers. This force can be measured when separating the two structures. Pull out strength provides a quantitative outcome that is related to the most rigid collagen connections. In experimental tendon research, pull-out strength has frequently been used as a measure for tendon adhesions^{7, 29, 109}. In two recent studies on prevention of nerve adhesion, the force required to avulse the nerve at a 45° angle to the neural bed was measured^{38, 68}. Unfortunately, no information was provided regarding the standardization of the nerve length involved. Thus far, a well defined method of quantifying nerve adhesions is lacking. In this thesis, the quantification of nerve adhesions will be approached biomechanically.

1.3.5 SUMMARY OF EXPERIMENTAL METHODS AVAILABLE FOR EXPERIMENTAL EVALUATION OF RECOVERY AFTER PERIPHERAL NERVE INJURY

Category of Assessment	Type of Assessment	Used for this Thesis
Histology	Quantitative (morphological) analysis of nerve fibers	- *
	Confocal laser scanning microscopy of regenerating axons	-
	Retrograde tracing of regenerating axons	- **
	Morphological analysis of neural scarring	-
Neurophysiology	Electroneurography	-
	Electromyography	-
	Magnetoneurography	+
Function of target organs	Footprint / walking track analysis	+
	Muscle strength and weight evaluation	+
	Sensory function evaluation	- **
	Sweating quantification	-
Biomechanics	Neural tensile forces	+
	Neural adhesions	+

Table 1. Summary of evaluation techniques per category, reviewed in the introduction. Furthermore, it is indicated whether the assessment technique is subject of further investigation in this thesis. One asterisk (*) is placed at “quantitative (morphological) analysis of nerve fibers”. In Chapter 5 histological sections are used not to (morphologically) quantify nerve fibers, but to quantify fascicular/non-fascicular tissue architecture. A double asterisk (**) is placed at “retrograde tracing of regenerating axons” and “sensory function evaluation”. Both techniques were used in non published pilot studies prior to this thesis.

1.4 General aim and outline of the thesis

This thesis aims to enable a more critical appraisal of underlying fundamental problems causing clinical symptoms of peripheral nerve injury. The rat sciatic nerve model is used to provide quantifiable experimental techniques to assess physiological and pathophysiological processes involved in peripheral nerve injury. All experiments and models designed for this thesis concentrate on the site of the peripheral nerve that is liable to injury (i.e. problems at the site of injury as described in the introduction).

The study in **chapter 2** is designed to investigate different techniques of functional evaluation, i.e. footprint analysis, after sciatic nerve injury in rats. The widely accepted but labor intensive walking track analysis is compared to a time-saving digitized static footprint analysis. The aim of this study is to validate the correlation between different techniques of footprint analysis in a large number of animals and confirm the efficacy of static footprint analysis.

In **chapter 3** the feasibility of ex vivo MNG measurements of the isolated rat sciatic nerve is studied. The aim of this study is to design a custom made recording chamber allowing for accurate control of conduction distances and temperature. Reduction of the stimulus artifact, reproducibility of signals and ex vivo nerve viability are subject of investigation.

Chapter 4 reports on the recovery pattern of neurophysiological features and function of target organs after rat sciatic nerve transection followed by direct repair. The major aim of this study is to provide an accurate data set of neurophysiological recovery with time. The increased accuracy of the MNG data (**chapter 3**) sheds new light on several issues relevant to experimental studies of nerve regeneration. These include the relation of the neurophysiological MNG variables to the indirect evaluation variables muscle weight and footprint analysis (**chapter 2**), and an assessment of the influence of autotomy and/or contracture on outcome variables.

The main objective of **chapter 5** is to determine how stretch is distributed along the nerve relative to location of particular nerve segments. Tensile properties of peripheral nerves are of paramount importance in nerve repair. Deformation (strain) in joint and non-joint regions of rat median and sciatic nerves is measured in situ during limb movement. In addition, isolated samples of joint and non-joint regions of both nerves are examined for differences in tensile properties and differences in fascicular/non-fascicular tissue architecture.

The study in **chapter 6** aims to develop an objective method of quantifying nerve adhesions. A biomechanical technique is used to determine the strength of neural adhesions. The model is validated in different types of nerve injury and used for the evaluation of the efficacy of an autocrosslinked hyaluronic acid (Hyaloglide) gel as an anti adhesion therapy. The effect of Hyaloglide gel on functional recovery is measured by static footprint analysis in time after crush injury (**chapter 2**).

Chapter 7 comprises a study on the use of ReGeneraTing Agents (RGTA) after peripheral nerve injury. The aim of this study is to assess the effect of RGTA (dextran

derivatives with heparin-like properties) on extraneural fibrosis and regeneration after crush injury in a rat sciatic nerve model. To assess the anti adhesion effect of RGTAs, the biomechanical model described in chapter 6 is used. RGTAs effect on nerve regeneration is studied using ex vivo MNG (**chapter 3 & 4**) and their effect on functional recovery is measured by static footprint analysis (**chapter 2**).

Finally, in **chapter 8**, the most important results are summarized and discussed for their implications.

References

- Adanali G, Verdi M, Tuncel A, et al: Effects of hyaluronic acid-carboxymethylcellulose membrane on extraneural adhesion formation and peripheral nerve regeneration. *J Reconstr Microsurg* 19:29-36, 2003
- Bain JR, Mackinnon SE, Hunter DA: Functional evaluation of complete sciatic, peroneal, and posterior tibial nerve lesions in the rat. *Plast Reconstr Surg* 83:129-138, 1989
- Baranowski AP, Priestley JV, McMahon SB: The consequence of delayed versus immediate nerve repair on the properties of regenerating sensory nerve fibres in the adult rat. *Neurosci Lett* 168:197-200, 1994
- Bervar M: Video analysis of standing—an alternative footprint analysis to assess functional loss following injury to the rat sciatic nerve. *J Neurosci Methods* 102:109-116, 2000
- Carr MM, Best TJ, Mackinnon SE, et al: Strain differences in autotomy in rats undergoing sciatic nerve transection or repair. *Ann Plast Surg* 28:538-544, 1992
- Cavaletti G, Oggioni N, Sala F, et al: Effect on the peripheral nervous system of systemically administered dimethylsulfoxide in the rat: a neurophysiological and pathological study. *Toxicology Letters* 118:103-107, 2000
- Constantinescu MA, Greenwald DP, Amarante MT, et al: Effects of laser versus scalpel tenolysis in the rabbit flexor tendon. *Plast Reconstr Surg* 97:595-601, 1996
- Danielsson P, Dahlin L, Povlsen B: Tubulization increases axonal outgrowth of rat sciatic nerve after crush injury. *Exp Neurol* 139:238-243, 1996
- Davison SP, McCaffrey TV, Porter MN, et al: Improved nerve regeneration with neutralization of transforming growth factor-beta1. *Laryngoscope* 109:631-635, 1999
- De Koning P, Brakkee JH, Gispen WH: Methods for producing a reproducible crush in the sciatic and tibial nerve of the rat and rapid and precise testing of return of sensory function. Beneficial effects of melanocortins. *Journal of the Neurological Sciences* 74:237-246, 1986
- de Medinaceli L, Freed WJ, Wyatt RJ: An index of the functional condition of rat sciatic nerve based on measurements made from walking tracks. *Exp Neurol* 77:634-643, 1982
- Dellon AL, Mackinnon SE: Selection of the appropriate parameter to measure neural regeneration. *Ann Plast Surg* 23:197-202, 1989
- den Dunnen WF, van der Lei B, Schakenraad JM, et al: Poly(DL-lactide-epsilon-caprolactone) nerve guides perform better than autologous nerve grafts. *Microsurgery* 17:348-357, 1996
- Dijkstra JR, Meek MF, Robinson PH, et al: Methods to evaluate functional nerve recovery in adult rats: walking track analysis, video analysis and the withdrawal reflex. *J Neurosci Methods* 96:89-96, 2000
- Dorfman LJ: Quantitative clinical electrophysiology in the evaluation of nerve injury and regeneration. *Muscle Nerve* 13:822-828, 1990
- Ferretti A, Boschi E, Stefani A, et al: Angiogenesis and nerve regeneration in a model of human skin equivalent transplant. *Life Sci* 73:1985-1994, 2003
- Forman DS, Wood DK, DeSilva S: Rate of regeneration of sensory axons in transected rat sciatic nerve repaired with epineurial sutures. *Journal of the Neurological Sciences* 44:55-59, 1979
- Fritsch B, Sonntag R: Sequential double labelling with different fluorescent dyes coupled to dextran amines as a tool to estimate the accuracy of tracer application and of regeneration. *J Neurosci Methods* 39:9-17, 1991
- Frykman GK, McMillan PJ, Yegge S: A review of experimental methods measuring peripheral nerve regeneration in animals. *Orthopedic Clinics of North America* 19:209-219, 1988
- Fugleholm K, Schmalbruch H, Krarup C: Post reinnervation maturation of myelinated nerve fibers in the cat tibial nerve: chronic electrophysiological and morphometric studies. *J Peripher Nerv Syst* 5:82-95, 2000
- Fukuoka Y, Komori H, Kawabata S, et al: Visualization of incomplete conduction block by neuromagnetic recording. *Clin Neurophysiol* 115:2113-2122, 2004
- Fukuoka Y, Komori H, Kawabata S, et al: Imaging of neural conduction block by neuromagnetic recording. *Clin Neurophysiol* 113:1985-1992, 2002
- Geuna S, Tos P, Battiston B, et al: Morphological analysis of peripheral nerve regenerated by means of vein grafts filled with fresh skeletal muscle. *Anat Embryol (Berl)* 201:475-482, 2000
- Gordon T, Yang JF, Ayer K, et al: Recovery potential of muscle after partial denervation: a comparison between rats and humans. *Brain Res Bull* 30:477-482, 1993
- Gorgulu A, Imer M, SimYek O, et al: The effect of aprotinin on extraneural scarring in peripheral nerve surgery: an experimental study. *Acta Neurochir (Wien)* 140:1303-1307, 1998
- Gorgulu A, Uzal C, Doganay L, et al: The effect of low-dose external beam radiation on extraneural scarring after peripheral nerve surgery in rats. *Neurosurgery* 53:1389-1395; discussion 1395-1386, 2003
- Haase P, Payne JN: Comparison of the efficiencies of true blue and diamidino yellow as retrograde tracers in the peripheral motor system. *J Neurosci Methods* 35:175-183, 1990
- Harsh C, Archibald SJ, Madison RD: Double-labeling of saphenous nerve neuron pools: a model for determining the accuracy of axon regeneration at the single neuron level. *J Neurosci Methods* 39:123-130, 1991
- Hatano I, Suga T, Diao E, et al: Adhesions from flexor tendon surgery: an animal study comparing surgical techniques. *J Hand Surg [Am]* 25:252-259, 2000
- Heijke GC, Klopper PJ, Baljet B, et al: Method for morphometric analysis of axons in experimental peripheral nerve reconstruction. *Microsurgery* 20:225-232, 2000
- Heijke GC, Klopper PJ, Van_Doorn IB, et al: Processed porcine collagen tubulization versus conventional suturing in peripheral nerve reconstruction: an experimental study in rabbits. *Microsurgery* 21:84-95, 2001
- Hentz VR, Rosen JM, Xiao SJ, et al: The nerve gap dilemma: a comparison of nerves repaired end to end under tension with nerve grafts in a primate model. *J Hand Surg [Am]* 18:417-425, 1993
- Herzog J, Kummel H: Fixation of transsynaptically transported WGA-HRP and fluorescent dyes used in combination. *J Neurosci Methods* 101:149-156, 2000
- Hobson MI, Brown R, Green CJ, et al: Inter-relationships between angiogenesis and nerve regeneration: a histochemical study. *Br J Plast Surg* 50:125-131, 1997
- Hobson MI, Green CJ, Terenghi G: VEGF enhances intraneural angiogenesis and improves nerve regeneration after axotomy. *J Anat* 197 Pt 4:591-605, 2000
- Hovius SE, Stevens HP, van Nierop PW, et al: Allogeneic transplantation of the radial side of the hand in

- the rhesus monkey: I. Technical aspects. *Plast Reconstr Surg* 89:700-709, 1992
37. Hunter JM: Recurrent carpal tunnel syndrome, epineural fibrous fixation, and traction neuropathy. *Hand Clin* 7:491-504, 1991
 38. Ikeda K, Yamauchi D, Osamura N, et al: Hyaluronic acid prevents peripheral nerve adhesion. *Br J Plast Surg* 56:342-347, 2003
 39. Jaquet JB. *Median and Ulnar Nerve Injuries: Prognosis and Predictors for Clinical Outcome*. Rotterdam: ErasmusMC Rotterdam; 2004.
 40. Jeronimo A, Jeronimo CA, Rodrigues Filho OA, et al: Microscopic anatomy of the sural nerve in the postnatal developing rat: a longitudinal and lateral symmetry study. *J Anat* 206:93-99, 2005
 41. Kanaya F, Firrell JC, Breidenbach WC: Sciatic function index, nerve conduction tests, muscle contraction, and axon morphometry as indicators of regeneration. *Plast Reconstr Surg* 98:1264-1274, 1996
 42. Kennedy WR, Navarro X, Kamei H: Reinnervation of sweat glands in the mouse: axonal regeneration versus collateral sprouting. *Muscle Nerve* 11:603-609, 1988
 43. Kerns JM, Braverman B, Mathew A, et al: A comparison of cryoprobe and crush lesions in the rat sciatic nerve. *Pain* 47:31-39, 1991
 44. Kim DH, Connolly SE, Gillespie JT, et al: Electrophysiological studies of various graft lengths and lesion lengths in repair of nerve gaps in primates. *J Neurosurg* 75:440-446, 1991
 45. Krarup C, Archibald SJ, Madison RD: Factors that influence peripheral nerve regeneration: an electrophysiological study of the monkey median nerve. *Ann Neurol* 51:69-81, 2002
 46. Kuypers PD, Gielen FL, Wai RT, et al: A comparison of electric and magnetic compound action signals as quantitative assays of peripheral nerve regeneration. *Muscle Nerve* 16:634-641, 1993
 47. Kuypers PD, van Egeraat JM, Dudok v Heel M, et al: A magnetic evaluation of peripheral nerve regeneration: I. The discrepancy between magnetic and histologic data from the proximal segment. *Muscle Nerve* 21:739-749, 1998
 48. Kuypers PD, van Egeraat JM, van Briemen LJ, et al: A magnetic evaluation of peripheral nerve regeneration: II. The signal amplitude in the distal segment in relation to functional recovery. *Muscle Nerve* 21:750-755, 1998
 49. Kwan MK, Wall EJ, Massie J, et al: Strain, stress and stretch of peripheral nerve. Rabbit experiments in vitro and in vivo. *Acta Orthop Scand* 63:267-272, 1992
 50. Lanciego JL, Luquin MR, Guillén J, et al: Multiple neuroanatomical tracing in primates. *Brain Res Brain Res Protoc* 2:323-332, 1998
 51. Lane JM, Bora FWJ, Pleasure D: Neuroma scar formation in rats following peripheral nerve transection. *Journal of Bone and Joint Surgery American Volume* 60:197-203, 1978
 52. Liu XL, Arai T, Sondell M, et al: Use of chemically extracted muscle grafts to repair extended nerve defects in rats. *Scand J Plast Reconstr Surg Hand Surg* 35:337-345, 2001
 53. Lowdon IM, Seaber AV, Urbaniak JR: An improved method of recording rat tracks for measurement of the sciatic functional index of de Medinaceli. *J Neurosci Methods* 24:279-281, 1988
 54. Lundborg G: A 25-year perspective of peripheral nerve surgery: evolving neuroscientific concepts and clinical significance. *J Hand Surg [Am]* 25:391-414, 2000
 55. Lundborg G: Brain plasticity and hand surgery: an overview. *J Hand Surg [Br]* 25:242-252, 2000
 56. Lundborg G, Rydevik B: Effects of stretching the tibial nerve of the rabbit. A preliminary study of the intraneural circulation and the barrier function of the perineurium. *J Bone Joint Surg Br* 55:390-401, 1973
 57. MacKinnon M, Dellon AL: *Surgery of the Peripheral Nerve*. New York: Thieme Medical Publishers, Inc,

- 1988,
58. Mackinnon SE, Dellon AL, O'Brien JP: Changes in nerve fiber numbers distal to a nerve repair in the rat sciatic nerve model. *Muscle Nerve* 14:1116-1122, 1991
59. Maeda T, Hori S, Sasaki S, et al: Effects of tension at the site of coaptation on recovery of sciatic nerve function after neurotomy: evaluation by walking-track measurement, electrophysiology, histomorphometry, and electron probe X-ray microanalysis. *Microsurgery* 19:200-207, 1999
60. Meek MF, Van Der Werff JF, Nicolai JB, et al: Biodegradable p(DLLA-epsilon-CL) nerve guides versus autologous nerve grafts: electromyographic and video analysis. *Muscle Nerve* 24:753-759, 2001
61. Mert T, Gunes Y, Guven M, et al: Comparison of nerve conduction blocks by an opioid and a local anesthetic. *Eur J Pharmacol* 439:77-81, 2002
62. Mert T, Gunes Y, Guven M, et al: Effects of calcium and magnesium on peripheral nerve conduction. *Pol J Pharmacol* 55:25-30, 2003
63. Naumann T, Hartig W, Frotscher M: Retrograde tracing with Fluoro-Gold: different methods of tracer detection at the ultrastructural level and neurodegenerative changes of back-filled neurons in long-term studies. *J Neurosci Methods* 103:11-21, 2000
64. Navarro X, Verdú E, Wendelschafer-Crabb G, et al: Immunohistochemical study of skin reinnervation by regenerative axons. *Journal of Comparative Neurology* 380:164-174, 1997
65. Nishiura Y, Haapaniemi T, Dahlin LB: Hyperbaric oxygen treatment has different effects on nerve regeneration in acellular nerve and muscle grafts. *J Peripher Nerv Syst* 6:73-78, 2001
66. Novikova L, Novikov L, Kellerth JO: Persistent neuronal labeling by retrograde fluorescent tracers: a comparison between Fast Blue, Fluoro-Gold and various dextran conjugates. *J Neurosci Methods* 74:9-15, 1997
67. Ochs S, Pourmand R, Si K, et al: Stretch of mammalian nerve in vitro: effect on compound action potentials. *J Peripher Nerv Syst* 5:227-235, 2000
68. Ohsumi H, Hirata H, Nagakura T, et al: Enhancement of perineurial repair and inhibition of nerve adhesion by viscous injectable pure alginate sol. *Plast Reconstr Surg* 116:823-830, 2005
69. Ozgenel GY: Effects of hyaluronic acid on peripheral nerve scarring and regeneration in rats. *Microsurgery* 23:575-581, 2003
70. Ozgenel GY, Filiz G: Effects of human amniotic fluid on peripheral nerve scarring and regeneration in rats. *J Neurosurg* 98:371-377, 2003
71. Palatinsky EA, Maier KH, Touhalisky DK, et al: ADCON-T/N reduces in vivo perineurial adhesions in a rat sciatic nerve reoperation model. *J Hand Surg [Br]* 22:331-335, 1997
72. Pan YA, Misgeld T, Lichtman JW, et al: Effects of neurotoxic and neuroprotective agents on peripheral nerve regeneration assayed by time-lapse imaging in vivo. *J Neurosci* 23:11479-11488, 2003
73. Paparounas K, O'Hanlon GM, O'Leary CP, et al: Anti-ganglioside antibodies can bind peripheral nerve nodes of Ranvier and activate the complement cascade without inducing acute conduction block in vitro. *Brain* 122 (Pt 5):807-816, 1999
74. Petersen J, Russell L, Andrus K, et al: Reduction of extraneural scarring by ADCON-T/N after surgical intervention. *Neurosurgery* 38:976-983; discussion 983-974, 1996
75. Puigdemivol-Sanchez A, Prats-Galino A, Ruano-Gil D, et al: Fast blue and diamidino yellow as retrograde tracers in peripheral nerves: efficacy of combined nerve injection and capsule application to transected nerves in the adult rat. *J Neurosci Methods* 95:103-110, 2000
76. Ramon y Cajal S: *The structure and connexions of neurons*. Nobel Lecture 1906
77. Reiner A, Veenman CL, Medina L, et al: Pathway tracing using biotinylated dextran amines. *J Neurosci*

- Methods* 103:23-37, 2000
78. Richmond FJ, Gladdy R, Creasy JL, et al: Efficacy of seven retrograde tracers, compared in multiple-labelling studies of feline motoneurons [published erratum appears in *J Neurosci Methods* 1995 May;58(1-2):221]. *J Neurosci Methods* 53:35-46, 1994
 79. Rodkey WG, Cabaud HE, McCarroll HRJ: Neurorrhaphy after loss of a nerve segment: comparison of epineurial suture under tension versus multiple nerve grafts. *J Hand Surg [Am]* 5:366-371, 1980
 80. Rushton WA: A theory of the effects of fibre size in medullated nerve. *J Physiol* 115:101-122, 1951
 81. Rydevik BL, Kwan MK, Myers RR, et al: An in vitro mechanical and histological study of acute stretching on rabbit tibial nerve. *J Orthop Res* 8:694-701, 1990
 82. Saimo T, Matsuura M, Satoh Y: Application of real-time confocal microscopy to intracellular calcium ion dynamics in rat arterioles. *Histochem Cell Biol* 117:295-305, 2002
 83. Sangster CL, Galea MP, Fan R, et al: A method for processing fluorescent labelled tissue into methacrylate: a qualitative comparison of four tracers. *J Neurosci Methods* 89:159-165, 1999
 84. Seckel BR: Enhancement of peripheral nerve regeneration. *Muscle Nerve* 13:785-800, 1990
 85. Seddon HJ: *Surgical disorders of the peripheral nerves*. Livingstone C, editor. New York: 1975,
 86. Shen N, Zhu J: Application of sciatic functional index in nerve functional assessment. *Microsurgery* 16:552-555, 1995
 87. Smith RS, Koles ZJ: Myelinated nerve fibers: computed effect of myelin thickness on conduction velocity. *Am J Physiol* 219:1256-1258, 1970
 88. Sondell M, Lundborg G, Kanje M: Vascular endothelial growth factor has neurotrophic activity and stimulates axonal outgrowth, enhancing cell survival and Schwann cell proliferation in the peripheral nervous system. *Journal of Neuroscience* 19:5731-5740, 1999
 89. Sporel Ozakat RE, Edwards PM, Hepgul KT, et al: A simple method for reducing autotomy in rats after peripheral nerve lesions. *J Neurosci Methods* 36:263-265, 1991
 90. Sterne GD, Brown RA, Green CJ, et al: Neurotrophin-3 delivered locally via fibronectin mats enhances peripheral nerve regeneration. *Eur J Neurosci* 9:1388-1396, 1997
 91. Sterne GD, Coulton GR, Brown RA, et al: Neurotrophin-3-enhanced nerve regeneration selectively improves recovery of muscle fibers expressing myosin heavy chains 2b. *Journal of Cell Biology* 139:709-715, 1997
 92. *Sunderland: Nerve Injuries and their Repair. A Critical appraisal*. London: Churchill Livingstone, 1991, pp 213-219 p
 93. *Sunderland S: The anatomy and physiology of nerve injury*. *Muscle Nerve* 13:771-784, 1990
 94. Terzis J, Faibisoff B, Williams B: The nerve gap: suture under tension vs. graft. *Plast Reconstr Surg* 56:166-170, 1975
 95. Varejao AS, Cabrita AM, Meek MF, et al: Motion of the foot and ankle during the stance phase in rats. *Muscle Nerve* 26:630-635, 2002
 96. Varejao AS, Cabrita AM, Patricio JA, et al: Functional assessment of peripheral nerve recovery in the rat: gait kinematics. *Microsurgery* 21:383-388, 2001
 97. Varejao AS, Meek MF, Ferreira AJ, et al: Functional evaluation of peripheral nerve regeneration in the rat: walking track analysis. *J Neurosci Methods* 108:1-9, 2001
 98. Verdu E, Buti M, Navarro X: The effect of aging on efferent nerve fibers regeneration in mice. *Brain Res* 696:76-82, 1995
 99. Verdu E, Ceballos D, Vilches JJ, et al: Influence of aging on peripheral nerve function and regeneration. *J*

Peripher Nerv Syst 5:191-208, 2000

100. Vleggeert-Lankamp CL, van den Berg RJ, Feirabend HK, et al: Electrophysiology and morphometry of the Aalpha- and Abeta-fiber populations in the normal and regenerating rat sciatic nerve. *Exp Neurol* 187:337-349, 2004
101. Walbeehm ET. *The role of the proximal segment in peripheral nerve regeneration*. Rotterdam: Erasmus University Rotterdam; 2004.
102. Walbeehm ET, Dudok_van_Heel EB, Kuypers PD, et al: Nerve compound action current (NCAC) measurements and morphometric analysis in the proximal segment after nerve transection and repair in a rabbit model. *J Peripher Nerv Syst* 8:108-115, 2003
103. Wall EJ, Kwan MK, Rydevik BL, et al: Stress relaxation of a peripheral nerve. *J Hand Surg [Am]* 16:859-863, 1991
104. Wijesinghe RS, Gielen FL, Wikswo JP: A model for compound action potentials and currents in a nerve bundle. I: The forward calculation. *Annals of Biomedical Engineering* 19:43-72, 1991
105. Wijesinghe RS, Gielen FL, Wikswo JP: A model for compound action potentials and currents in a nerve bundle. III: A comparison of the conduction velocity distributions calculated from compound action currents and potentials. *Annals of Biomedical Engineering* 19:97-121, 1991
106. Wijesinghe RS, Wikswo JP: A model for compound action potentials and currents in a nerve bundle. II: A sensitivity analysis of model parameters for the forward and inverse calculations. *Annals of Biomedical Engineering* 19:73-96, 1991
107. Wikswo JP, Barach JP, Freeman JA: Magnetic field of a nerve impulse: first measurements. *Science* 208:53-55, 1980
108. Wood RJ, Adson MH, VanBeek AL, et al: Controlled expansion of peripheral nerves: comparison of nerve grafting and nerve expansion/repair for canine sciatic nerve defects. *Journal of Trauma* 31:686-690, 1991
109. Zhao C, Amadio PC, Momose T, et al: The effect of suture technique on adhesion formation after flexor tendon repair for partial lacerations in a canine model. *J Trauma* 51:917-921, 2001
110. Zhao Q, Lundborg G, Danielsen N, et al: Nerve regeneration in a 'pseudo-nerve' graft created in a silicone tube. *Brain Res* 769:125-134, 1997

2

Static footprint analysis: a time-saving functional evaluation of nerve repair in rats

Xander Smit, Johan W. van Neck, Menno J. Ebeli and Steven E.R. Hovius

Department of Plastic and Reconstructive Surgery, Erasmus MC - University Medical Center Rotterdam,
The Netherlands

Scand J Plast Reconstr Surg Hand Surg. 2004;38(6):321-5.

Abstract.

Walking track analysis is a widely accepted technique for functional evaluation after sciatic nerve repair in rats, but it is labour-intensive. In 2000, Bervar described a time-saving digitized static footprint analysis. In that study there were good correlations between the traditional sciatic function index (SFI) and the newly-developed static sciatic index (SSI) and static toe spread factor (TSF), respectively. Despite promising results, static footprint analysis is still not widely used. The present study was designed to validate it. After transection of the sciatic nerve, end-to-end repair was assessed using video recorded dynamic and static footprints in 45 Wistar rats. We found an even better correlation between the SFI and both the SSI and the static TSF. In conclusion, static footprint analysis is a time-saving and easy technique for accurate functional assessment of peripheral nerve regeneration in rats.

Keywords: functional assessment, rat, peripheral nerve, regeneration, SFI, static footprint analysis.

Introduction

There is no perfect measure of nerve regeneration in experimental studies in rats¹¹, so various techniques have been used to evaluate peripheral nerve regeneration. The most commonly used method of functional assessment after nerve repair in the rat is walking track analysis. The sciatic function index (SFI), developed by de Medinaceli et al.⁵ and later adapted by Bain et al.¹, is calculated using three measures of hind leg footprints: the 1-5 toe spread (TS), the 2-4 toe spread (ITS) and the print length (PL). During the past two decades, many experimental studies on nerve regeneration have successfully used the SFI as a measure of functional loss^{7, 13, 15, 18}.

Different techniques have been used to obtain the footprints for walking track analysis. Initially, the rat was allowed to walk in a walkway leaving visible footprints by stepping in developer on X-ray film or ink or paint on paper^{5, 12}. In the late 1970s, Hruska et al.¹⁰ published a video recording method of analysing normal locomotion in rats. In 1994 Walker et al.²¹, introduced video-recorded footprint analysis to evaluate functional recovery in rats after nerve injury. This technique has been further developed by others using a mirror positioned at a 45° angle to see the footprints of a walking rat^{6, 14}.

The traditional and the new video techniques of walking track analysis are labour-intensive⁶, but in 2000 Bervar introduced a new method that enabled reliable and fast footprint analysis². In this video recording method, static footprints were used to assess the degree of functional loss, instead of the dynamic footprints that are necessary to calculate the SFI. The static TS and the static ITS were incorporated in a new index formula, resulting in the static sciatic index (SSI). The usefulness of the static toe spread factor (TSF) was also examined. The author showed a good correlation between the SSI and the SFI (0.94; $p < 0.001$) and found a similar correlation between the static TSF and the SFI. The main benefits of this static video recording were the ease and speed with which the essential footprints could be collected and analysed. However, to our knowledge no other workers have used this static footprint analysis to monitor functional recovery after sciatic nerve repair in the rat, and possibly, the lack of independent validation was the reason.

The aim of this study was therefore, to validate the correlation between the SFI and the SSI and static TSF respectively, in a large number of animals and confirm the efficacy of static footprint analysis.

Materials & Methods

SURGICAL PROCEDURE

We followed the guidelines for the care and use of laboratory animals laid down by the experimental animal committee of the Erasmus MC Rotterdam. Female Wistar rats (Harlan Netherlands B.V., Horst, The Netherlands) weighing roughly 200 g, were anaesthetized by inhalation of isoflurane and a mixture of oxygen and nitrous oxide. The right sciatic nerve was exposed through a gluteal muscle splitting incision. Under magnification the nerve was mobilized in the mid thigh, transected with micro scissors and immediately repaired with four to six epineural sutures of monofilament polyamide (10/0 Ethilon®, Ethicon Inc, Somerville). The muscle septum and the skin were closed with 5/0 polyglactin 910 (Vicryl®, Ethicon Inc, Somerville). Postoperatively, animals were housed in twos with free access to food and water. A total of 45 animals was included. This number decreased over time as animals were excluded because of autotomy or contracture or were killed for other experimental purposes. The number of animals counted at each measurement point is given in the legend to Fig. 1.

AUTOTOMY AND CONTRACTURE

The animals were intensively examined for signs of autotomy and contracture. All animals with severe wounds (absence of a part of the foot or severe infection) or animals with contractures were excluded from the study.

FOOTPRINT ANALYSIS

To obtain footprints, a Plexiglas runway (10 x 15 x 100 cm) was used with a mirror placed under the runway at an angle of 45°. This way, a split screen provided a lateral and a plantar view of the rat. Recordings were made of the hind feet using a digital video camera (Sony®, model DCR-TRV240E, Sony Corp., Japan) on a stand positioned 200 cm from the runway. When a fluorescent tubular lamp (90 cm) was used to illuminate from below, the whitened pressure points of the footprints were clearly visible on the plantar view (Fig. 1). Footprints were obtained preoperatively and at 2, 4, 6, 10, and 15 weeks postoperatively.

For dynamic gait analysis, walking movements were recorded until at least four complete runs had been collected. In the same session, static footprints were obtained by recording at least four occasional rest periods. For both dynamic and static assessment, three separate images of the operated (O) and unoperated (N) foot were loaded on a personal computer using commercial software (Studio DV®, version 1.1.0.15, Pinnacle Systems Inc, California). From the digitized footprints the different variables could be measured with the measure tool in Adobe® PhotoShop 4.0 (Adobe Systems Inc., California): the distance between the first and fifth toe (Toe Spread; TS); the distance between the second and fourth toe (Intermediate Toe Spread; ITS) and the distance from the heel to the top of the third toe (Print Length; PL) (Fig. 1b, c). In the static evaluation only the TS and ITS were measured (Fig. 1a).

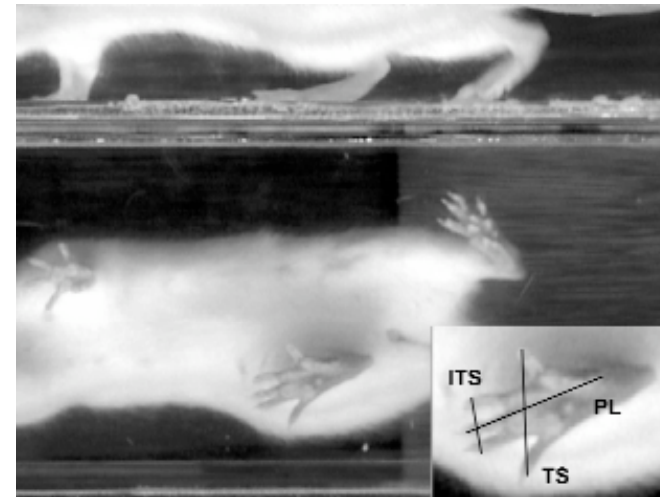


Figure 1a

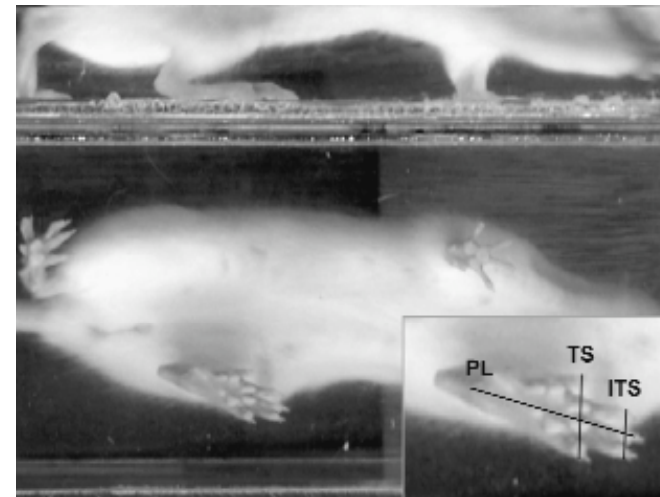


Figure 1b

Figure 1c

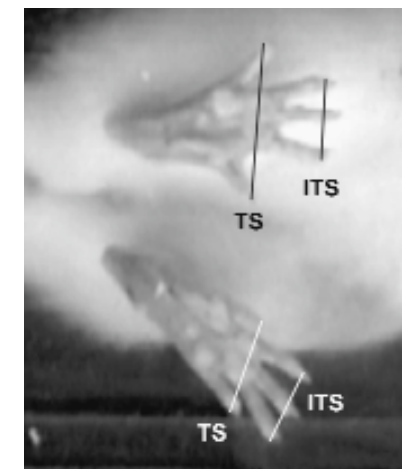


Figure 1. Footprints of a rat 6 weeks after transection of the sciatic nerve followed by end-to-end repair. Note the mirror image of the right and left footprint in the plantar view. (a) Lateral and plantar view (detail) of unoperated left hind feet. The maximal foot placing can be determined from the lateral view of the video screen. On the detailed footprint the whitened pressure points are visible, which are used to measure the toe spread (TS), intermediate toe spread (ITS) and print length (PL). (b) is similar to (a), for the operated right hind feet. (c) a detailed plantar view of a static footprint. The TS and ITS are marked.

The mean distances of three measurements were used to calculate the following factors (dynamic and static):

$$\text{Toe spread factor (TSF)} = (\text{OTS} - \text{NTS}) / \text{NTS}$$

$$\text{Intermediate toe spread factor (ITSF)} = (\text{OITS} - \text{NITS}) / \text{NITS}$$

$$\text{Print length factor (PLF)} = (\text{OPL} - \text{NPL}) / \text{NPL}$$

For the static TSF, an index score of 0 indicates no functional loss. To establish the set value for total impairment in the static TSF, the mean static TSF was calculated from measurable footprints of 22 animals one day postoperatively. This calculated value was also given to the static TSF, when no footprints were measurable.

To calculate the sciatic function index (SFI) the dynamic factors were incorporated in the formula:

$$\text{SFI} = (-38.3 \times \text{PLF}) + (109.5 \times \text{TSF}) + (13.3 \text{ ITSF}) - 8.8^1$$

The static sciatic index (SSI) developed by Bervar² was calculated using the static factors in the equation:

$$\text{SSI} = (108.44 \times \text{TSF}) + (31.85 \times \text{ITSF}) - 5.49$$

Each variable in both the SFI and SSI formulas was previously assessed using multiple regression analysis and ascribed an individual weight subject to their contribution to the sciatic function. The TSF was found to be the most discriminating factor in the SFI and SSI formula and was, therefore, allocated the largest weight. An increased PL, caused by loss of function, resulted in the negative weight of the PLF in the SFI formula. In both formulas an index score of 0 was defined as normal and an index of -100 indicated total impairment. When no footprints were measurable, the index score of -100 was given⁶.

STATISTICAL ANALYSIS

The data were analyzed with using the Statistical Package for the Social Sciences 10 (SPSS, Inc, Chicago) software. Regression analysis was done using Pearson's correlation coefficient of all measurable paired values of the SFI and SSI, and of the SFI and static TSF, of each animal on each measurement day. The residual SD was calculated to characterize the variability around the regression line.

RESULTS

The mean (SEM) static TSF on day 1 postoperatively was -0.66 (0.0095). Functional recovery assessed by the SFI, SSI and static TSF is shown in *Fig. 2*. The preoperative index values are given at time point 0 (SSI = -8.67, SFI = -7.68 and static TSF = -2.59). The SFI, SSI and the static TSF show a similar recovery pattern over time.

During the study six animals were excluded because of autotomy and 11 animals because of contractures. In *Table I* Pearson's correlation coefficient is shown for the intra-animal relation of the SFI and the SSI (R = 0.956; p < 0.001), and of the SFI and static TSF (R = 0.958; p < 0.001).

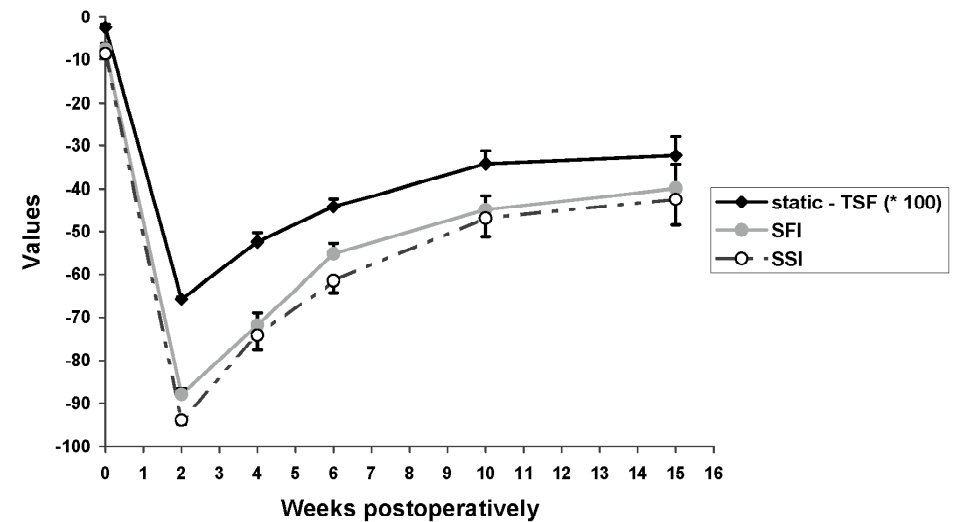


Figure 2. Mean (SEM) sciatic function index (closed circles), the static sciatic index (open circles) and the static toe spread factor x100 (closed diamonds) preoperatively (n=45) and at 2 weeks (n=44), 4 weeks (n=40), 6 weeks (n=30), 10 weeks (n=22), and 15 weeks (n=12) after nerve repair.

Variables	Degrees of freedom (df)	Correlation coefficient (R)	p value	Residual SD
SFI compared with SSI	163	0.956	< 0.001	8.56
SFI compared with static-TSF	163	0.958	< 0.001	8.39

Table I. Pearson's correlation coefficient for the intra-animal relation of the sciatic function index (SFI), the static sciatic index (SSI) and the static toe spread factor (TSF). The residual SD characterizes the variability around the regression line.

Discussion

We found an excellent correlation between the laborious sciatic function index and the time-saving static footprint analysis (static TSF and SSI) used to assess functional recovery after repair of rat sciatic nerves, and our results confirm those of Bervar².

Since its introduction, walking track analysis has been the subject of many discus-

sions^{3, 16, 21, 22}. In particular, the PL is considered to vary⁶. It has been shown that the PL obtained from a standing footprint does not correlate well with a dynamic PL². With this variable excluded, regression analysis was performed to find new coefficients for the TSF and the ITSF, resulting in a new and reliable index formula: the SSI². In 1978, Hasegawa⁹ had already shown that the TS and ITS were useful as individual variables to discriminate nerve function after different types of crush. The SSI formula integrates these two variables, derived from static footprints. We found an excellent correlation between the commonly used SFI and this new SSI. However, we found a similarly good correlation between the SFI and the static TSF, indicating the usefulness of the static TSF as an individual outcome measure of functional recovery. The effectiveness of the static TSF has been emphasised by Bervar² as well. A non-walking TSF was also examined by Hare et al.⁸. However, in this study, the non-walking TSF did not accurately reflect functional recovery. The non-walking toe spread was measured by manually suspending the rat by the scruff of the neck and marking the TS with its feet resting on the floor. This different technique for measuring the TS may explain the contrast with our results.

It should be noted that between full function and total impairment, the static TSF does not range from 0 to -1. We calculated a static TSF value of -0.66, reflecting total functional loss. This value can be allocated to the static TSF, in case no footprints are measurable as a result of total impairment.

A disadvantage of both the SFI and the static footprint analysis remains the exclusion of animals because of autotomy and contractures. In our study six animals (13%) were excluded because of autotomy and 11 (24%) because of contractures. To reduce the problem of autotomy the use of anti-nail-bite lotion is suggested¹⁷ or the use of Lewis rats, a strain that has a low incidence of autotomy⁴.

Over the years, the use of video analysis has been expanded. For example, the stance phase of a gait cycle can be used to assess stance duration and ankle angle; both valuable measures of functional recovery^{19, 20}. In addition, Meek et al.¹⁴ describe a scoring system of seven variables to evaluate the walking pattern of a rat. Such extensive, but labour-intensive, functional gait analyses indeed have been shown to accurately reflect nerve function and furthermore, still enable partial functional evaluation in rats with autotomy or contractures. However, it is obvious from other publications that most investigators interested in nerve function, calculate only the SFI and do not use other evaluation techniques. In these cases, the static footprint analysis provides a similar outcome compared to the SFI, but is achieved in less time. The use of the static TSF is preferable, as the supplementary value of the SSI over the static TSF has not been confirmed and the calculation of the static TSF is easier than the calculation of the SSI.

In a typical experiment with a group size of eight animals we estimate that it takes three to four hours for a complete traditional walking track analysis for each measurement point. Two components contribute to a roughly 40% reduction of the total time needed for the described static footprint analysis compared with the traditional walking track analysis (SFI). Firstly, recording and taking an image of a static footprint demands much less time than a dynamic footprint. Secondly, the use of digitized images facilitates the required actions for measuring the footprint variables.

The static footprint analysis described can easily be incorporated in an existing test battery. We conclude that static footprint analysis is a time-saving and reliable way of assessing functional recovery after injury to rat sciatic nerves.

Acknowledgements

We thank I. Hekking for the surgical assistance, J.F.M. Lange for constructing the equipment and S.J. Flood for carefully reading the manuscript. This work was supported by EC grant QLK3-CT-1999-00625.

References

1. Bain JR, Mackinnon SE, Hunter DA: Functional evaluation of complete sciatic, peroneal, and posterior tibial nerve lesions in the rat. *Plast Reconstr Surg* 83:129-138, 1989
2. Bervar M: Video analysis of standing—an alternative footprint analysis to assess functional loss following injury to the rat sciatic nerve. *J Neurosci Methods* 102:109-116, 2000
3. Brown CJ, Evans PJ, Mackinnon SE, et al: Inter- and intraobserver reliability of walking-track analysis used to assess sciatic nerve function in rats. *Microsurgery* 12:76-79, 1991
4. Carr MM, Best TJ, Mackinnon SE, et al: Strain differences in autotomy in rats undergoing sciatic nerve transection or repair. *Ann Plast Surg* 28:538-544, 1992
5. de Medinaceli L, Freed WJ, Wyatt RJ: An index of the functional condition of rat sciatic nerve based on measurements made from walking tracks. *Exp Neurol* 77:634-643, 1982
6. Dijkstra JR, Meek MF, Robinson PH, et al: Methods to evaluate functional nerve recovery in adult rats: walking track analysis, video analysis and the withdrawal reflex. *J Neurosci Methods* 96:89-96, 2000
7. Hare GM, Evans PJ, Mackinnon SE, et al: Walking track analysis: a long-term assessment of peripheral nerve recovery. *Plast Reconstr Surg* 89:251-258, 1992
8. Hare GM, Evans PJ, Mackinnon SE, et al: Walking track analysis: utilization of individual footprint parameters. *Ann Plast Surg* 30:147-153, 1993
9. Hasegawa K: A new method of measuring functional recovery after crushing the peripheral nerves in unanesthetized and unrestrained rats. *Experientia* 34:272-273, 1978
10. Hruska RE, Kennedy S, Silbergeld EK: Quantitative aspects of normal locomotion in rats. *Life Sci* 25:171-179, 1979
11. Kanaya F, Firrell JC, Breidenbach WC: Sciatic function index, nerve conduction tests, muscle contraction, and axon morphometry as indicators of regeneration. *Plast Reconstr Surg* 98:1264-1274, 1996

12. Lowdon IM, Seaber AV, Urbaniak JR: An improved method of recording rat tracks for measurement of the sciatic functional index of de Medinaceli. *J Neurosci Methods* 24:279-281, 1988
13. Maeda T, Hori S, Sasaki S, et al: Effects of tension at the site of coaptation on recovery of sciatic nerve function after neurotaphy: evaluation by walking-track measurement, electrophysiology, histomorphometry, and electron probe X-ray microanalysis. *Microsurgery* 19:200-207, 1999
14. Meek MF, Van Der Werff JE, Nicolai JP, et al: Biodegradable p(DLLA-epsilon-CL) nerve guides versus autologous nerve grafts: electromyographic and video analysis. *Muscle Nerve* 24:753-759, 2001
15. Shen N, Zhu J: Application of sciatic functional index in nerve functional assessment. *Microsurgery* 16:552-555, 1995
16. Shenaq JM, Shenaq SM, Spira M: Reliability of sciatic function index in assessing nerve regeneration across a 1 cm gap. *Microsurgery* 10:214-219, 1989
17. Sporel Ozakat RE, Edwards PM, Hepgul KT, et al: A simple method for reducing autotomy in rats after peripheral nerve lesions. *J Neurosci Methods* 36:263-265, 1991
18. Tarasidis G, Watanabe O, Mackinnon SE, et al: End-to-side neurotaphy: a long-term study of neural regeneration in a rat model. *Otolaryngol Head Neck Surg* 119:337-341, 1998
19. Varejao AS, Cabrita AM, Meek MF, et al: Motion of the foot and ankle during the stance phase in rats. *Muscle Nerve* 26:630-635, 2002
20. Varejao AS, Cabrita AM, Patricio JA, et al: Functional assessment of peripheral nerve recovery in the rat: gait kinematics. *Microsurgery* 21:383-388, 2001
21. Walker JL, Evans JM, Meade P, et al: Gait-stance duration as a measure of injury and recovery in the rat sciatic nerve model. *J Neurosci Methods* 52:47-52, 1994
22. Weber RA, Proctor WH, Warner MR, et al: Autotomy and the sciatic functional index. *Microsurgery* 14:323-327, 1993

3

Magnetoneurography: Recording biomagnetic fields for quantitative evaluation of isolated rat sciatic nerves

*Xander Smit*¹, *B. Stefan de Kool*^{1,2}, *Erik T. Walbeehm*¹, *E.B. Michiel Dudok van Heel*² †, *Johan W. van Neck*¹ and *Steven E.R. Hovius*¹

1) Department of Plastic and Reconstructive Surgery, Erasmus MC – University Medical Center Rotterdam, The Netherlands

2) Department of Clinical Neurophysiology, Erasmus MC - University Medical Center Rotterdam, The Netherlands

† Michiel Dudok van Heel unfortunately died on July 1st, 2002

J Neurosci Methods. 2003 May 30;125(1-2):59-63.

Abstract

Magnetoneurography (MNG) is a technique to record the biomagnetic action fields of peripheral nerves. The benefits of MNG in contrast to Electroneurography include the decreased signal disturbance caused by surrounding biological tissues and the use of a calibration pulse, both of which contribute to high reproducibility. MNG has proven to be a valuable tool to quantify peripheral nerve regeneration in rabbits. However, the most commonly used model to study the peripheral nervous system is the rat sciatic nerve. Up till now, the small size of the nerve impeded accurate MNG measurements in rat.

This report describes a custom made recording chamber which allows accurate control of conduction distances and temperature, and enables adequate MNG measurements of isolated sciatic nerves of Wistar rats. We applied biphasic stimulation with optimized grounding to reduce the stimulus artifact. A high reproducibility of signals was demonstrated. 'Ex vivo' nerve viability was assured for at least 2 hours after dissection.

In conclusion, MNG is a powerful tool to quantitatively evaluate the function of rat sciatic nerves and will be used for the early assessment of nerve regeneration.

Keywords: Peripheral nerve; Neurography; Magnetic; ex vivo; Rat; Quantification

Introduction

The rat sciatic nerve is often used for experimental studies on the peripheral nervous system. To examine the regeneration of injured rat sciatic nerves an elaborate test battery has been developed over the last decades. Morphometric, functional and electrophysiological nerve analysis of the rat has been described extensively^{1,2,6}.

Electrophysiological methods to analyse the rat sciatic nerve include electromyography (EMG) and electroneurography (ENG). Compound action potentials (CAPs) have previously been used for evaluation of nerve regeneration^{3,5,10}. However, the CAP recorded during ENG is a non consistent parameter as it depends heavily on the distance (hence, impedance) between the sensor and the nerve⁷. Consequently, ENG is less suitable for quantitative analysis. EMG evaluates motor function by measuring evoked or voluntary action potentials in muscles. Therefore, EMG is an indirect measure of the conduction capacity of the nerve⁴, limited to study the recovery of motor axons and not suitable for the early evaluation of nerve regeneration.

These drawbacks of electrophysiological testing are avoided when a magnetic recording technique is used: the Magnetoneurography (MNG) developed by Wikswo et al.¹⁶. Conducted action potentials through axons generate intracellular action currents, resulting in the so called Compound Action Currents (CACs). These CACs produce a magnetic field outside the nerve. In MNG, toroidal coil sensors record the changes in these biomagnetic fields. One advantage of MNG is that the impedance of surrounding tissues hardly influences the magnetic fields, which are directly related to the intra-axonal currents. Most importantly, the use of a calibration pulse allows signal amplitude calibration, enabling signal quantification^{7,14,15}. From the Compound Action Potential a rough distribution of fast and slowly conducting fibers can be made¹⁴. The MNG signal does not distinguish between motor and sensory fibers. In 'in vivo' rabbit studies, MNG was used for the quantification of peripheral nerve regeneration after microsurgical end-to-end repair^{7,8}. Thus far, accurate 'in vivo' MNG measurements of the small sized rat sciatic nerves were impeded due to an overlap of the stimulus artifact and the MNG signal.

In this report we describe a set up, developed to accurately make 'ex vivo' MNG measurements on rat sciatic nerves. The reduction of the stimulus artifact, the reproducibility of signals and the 'ex vivo' nerve viability were examined resulting in a set up that can reliably quantify the nerve's conduction capacity.

Materials & Methods

RECORDING CHAMBER

We designed a 12.5 x 20 x 7.5 cm chamber made of 1 cm thick Plexiglas (Figure 1). The exterior of the chamber was coated with aluminum to provide electro-magnetic shielding. Using a current-driven heating element mounted on the bottom of the chamber and a digital thermometer (Conrad #191027), the buffer solution's temperature was kept constant at 21 ± 0.1 °C.

Clamps on each side served to suspend the nerve. The stimulation cuff and the recording sensors were plugged into a moveable part on a rail, which made it possible to independently alter their position in relation to the nerve.

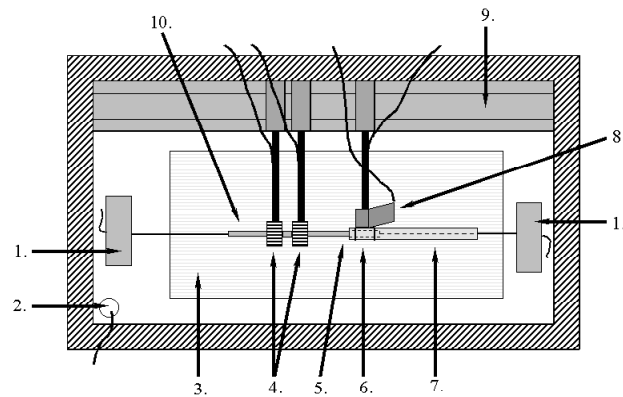


Figure 1. Schematic top view of recording chamber: (1) clamps; (2) thermometer; (3) heating pad; (4) sensors; (5) distal nerve end; (6) stimulation cuff cathode & anode; (7) silicone tube; (8) grounding connection; (9) rail; (10) proximal nerve end.

STIMULATION CUFF

The nerve was stimulated by a cuff which consisted of two circular silver wires (0.25mm diameter) placed 4.5 mm apart, where the proximal electrode served as the cathode and the distal electrode as the anode (Figure 1 & 2). To reduce the stimulus from spreading across the conducting medium, the electrodes were surrounded by a silicone tube (length 4 cm, diameter 3 mm). For optimal grounding, a large grounded silver strip was attached to the stimulation cuff, making the proximity to the stimulation point consistent.

MNG SENSORS

The MNG sensors consisted of a toroidal ferrite core (Magnetics YH40601, ID=3.05mm, OD=5.84mm, Height=1.52mm), wound 76 times with insulated copper wire (63µm diameter; Posyn insulation) (Figure 2). Also, a single insulated silver wire (Medwire Ag10T, Sigmund Cohen Co.) which was used to transmit the calibration signal, was wound around the coil. The coils were mounted on a 304 stainless steel rod, chosen because of its low magnetic permeability ($\mu_r=1.03$), thus minimizing the distortion of the magnetic signal. A silicone coating (Elastosil E41, Wacker Chemie) was used to insulate and protect the coils. Because of its low permittivity ($\epsilon_r=3$), this coating also

reduced the capacitive coupling of the stimulus artifacts to the sensor wires. Two identical sensors were interconnected, leaving a 10 mm space in between.

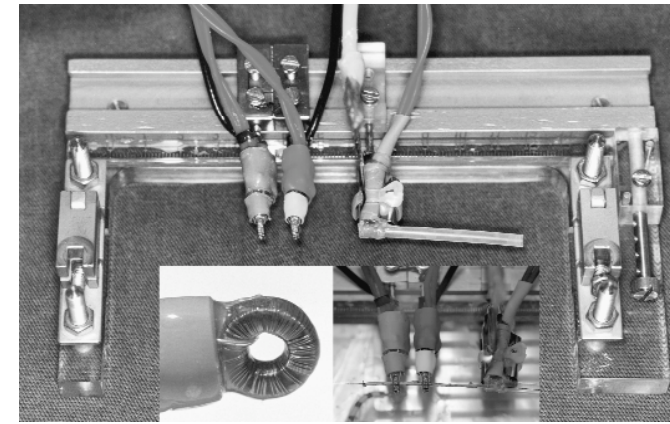


Figure 2. Rail plus stimulation cuff & sensors removed out of recording chamber. Two details: (1) MNG sensor with 76 copper windings and one calibration winding (left); (2) a sciatic nerve suspended in the recording chamber (right).

ANIMAL PREPARATION

All guidelines for the care and use of laboratory animals according to the experimental animal committee of the Erasmus MC Rotterdam were followed.

For all experiments, Wistar rats (female, ± 250 gram) were anaesthetized with Urethane (1ml/100gram). The sciatic nerve was exposed from its origin in the lumbar spine to distal to the trifurcation at knee level, to acquire a maximum length. To prevent axon leakage, the proximal part as well as the three branches of the sciatic nerve were ligated with a 6-0 suture (leaving ± 6 cm of string on each side) and were respectively transected proximally and distally to the knots. To approximate 'in vivo' length, the transected nerve was drawn along a wet surgical gauze and the distance was measured from knot to knot. In a pilot study, this procedure has exhibited good reproducibility and approximates 'in vivo' nerve length.

RECORDING SET UP & SIGNAL EVALUATION

The recording chamber was filled with a buffer solution (Ringers Lactate containing glucose, 1 g/L, at 21 ± 0.1 °C). The nerve was guided through the recording sensors and the stimulation cuff and stretched to 'in vivo' length by clamping the two sutures in the recording chamber (Figure 2). By applying distal stimulation, only those axons present in the distal nerve segment were recorded. Hence, signals of non relevant cut branches were avoided. The nerve end was stimulated with a biphasic constant current pulse of 50 µs delivered by two isolated stimulus units (Digitimer DS3), connected in parallel. For monophasic stimulation one unit was turned off. To guarantee supra maximal stimulation, the stimulator was finally set at 1.4 times the strength of the current which produced a maximal signal¹¹. Every time the stimulation cuff changed position the maximal stimulus was redetermined. Nerve Compound Action Currents (NCACs) were compared to a 1µA calibration signal, converted to voltages, and analyzed on a per-

sonal computer using custom-made software (DataCorr3 written in VBA for MS Excel). In each recording set up four consecutive batches of 256 CACs were recorded and averaged. From this averaged signal, the 1st peak amplitude was calculated from the maximum of the 1st peak to the baseline of the signal. Conduction Velocity was calculated per sensor using the distance from the stimulation cuff to the sensor and the time (latency) from the initial stimulus to the 1st peak.

Results

The sciatic nerves were carefully dissected and they ranged in length between 38 and 43 mm.

In an effort to reduce the stimulus artifact we tested biphasic stimulation instead of monophasic stimulation. The decaying tail of the biphasic stimulus artifact affects the baseline of the recorded signal to a lesser degree (Figure 3).

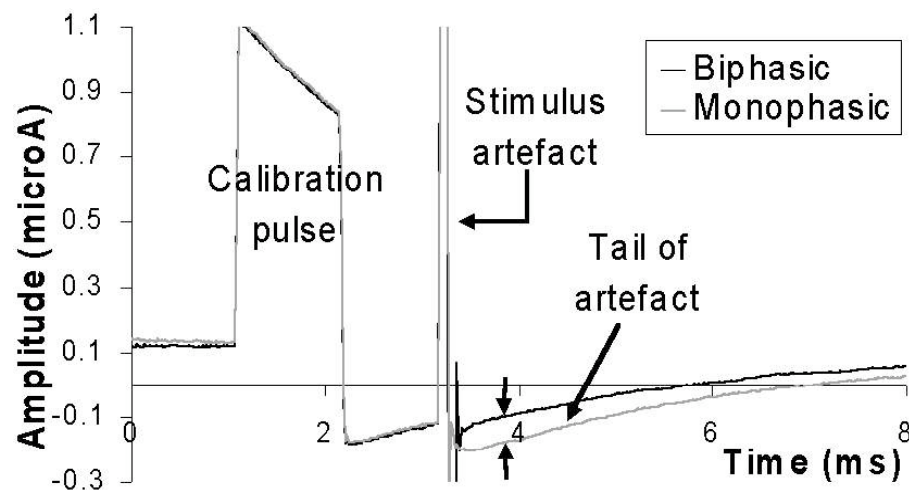


Figure 3. Signals with mono- and biphasic stimulation.

Note the disturbance of the baseline by monophasic stimulation (lower arrow).

The test-retest reproducibility of the MNG signals was determined by recording the CACs of one nerve in four consecutive measurements, in which the two recording sensors were removed and repositioned at 15 mm (Sensor 1: S1) and 5 mm (Sensor 2: S2) from the proximal nerve end. The stimulator cuff cathode was placed 3 mm from the distal nerve end. The CACs in 5 different nerves were evaluated, and this demonstrated that only small differences occur in consecutive measurements of one nerve (mean variability of 2.92% (S1) and 3.04% (S2) for the 1st peak amplitude and 4.16% (S1) and

2.35% (S2) for the conduction velocity).

To determine the influence of time and the position of the recording sensors for the conduction capacity of the isolated nerve, viability measurements were carried out. The 1st peak amplitude and the conduction velocity were recorded at 5, 10, 15 and 20 mm from the proximal nerve end and were assessed every 30 minutes until 3.5 hours after dissection. The stimulator cuff cathode was again positioned 3 mm from the distal nerve end. The mean percentages of the 1st peak amplitude and the conduction velocity are shown in Figure 4 and 5. Maintaining a margin of 10 mm between the proximal nerve end and the sensor, signals varied less than 5 % 2 hours after dissection.

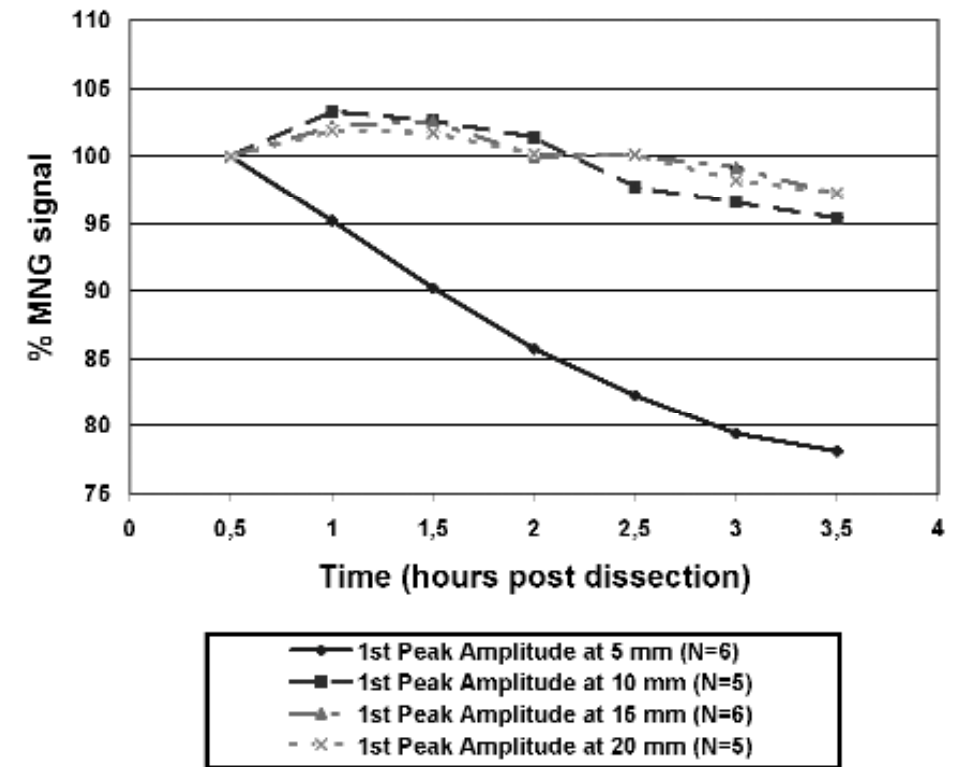


Figure 4. Change of 1st peak amplitude in time; recorded at 5, 10, 15 and 20 mm from the proximal nerve end. The mean signal of each 1st measurement (30 minutes after isolation of the nerve) is defined 100% (SE bars are shown).

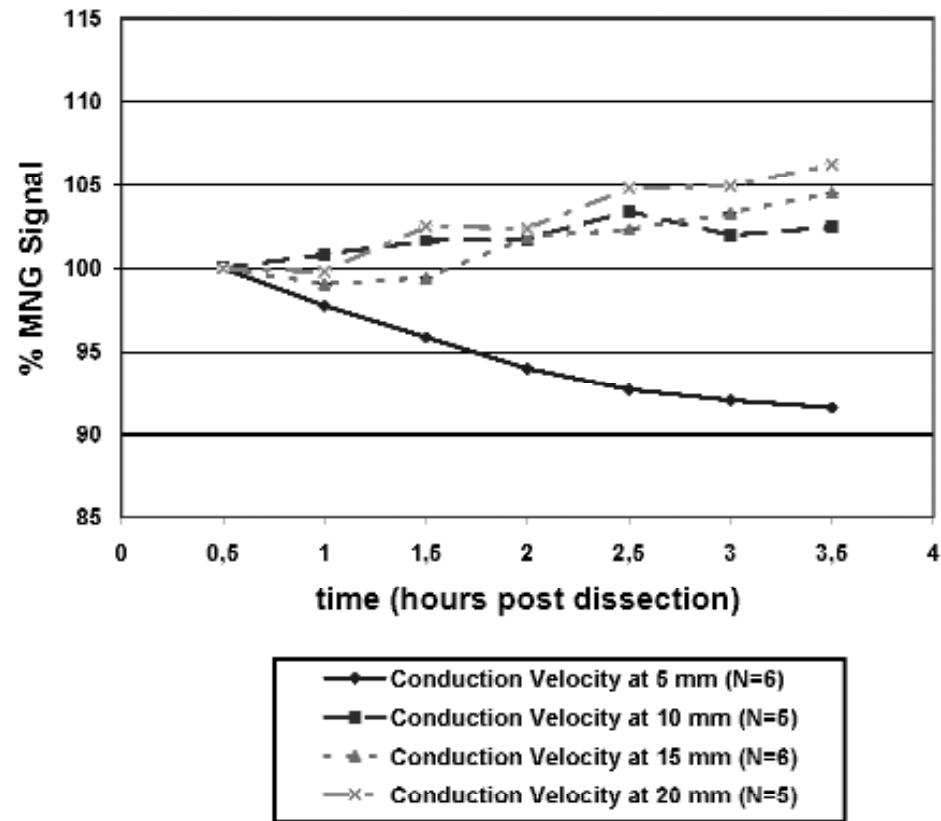


Figure 5. Change of conduction velocity in time; recorded at 5, 10, 15 and 20 mm from the proximal nerve end. The mean signal of each 1st measurement (30 minutes after isolation of the nerve) is defined 100% (SE bars are shown).

Discussion

This report describes the development of an 'ex vivo' experimental set up for magnetoneurographic measurements of rat sciatic nerves. The advantages of this 'ex vivo' set up are multiple. First, the temperature of the buffer solution can accurately be maintained at a constant temperature. This is important, as a change in temperature greatly influences the reproducibility of neurophysiological measurements⁹. Furthermore, small errors in adjusting the distances between the nerve ends and the stimulator and sensors induce relatively great effects on the derived signals in these small sized nerves. The mean variability (<5%) demonstrates that our design of the recording chamber allows for a precise and reproducible set up.

The electrical stimulus needed to effectuate a conducted action potential in the nerve also causes a magnetic field, resulting in a stimulus artifact. Biphasic stimulation and optimal grounding decrease the decaying tail of the stimulus artefact. This results

in less distortion of the signal baseline, ensuring less error in the calculation of the 1st peak amplitude. The available conducting distance is increased by isolation of the nerve. Interference between the signal and the stimulus artefact is minimized by this increased conducting distance ('ex vivo' vs. 'in vivo') and the diminished stimulus artefact.

An inherent side effect of 'ex vivo' measurements is a decrease in nerve viability over time. Neurophysiological signals derived 'ex vivo' fade in time, especially when measured close to a nerve end^{12,13}. However, provided that the sensor is placed at a minimal distance of 10 mm from the proximal nerve end, we can assure a period of 2 hours in which the change in MNG signals is less than 5%. To put this in perspective, the time necessary for determining the stimulus maximum and four consecutive measurements is approximately 20 minutes.

A disadvantage of the described 'ex vivo' technique is that no longitudinal measurements can be made, in order to follow regeneration of a nerve. The MNG model is based on the distal stimulation and the proximal recording of a repaired nerve. This way, only those axons with regenerating fibers are stimulated and recorded. Most experimental studies on the enhancement of peripheral nerve regeneration concentrate on a maximal outgrowth of axons over a nerve lesion. MNG provides an early and quantitative measure of these regenerated axons. In contrast to EMG or Walking Track Analysis, the outcome of MNG is directly related to the regenerated nerve's conduction capacity. MNG can be used in different models of nerve injury (crush, transection, grafts), used to test a hypothesis of increase in speed or quantity of axon regeneration. Five weeks after end to end repair following nerve transection, a first weak signal can be recorded with MNG (our unpublished results).

In conclusion, we have developed an experimental set up for magnetoneurography of the rat sciatic nerve. It will be a powerful supplementary tool in experimental studies of the peripheral nervous system.

Acknowledgements

The surgical assistance of Mrs. I. Hekking is gratefully acknowledged. The authors also thank Mr. M.J. Ebeli for helping with the experiments and converting the rough data, and Mrs. A.E. Huntington for carefully reading the manuscript.

References

1. Dellon AL, Mackinnon SE: Selection of the appropriate parameter to measure neural regeneration. *Ann Plast Surg* 23:197-202, 1989
2. Dijkstra JR, Meek MF, Robinson PH, et al: Methods to evaluate functional nerve recovery in adult rats: walking track analysis, video analysis and the withdrawal reflex. *J Neurosci Methods* 96:89-96, 2000
3. Dubuisson AS, Beuermann RW, Kline DG: Sciatic nerve regeneration across gaps within collagen chambers: the influence of epidermal growth factor. *J Reconstr Microsurg* 9:341-346; discussion 346-347, 1993

4. Frykman GK, McMillan PJ, Yegge S: A review of experimental methods measuring peripheral nerve regeneration in animals. *Orthopedic Clinics of North America* 19:209-219, 1988
5. Gramsbergen A, IJkema-Paassen J, Meek MF: Sciatic nerve transection in the adult rat: abnormal EMG patterns during locomotion by aberrant innervation of hindleg muscles. *Exp Neurol* 161:183-193, 2000
6. Kanaya F, Firrell JC, Breidenbach WC: Sciatic function index, nerve conduction tests, muscle contraction, and axon morphometry as indicators of regeneration. *Plast Reconstr Surg* 98:1264-1274, 1996
7. Kuypers PD, Gielen FL, Wai RT, et al: A comparison of electric and magnetic compound action signals as quantitative assays of peripheral nerve regeneration. *Muscle Nerve* 16:634-641, 1993
8. Kuypers PD, van Egeraat JM, van Briemen LJ, et al: A magnetic evaluation of peripheral nerve regeneration: II. The signal amplitude in the distal segment in relation to functional recovery. *Muscle Nerve* 21:750-755, 1998
9. Rutkove SB: Effects of temperature on neuromuscular electrophysiology. *Muscle Nerve* 24:867-882, 2001
10. Shen N, Zhu J: Application of sciatic functional index in nerve functional assessment. *Microsurgery* 16:552-555, 1995
11. Spaans F. *Klinische Electromyografie*. Alphen a/d Rijn / Brussel: Stafleu's BV; 1981. p 118.
12. van Egeraat JM, Stasaski R, Barach JP, et al: The biomagnetic signature of a crushed axon. A comparison of theory and experiment. *Biophysical Journal* 64:1299-1305, 1993
13. van Egeraat JM, Wikswo JP: A model for axonal propagation incorporating both radial and axial ionic transport. *Biophysical Journal* 64:1287-1298, 1993
14. Wijesinghe RS, Gielen FL, Wikswo JP: A model for compound action potentials and currents in a nerve bundle. III: A comparison of the conduction velocity distributions calculated from compound action currents and potentials. *Annals of Biomedical Engineering* 19:97-121, 1991
15. Wijesinghe RS, Wikswo JP: A model for compound action potentials and currents in a nerve bundle. II: A sensitivity analysis of model parameters for the forward and inverse calculations. *Annals of Biomedical Engineering* 19:73-96, 1991
16. Wikswo JP, Barach JP, Freeman JA: Magnetic field of a nerve impulse: first measurements. *Science* 208:53-55, 1980

4

Recovery of neurophysiological features with time after rat sciatic nerve repair: a magneto-neurographic study

*Xander Smit¹, B.S. (Stefan) de Kool^{1,2}, Joleen H. Blok², Gerhard H. Visser²,
Steven E.R. Hovius¹, Johan W. van Neck¹*

- 1) Department of Plastic and Reconstructive Surgery, Erasmus MC - University Medical Center Rotterdam, The Netherlands
- 2) Department of Clinical Neurophysiology, Erasmus MC - University Medical Center, Rotterdam, The Netherlands

Accepted in J Peripher Nerv Syst

Abstract

Experimental assessment of peripheral nerve regeneration in rats by electrophysiology is controversial due to low reproducibility of electrophysiological indicators and diminished quantitative evaluation in conventional experimental set ups. Magnetoneurography (MNG) counteracts these drawbacks by magnetically recording electrophysiological signals *ex vivo*, thereby providing accurate and quantitative data.

In 50 rats, sciatic nerve transection was followed by direct repair. MNG outcome parameters, footprints (static-TSF; function) and muscle weight (MW) were studied for their recovery pattern from 2 to 24 weeks. By using MNG, we showed that the regeneration process still continues when functional recovery (static-TSF) becomes stagnant. With regression analysis MNG parameters amplitude, amplitude area and conduction velocity demonstrated moderate significant correlation with MW, whereas conduction velocity was not significantly associated with static-TSF. No significant association exists between MW and static-TSF. A Kaplan Meier survival curve revealed that autotomy / contracture of rat hind paws was not related to decreased MNG outcome values.

In conclusion, this study highlights and discusses the dissimilarities between direct (MNG) and indirect (static-TSF & MW) assessment techniques of the regeneration process. We emphasize the significance of MNG as a direct derivative of the axon regeneration in experimental rat studies. Additionally, we stress the must for right – left ratios, as neurophysiological indicators vary with age and we confute possible bias in footprint analysis caused by exclusion of autotomy / contracture animals.

Keywords: peripheral nerve, rat, electrophysiology, magnetoneurography, function, footprint, muscle weight, autotomy

Introduction

When studying early regeneration of peripheral nerves after traumatic lesions, the choice of evaluation technique is critical. Immunohistochemical methods can give an impression of axonal outgrowth. However, they do not provide insight into the capacity of the regenerated nerve to conduct an electrical signal, that is, provide insight into the nerve's functional recovery.

In this study, we present neurophysiological (functional) data that were collected from regenerating rat sciatic nerves. These data were obtained using magnetoneurography (MNG), a powerful neurophysiological technique that is based on the magnetic recording of intra-axonal currents, which together produce a compound nerve action current (CNAC). Thus, the CNAC derived by MNG is directly related to the conduction capacity of a nerve^{12-15,33}.

Recently, we developed an *ex vivo* experimental set up allowing for precise and highly reproducible MNG measurements of healthy rat sciatic nerves²⁷. Recent studies showed that *in vitro* nerve measurements, enabling high reproducibility and signal quantification, can be performed with electroneurography (ENG) using bath solutions in one or multiple compartment recording chambers^{5,6,22-24,32}. However, the main advantage of MNG over ENG is that magnetic fields are less influenced by the impedance of biological tissue surrounding the nerve, and by the position of the nerve in relation the sensor^{11, 35-38}. By eliminating these confounding factors, MNG provides a more direct view on nerve physiology and results in an increased reproducibility compared to conventional ENG^{11,35-37}. In contrast to electromyography (EMG), MNG is a direct measure of the conduction capacity of the nerve. Previous reports studying different measures of neural regeneration lack the use of such an accurate electrophysiological technique^{4, 9,26}.

The major aim of this study was to provide an accurate data set of neurophysiological recovery with time after injury of rat sciatic nerves, using the MNG outcome variables CNAC amplitude and area, and conduction velocity. Once obtained, this set may serve as reference for future studies that, for example, aim to evaluate therapeutical interventions during the regenerative process. Furthermore, we will use the increased accuracy of the MNG data compared to previously obtained electrophysiological results to shed new light on several issues relevant to experimental studies of nerve regeneration. These include the relation of the abovementioned neurophysiological variables to the indirect evaluation variables muscle weight and footprint analysis, and an assessment of the influence of autotomy and/or contracture on outcome variables.

Materials & Methods

SURGICAL PROCEDURE

The experimental protocol was approved by the Animal Experiments Committee under the national Experiments on Animals Act and adhered to the rules laid down in this national law that serves the implementation of "Guidelines on the protection of experimental animals" by the Council of Europe (1986), Directive 86/609/EC. In total 50 female Wistar rats (Harlan Netherlands B.V., Horst, The Netherlands) weighing 200 ± 10 g (11 weeks old), were anaesthetised by inhalation of isoflurane and a mixture of oxygen and nitrous oxide. The right sciatic nerve was exposed through a gluteal muscle splitting incision. Under magnification the nerve was mobilised in the mid thigh, transected with micro scissors and immediately repaired with four to six epineural sutures 10/0 Ethilon® (Ethicon Inc, Somerville). The muscle septum and the skin were closed with 5/0 Vicryl® (Ethicon Inc, Somerville). Following surgery, animals were housed in pairs, and had access to food and water ad libitum.

MNG MEASUREMENTS

MNG end point measurements were carried out 2, 5, 8, 12, 16 and 24 weeks (all $N=10$, except week 2 and 5: $N=5$) after transection and repair, according to the ex vivo MNG technique as described earlier²⁷. In short, animals were anaesthetized with Urethane i.p. 12.5% (1ml/100gram). The sciatic nerve was exposed from its origin in the lumbar spine to distal to the trifurcation at knee level, to acquire a segment of maximum length. To prevent axon leakage, the proximal part as well as the three branches of the sciatic nerve were ligated with a 6-0 suture and were transected proximally and distally to the knots, respectively. The MNG recording chamber was filled with a buffer solution (Ringers Lactate containing glucose, 1 g/L, at 21 ± 0.1 °C). The nerve was guided through the recording sensor coils as well as the stimulation cuff and stretched to 'in vivo' length by clamping the two sutures in the recording chamber. The distal nerve end was stimulated with a biphasic constant current pulse of 50 μ s delivered by two isolated stimulus units (Digitimer DS3), connected in parallel. To guarantee supra maximal stimulation, the stimulator was finally set to 1.4 times the strength of the lowest current that produced a maximal signal. Every time the stimulation cuff changed position this stimulus strength was redetermined.

MNG RECORDING SET UP

Both the right (operated) and left (control) sciatic nerve were measured (Fig. 1). In the recording setting of the right nerve, the stimulation cuff cathode was positioned 10 mm distal to the suture line. Sensor 1 and sensor 2 were positioned 4 mm and 14 mm proximal to the suture line, respectively. By applying distal stimulation and proximal recording, only axons with fibers regenerating across the lesion were stimulated and recorded. For the contra lateral (unoperated) nerve similar recording settings were used, and an imaginary suture line was created at the same distance from the distal nerve end as present in the repaired nerve.

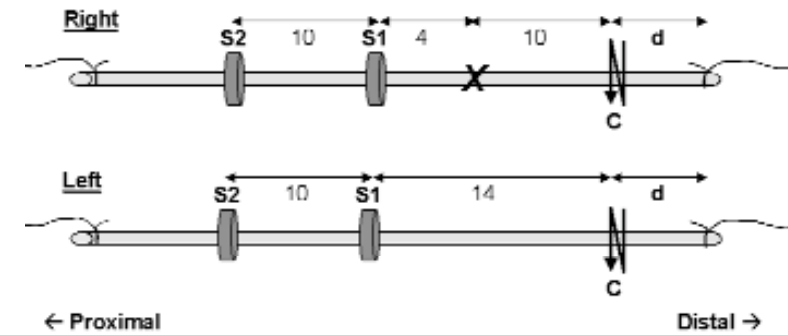


Figure 1. Experimental set up for the operated, right nerve and control, left nerve. C = cathode of stimulator; d = distance between distal nerve end and cathode; S1 = sensor 1; S2 = sensor 2; X = suture line.

SIGNAL EVALUATION

Each signal was calibrated by means of an accompanying one microampere calibration signal, which was recorded prior to every stimulus. Next, CNACs were analyzed on a personal computer using custom-made software (DataCorr3 written in VBA for MS Excel). In each recording set up, 2 to 4 consecutive batches of 256 CNACs were recorded and averaged. Further analyses were performed using MatLab (The MathWorks, Natick, MA). First, the baseline drift in a 4 ms window containing the MNG response was estimated using a linear interpolation of the signal samples immediately preceding and following this window. After correction for this drift, the following variables were calculated from the signal (Fig. 2):

- (1) 1st peak amplitude (1PA), from the maximum of the 1st peak to the baseline of the signal.
- (2) peak-peak amplitude (PPA), from the maximum of the 1st peak to the minimum of the 2nd peak.
- (3) area (A), determined as the area below the CNAC and between the 1st and the 2nd peak. Since both peaks in the signal are fairly symmetrical, this area is approximately equal to half of the total signal area. However, our area measure is much easier to determine than total area, because in many cases signal onset coincided with the stimulus artefact and stimulus offset was difficult to determine due to small, late components.
- (4) conduction velocity (CV), calculated as Dx/Dt , with Dx the distance from the stimulation cuff cathode to the sensor and Dt the latency from the stimulus onset to the maximum of the 1st peak of the signal.

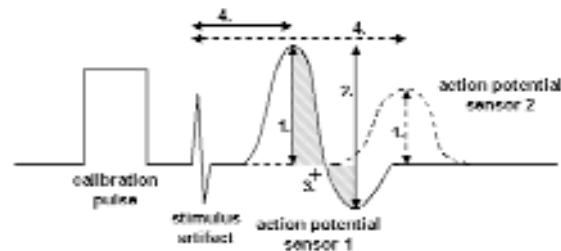


Figure 2. Schematic example of an MNG signal as recorded by sensor 1 (solid line) and sensor 2 (dashed line), with from left to right (early to late) the calibration pulse, the stimulus artefact, and the action current. Signals are quantified using: 1. 1st peak amplitude; 2. peak-peak amplitude (sensor 1 only); 3. area below the signal (shaded; sensor 1 only); 4. peak latency used to calculate the conduction velocity.

The biphasic character of the signal derived from sensor 1 enabled calculation of all of these variables. Because of the generally monophasic character of the signal recorded with sensor 2, only the 1PA and the CV were calculated for this sensor.

FOOTPRINT ANALYSIS

Static footprint analysis was performed 2, 4, 6, 10, 15, 19 and 24 weeks after surgery, following the procedure described elsewhere²⁸. From the digitized footprints the distance between the first and fifth toe (Toe Spread; TS) was measured. The averaged distances of three measurements were used to calculate the static Toe Spread Factor (TSF) = (OTS – NTS) / NTS (O=operated/right; N=normal/left). A value of –0.66 was allocated to the static TSF, in case no footprints were measurable due to total impairment²⁸.

AUTOTOMY AND CONTRACTURE

The animals were meticulously examined for signs of autotomy and contracture. All animals with absence of a part of the foot and/or showing contracture were excluded from footprint analysis.

MUSCLE WEIGHT

Directly after dissection of the nerve at each MNG measurement time point, the gastrocnemius muscles were carefully dissected and detached from their origin and insertion, and weighed immediately. Muscle weight was expressed as the ratio of the right (operated) over the left (control) muscle weight.

STATISTICAL ANALYSIS

The data were analyzed using the Statistical Package for the Social Sciences version 10 (SPSS, Chicago, IL) software. Statistical significance was accepted at $p < 0.05$. Individual statistical tests are mentioned where used. Error bars accompanying means illustrate the standard error of the mean (SEM).

Results

ELECTROPHYSIOLOGY: MNG

In Figure 3, the postoperative time course of all neurophysiological variables (1PA, PPA, A and CV), expressed as right - left ratios, is presented. In repaired nerves, no CNACs could be recorded two weeks postoperatively, whereas five weeks postoperatively, neurophysiological values could be calculated from the earliest detectable CNACs. At this point in time (5 weeks), all MNG variables recorded from the regenerating nerve show a recovery to 14-21 % of control values, except for CV of sensor 2 (35%). With increasing time postoperatively, 1PA, PPA, A and CV ratios increase, except for the CV ratio of sensor 2, which drops 12 weeks after surgery. Means of different points in time were declared to be significantly different from each other ($p < 0.05$) by an analysis of

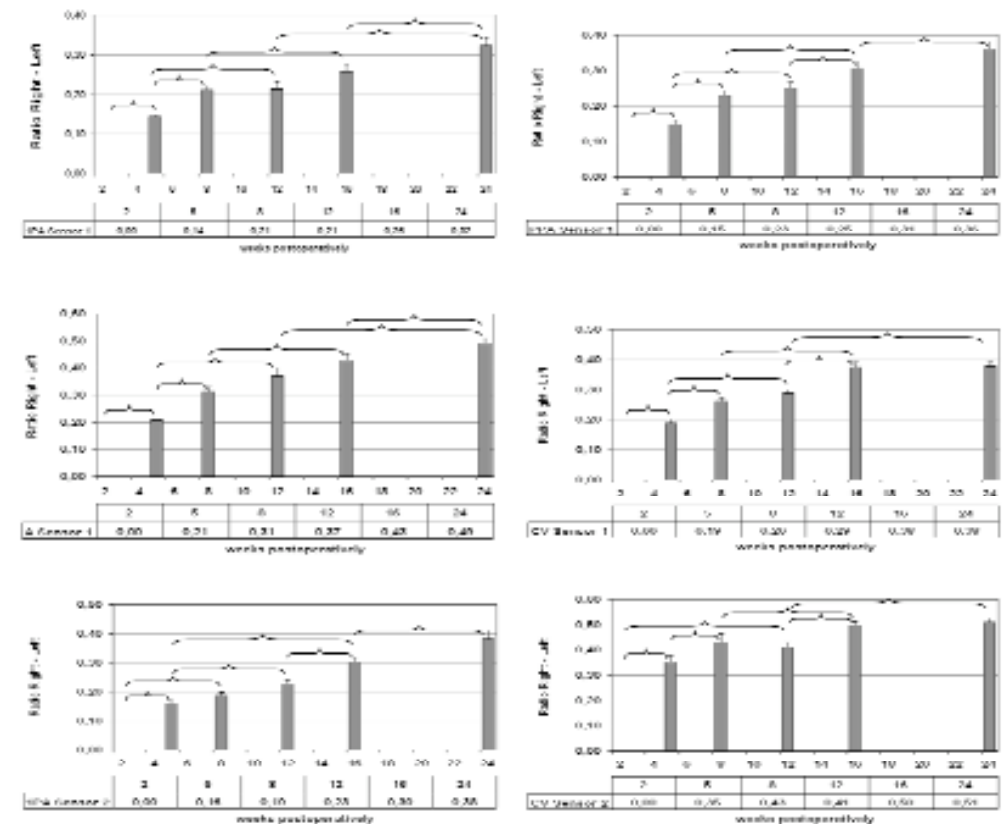


Figure 3. Recovery pattern with time after surgery of the various neurophysiological (MNG) variables, represented as right-left ratios in bars and in number below the respective point in time. Error bars represent standard errors of the mean (SEM). Accolades indicate statistically significant differences ($p < 0.05$) between adjacent or next-adjacent points in time.

variance (ANOVA)-protected least significant difference (LSD) test.

In principle, the observed changes with time may not only be caused by the regenerative process, but also by maturation of the animal. To allow assessment of normal neurophysiological changes with age, the values of the MNG outcome variables of the left (control) nerves are summarized in *Figure 4*.

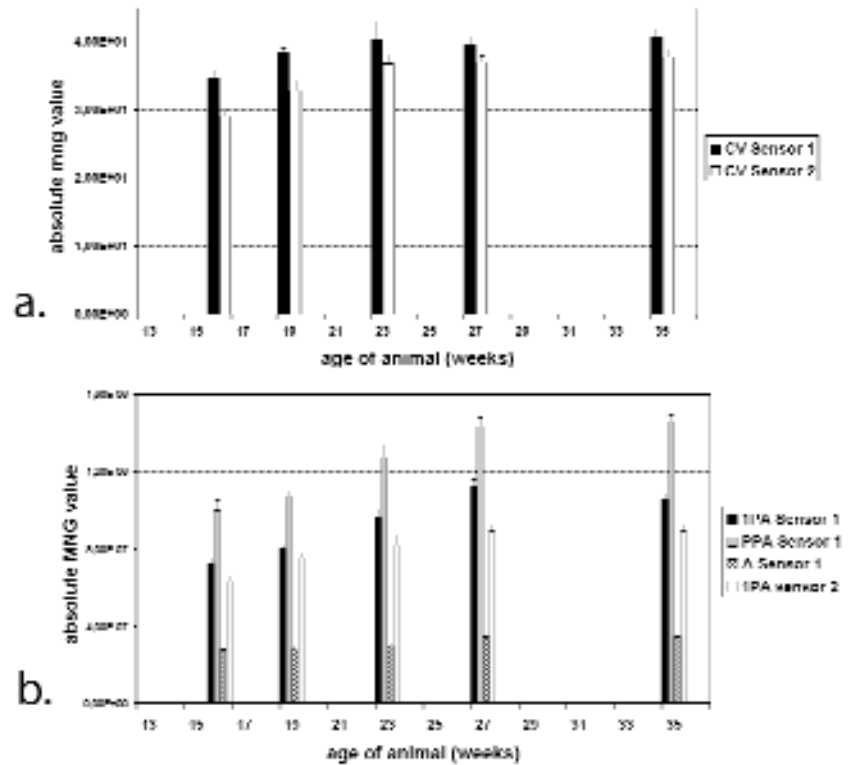
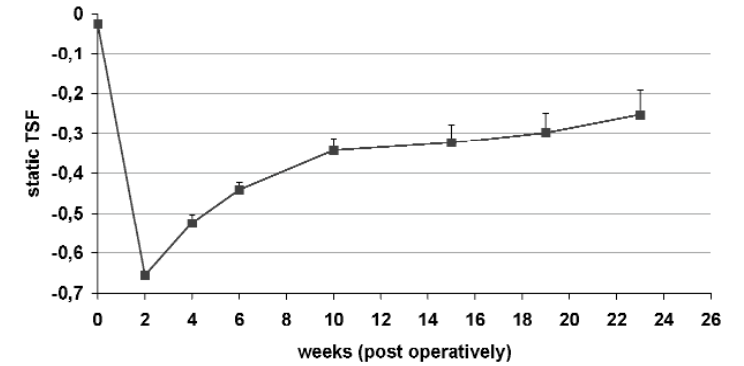


Figure 4. MNG outcome variables of healthy, right nerves as a function of age of the animal: (a) conduction velocity (CV) of sensor 1 & 2, (b) 1st peak amplitude (1PA) of sensor 1 & 2, peak-peak amplitude (PPA) and area (A) of sensor 1. Error bars represent standard errors of the mean.

FOOTPRINT ANALYSIS

The mean static TSF is shown as a function of time in *Figure 5*. The mean preoperative value was -0.026 and after 4 weeks the first distinct signs of functional recovery could be observed (-0.524).

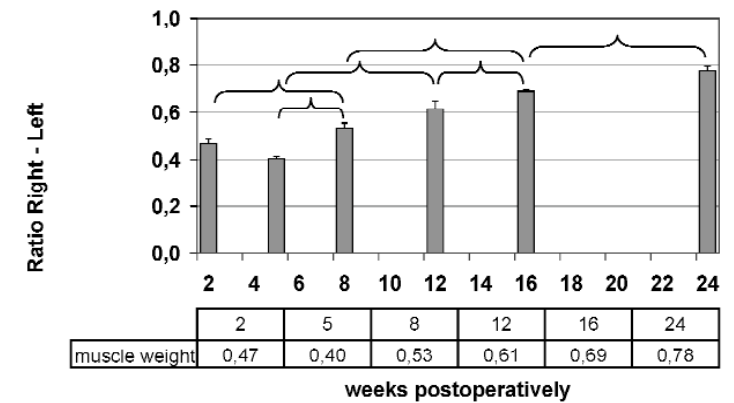
Figure 5. Mean static TSF as a function of time after surgery. Error bars represent standard errors of the mean.



MUSCLE WEIGHT

The recovery pattern of the muscle weight (MW) ratio after nerve repair is depicted in *Fig. 6*. Again, an ANOVA-protected LSD test was used to test for statistical significance of differences between means at various points in time. Five weeks postoperatively, the lowest ratio (0.40) was observed. Thereafter, recovery of MW ratio starts, and continues until at least 24 weeks after surgery (as demonstrated by the significant increase in MW ratio between 16 and 24 weeks in *Fig. 6*).

Figure 6. Right-left muscle weight ratio as a function of time after surgery. Error bars represent standard errors of the mean. Accolades indicate statistically significant differences ($p < 0.05$) between adjacent or next adjacent points in time.



CORRELATION MNG, FOOTPRINT ANALYSIS AND MUSCLE WEIGHT

Correlation analysis was performed to determine the association between the outcome variables of MNG, MW and static TSF. Spearman's correlation coefficient was calculated using data of individual animals.

Table 1 shows the correlation coefficients between MNG variables and static TSF, and between the MNG variables and MW. At two weeks, no detectable CNACs and no measurable footprints could be recorded. Therefore, week 2 is not included in the correlation analysis. Significant correlation coefficients between MNG variables and static TSF were found except for the CV of sensor 1 and 2. The correlation coefficients relat-

ing MNG variables and MW ratio (5 - 24 weeks) were all statistically significant and all higher than coefficients regarding the static TSF. No significant correlation ($r = 0.309$; $p=0.151$) was found between MW ratio and static TSF.

AUTOTOMY AND CONTRACTURES IN RELATION TO MNG AND MUSCLE WEIGHT

Autotomy and contracture caused animal exclusion from footprint analysis. A total of 12 (24%) animals displayed contractures between week 1 and week 24. Six (12%) animals displayed autotomy, all between week 2 and week 6.

To assess whether the incidence of autotomy and/or contracture is related to an altered neurophysiological feature and / or muscle weight, a Kaplan-Meier survival analysis was performed. No significant differences were found between normal rats and rats displaying autotomy and/or contractures.

		5 - 24 weeks	5 - 24 weeks
		static TSF	muscle weight
1PA sensor 1	Spearman's Correlation	0,524 **	0,658 **
	Sig. (2-tailed)	0,009	0,000
	N	24	34
PPA sensor 1	Spearman's Correlation	0,518 **	0,665 **
	Sig. (2-tailed)	0,009	0,000
	N	24	34
CV sensor 1	Spearman's Correlation	0,395	0,726 **
	Sig. (2-tailed)	0,056	0,000
	N	24	34
A sensor 1	Spearman's Correlation	0,550 **	0,705 **
	Sig. (2-tailed)	0,005	0,000
	N	24	34
1PA sensor 2	Spearman's Correlation	0,617 **	0,763 **
	Sig. (2-tailed)	0,001	0,000
	N	24	34
CV sensor 2	Spearman's Correlation	0,251	0,560 **
	Sig. (2-tailed)	0,236	0,001
	N	24	34

Table 1 Spearman's correlation coefficients, indicating the strength of the association between 1st peak amplitude (1PA), peak peak amplitude (PPA), area (A) and conduction velocity (CV) on the one hand and the static TSF and Muscle Weight on the other. Asterisks indicate a significant correlation at significance level $p < 0.05$.

Discussion

The MNG technique we used allows for robust and highly reproducible neurophysiological measurements²⁷. Consequently, more profound conclusions can be drawn on the experimental outcome after nerve injury than from previous studies where EMG or ENG (accompanied by the disadvantages mentioned in the Introduction) was used to study the electrophysiology of nerve regeneration and its relation to other outcome measures^{4,9,26}.

Here, an experimental invasive toroidal coil method is used to obtain reproducible, quantifiable MNG signals. Due to its invasive character, diagnostic clinical use of this method must be primarily sought peri-operatively. However there is a non-invasive MNG technique, SQUID (Superconducting Quantum Interference Device) based MNG, by which magnetic fields generated by CNACs inside the body, can be recorded non invasively without contact to the body. Due to the relatively long distance between nerve and sensor, this method is more prone to field disturbances and up to now the signal to noise ratio is less. Further developments of this SQUID based MNG technique may possibly allow clinical applications, i.e. non-invasive recording of magnetic fields induced by CACs in regenerating nerves. Notably, using this technique, propagating CACs and conduction blocks have already been studied in vivo^{5,6} and non-invasively in patients^{16,17}.

As mentioned earlier, in vitro ENG measurements can also be performed by placing the experimental nerve in a single or multiple compartment chamber. In contrast to MNG, where magnetic fields are measured, electrical insulation between different compartments is a strict condition when using in vitro ENG. However, a major advantage of these multiple compartment chambers is that they allow for evaluation of local drug influence on the nerve's conduction capacity²²⁻²⁴. In case of a bath solution in a single compartment chamber, special attention should be paid to the stimulating tube and the elimination of electrical artifacts^{5,6}.

Neurophysiological experiments of nerve regeneration are known to require long term study end points. EMG studies in particular, demand a long period for axons to reach the muscle^{7,18,19}. Our results, however, demonstrate that 8 weeks after nerve repair, MNG values of sensor 1 (1PA, PPA, A and CV) have already reached approximately two thirds of the values measured 24 weeks postoperatively (at 8 weeks: $\pm 25\%$ of control value; at 24 weeks: $\pm 40\%$ of control value). Thus, recovery of neurophysiological signals is primarily established within the early weeks of regeneration.

Two weeks after nerve repair, no CNACs could be recorded. This finding suggests either that axon sprouts were too immature to conduct recordable action currents, or that ingrowing axons did not reach the stimulation point 10 mm distal to the lesion at that time. The first CNACs were recorded at the subsequent measure point in time, five weeks after surgery. The high value of the CV for sensor 2 (35% of control) after just five weeks of regeneration is the result of the relatively large conducting distance proximal to the lesion. For a proper understanding of this phenomenon, we would like to stress again that we applied distal stimulation and proximal recording. Nerve fibers with

regenerating axons have a larger caliber and, hence, a higher CV in the proximal segment than in the distal segment^{12, 13, 33}. This implies that the measured CV will be a weighted average of the two CV values, with the weights determined by the lengths of the conduction distances in the distal and proximal segment. The longer proximal conduction distance to sensor 2 than to sensor 1 leads to higher CV values for the former.

It may be expected that conducting capacity of repaired nerves increases with advancing regeneration. Indeed, 1PA, PPA, A and CV of sensor 1 display an increase in time, and MNG values differ significantly between either adjacent or next- adjacent measuring points. The recovery pattern of the CV of sensor 2 does not follow such a structured increase, however. The minor collapse seen after 12 weeks may be caused by a temporal drop in conduction velocity in the proximal segment¹⁵, in combination with the aforementioned influence of a relatively large length of the proximal segment.

Electrophysiological changes in aging animals have been reported extensively^{10, 25, 30, 31, 34}. Postnatal maturation, with increasing conduction velocities of nerve fibers to reach adult values, is followed by a decrease in conduction capacity in the older animal (i.e. rat > 1 year). Our results demonstrate an increase of all MNG variables of control (healthy) nerves with increasing animal age (Fig. 4). The eldest animals in this study were 35 weeks of age (11 weeks plus 24 experimental weeks). Up to this age, conduction capacity as assessed by MNG variables continued to improve. Within this context, we emphasize the need of right - left ratios in longitudinal studies.

Previously, we reported that static footprint analysis (static TSF) is an accurate technique for the functional assessment of peripheral nerve regeneration in rats, and similar to the traditionally used Sciatic Function Index obtained by walking track analysis²⁸. Theoretically, it might be expected that the functional capacity of a regenerating nerve is related to its conduction capacity. Nevertheless, Table 1 shows that only moderate correlations were found between static TSF (function) and MNG variables (conduction capacity). The correlation between static TSF and CV of sensor 1 and 2 is low and not significant. This finding may partially be explained by, again, the relatively large influence of the proximal segment on the CV. However, it is clear that no significant relation exists between function measured by footprint analysis and conduction velocity.

The moderate correlation between function (static TSF) and conduction capacity (MNG variables) may be explained by the difference in recovery pattern as measured by static TSF and MNG. After approximately 10 weeks, static TSF recovery levels off, whereas in case of MNG, neurophysiological variables still increase significantly after this period. This plateau phase has been described in previous studies using the sciatic function index^{8, 20}. Thus, the process of axon regeneration continues, even though improvement of function appears to stagnate. It might be concluded that maturation of axons does not have consequences for final function. This would probably be true if static TSF was an adequate measure of final nerve function. However, it is more likely that spreading of the toes already can be established by ingrowth of relatively few or immature axons.

Atrophy of the gastrocnemius muscle is responsible for a decrease in muscle weight, with a minimum measured 5 weeks after transection. Subsequently, reinnervation of the muscle causes a significant increase in MW up to at least 24 weeks after surgery.

Compared to the correlation between MNG and static TSF, a relatively strong correlation was found between all neurophysiological variables (MNG) and MW (Table 1). An increase in number and / or maturation of regenerated nerve fibers is, therefore, related to the weight of the muscle. It is important to note that this relation does not provide information on muscle function. There was no significant relation between static TSF and MW. Apparently, both indirect measures are totally different derivatives of the regeneration process. For that reason, we recommend use of a more direct measure of the process such as MNG for studies of nerve fiber regeneration after injury.

For decades, footprint analysis has been promoted as an outcome measure in experimental studies on nerve regeneration^{2, 3, 8, 21}. A widely discussed drawback of this evaluation technique is the loss of animals due to autotomy and contracture of the rat's hind paw^{1, 20, 29}. Up to now, there is no experimental proof of whether animals displaying autotomy and / or contracture also demonstrate poor nerve regeneration. If so, exclusion of these animals would generate a bias. From this study, we conclude that autotomy and / or contracture are not related to a relatively poor conduction capacity of the nerve.

During the process of axon regeneration, the nerve's conduction capacity provides information on speed of axon maturation and quantity of axon ingrowth. We conclude that MNG is a sound methodology to obtain accurate, quantifiable neurophysiological signals early in the regeneration process. This study demonstrated that recovery patterns as assessed by MNG, a direct measure of axon regeneration, and by indirect measures like MW and static TSF, vary significantly. Furthermore, we demonstrated no existing relation between poor conduction capacity and autotomy / contracture, and we showed that the process of regeneration does not stop when functional recovery measured by static TSF becomes stagnant.

Acknowledgements

The authors are grateful to Erik Walbeehm for helpful and constructive advice and to Ineke Hekking for surgical assistance. This research was supported by EC grant QLK3-CT-1999-00625.

References

1. Carr MM, Best TJ, Mackinnon SE, et al: Strain differences in autotomy in rats undergoing sciatic nerve transection or repair. *Ann Plast Surg* 28:538-544, 1992
2. de Medinaceli L, Freed WJ, Wyatt RJ: An index of the functional condition of rat sciatic nerve based on measurements made from walking tracks. *Exp Neurol* 77:634-643, 1982
3. Dijkstra JR, Meek MF, Robinson PH, et al: Methods to evaluate functional nerve recovery in adult rats: walking track analysis, video analysis and the withdrawal reflex. *J Neurosci Methods* 96:89-96, 2000

4. Frykman GK, McMillan PJ, Yegge S: A review of experimental methods measuring peripheral nerve regeneration in animals. *Orthopedic Clinics of North America* 19:209-219, 1988
5. Fukuoka Y, Komori H, Kawabata S, et al: Visualization of incomplete conduction block by neuromagnetic recording. *Clin Neurophysiol* 115:2113-2122, 2004
6. Fukuoka Y, Komori H, Kawabata S, et al: Imaging of neural conduction block by neuromagnetic recording. *Clin Neurophysiol* 113:1985-1992, 2002
7. Gramsbergen A, Ijkema-Paassen J, Meek MF: Sciatic nerve transection in the adult rat: abnormal EMG patterns during locomotion by aberrant innervation of hindleg muscles. *Exp Neurol* 161:183-193, 2000
8. Hare GM, Evans PJ, Mackinnon SE, et al: Walking track analysis: a long-term assessment of peripheral nerve recovery. *Plast Reconstr Surg* 89:251-258, 1992
9. Kanaya F, Firrell JC, Breidenbach WC: Sciatic function index, nerve conduction tests, muscle contraction, and axon morphometry as indicators of regeneration. *Plast Reconstr Surg* 98:1264-1274, 1996
10. Kurokawa K, Mimori Y, Tanaka E, et al: Age-related change in peripheral nerve conduction: compound muscle action potential duration and dispersion. *Gerontology* 45:168-173, 1999
11. Kuypers PD, Gielen FL, Wai RT, et al: A comparison of electric and magnetic compound action signals as quantitative assays of peripheral nerve regeneration. *Muscle Nerve* 16:634-641, 1993
12. Kuypers PD, van Egeraat JM, Dudok v Heel M, et al: A magnetic evaluation of peripheral nerve regeneration: I. The discrepancy between magnetic and histologic data from the proximal segment. *Muscle Nerve* 21:739-749, 1998
13. Kuypers PD, van Egeraat JM, Godschalk M, et al: Loss of viable neuronal units in the proximal stump as possible cause for poor function recovery following nerve reconstructions. *Exp Neurol* 132:77-81, 1995
14. Kuypers PD, van Egeraat JM, van Briemen LJ, et al: A magnetic evaluation of peripheral nerve regeneration: II. The signal amplitude in the distal segment in relation to functional recovery. *Muscle Nerve* 21:750-755, 1998
15. Kuypers PD, Walbeehm ET, Heel MD, et al: Changes in the compound action current amplitudes in relation to the conduction velocity and functional recovery in the reconstructed peripheral nerve. *Muscle Nerve* 22:1087-1093, 1999
16. Mackert BM: Magnetoneurography: theory and application to peripheral nerve disorders. *Clin Neurophysiol* 115:2667-2676, 2004
17. Mackert BM, Curio G, Burghoff M, et al: Magnetoneurographic 3D localization of conduction blocks in patients with unilateral S1 root compression. *Electroencephalogr Clin Neurophysiol* 109:315-320, 1998
18. Maeda T, Hori S, Sasaki S, et al: Effects of tension at the site of coaptation on recovery of sciatic nerve function after neuroorrhaphy: evaluation by walking-track measurement, electrophysiology, histomorphometry, and electron probe X-ray microanalysis. *Microsurgery* 19:200-207, 1999
19. McDonald CM, Carter GT, Fritz RC, et al: Magnetic resonance imaging of denervated muscle: comparison to electromyography. *Muscle Nerve* 23:1431-1434, 2000
20. Meek MF, Den Dunnen WF, Schakenraad JM, et al: Long-term evaluation of functional nerve recovery after reconstruction with a thin-walled biodegradable poly (DL-lactide-epsilon-caprolactone) nerve guide, using walking track analysis and electrostimulation tests. *Microsurgery* 19:247-253, 1999
21. Meek MF, Van Der Werff JE, Nicolai JP, et al: Biodegradable p(DLLA-epsilon-CL) nerve guides versus autologous nerve grafts: electromyographic and video analysis. *Muscle Nerve* 24:753-759, 2001
22. Mert T, Gunes Y, Guven M, et al: Comparison of nerve conduction blocks by an opioid and a local anesthetic. *Eur J Pharmacol* 439:77-81, 2002

23. Mert T, Gunes Y, Guven M, et al: Effects of calcium and magnesium on peripheral nerve conduction. *Pol J Pharmacol* 55:25-30, 2003
24. Paparounas K, O'Hanlon GM, O'Leary CP, et al: Anti-ganglioside antibodies can bind peripheral nerve nodes of Ranvier and activate the complement cascade without inducing acute conduction block in vitro. *Brain* 122 (Pt 5):807-816, 1999
25. Schmelzer JD, Low PA: Electrophysiological studies on the effect of age on caudal nerve of the rat. *Exp Neurol* 96:612-620, 1987
26. Shen N, Zhu J: Application of sciatic functional index in nerve functional assessment. *Microsurgery* 16:552-555, 1995
27. Smit X, Stefan_de_Kool B, Walbeehm ET, et al: Magnetoneurography: recording biomagnetic fields for quantitative evaluation of isolated rat sciatic nerves. *J Neurosci Methods* 125:59-63, 2003
28. Smit X, van Neck JW, Ebeli MJ, et al: Static footprint analysis: a time-saving functional evaluation of nerve repair in rats. *Scand J Plast Reconstr Surg Hand Surg* 38:321-325, 2004
29. Sporel Ozakat RE, Edwards PM, Hepgul KT, et al: A simple method for reducing autotomy in rats after peripheral nerve lesions. *J Neurosci Methods* 36:263-265, 1991
30. Verdu E, Buti M, Navarro X: The effect of aging on efferent nerve fibers regeneration in mice. *Brain Res* 696:76-82, 1995
31. Verdu E, Ceballos D, Vilches JJ, et al: Influence of aging on peripheral nerve function and regeneration. *J Peripher Nerv Syst* 5:191-208, 2000
32. Vleggeert-Lankamp CL, van den Berg RJ, Feirabend HK, et al: Electrophysiology and morphometry of the Aalpha- and Abeta-fiber populations in the normal and regenerating rat sciatic nerve. *Exp Neurol* 187:337-349, 2004
33. Walbeehm ET, Dudok_van_Heel EB, Kuypers PD, et al: Nerve compound action current (NCAC) measurements and morphometric analysis in the proximal segment after nerve transection and repair in a rabbit model. *J Peripher Nerv Syst* 8:108-115, 2003
34. Wheeler SJ: Effect of age on sensory nerve conduction velocity in the horse. *Res Vet Sci* 48:141-144, 1990
35. Wijesinghe RS, Gielen FL, Wikswo JP: A model for compound action potentials and currents in a nerve bundle. I: The forward calculation. *Annals of Biomedical Engineering* 19:43-72, 1991
36. Wijesinghe RS, Gielen FL, Wikswo JP: A model for compound action potentials and currents in a nerve bundle. III: A comparison of the conduction velocity distributions calculated from compound action currents and potentials. *Annals of Biomedical Engineering* 19:97-121, 1991
37. Wijesinghe RS, Wikswo JP: A model for compound action potentials and currents in a nerve bundle. II: A sensitivity analysis of model parameters for the forward and inverse calculations. *Annals of Biomedical Engineering* 19:73-96, 1991
38. Wikswo JP, Jr., van Egeraat JM: Cellular magnetic fields: fundamental and applied measurements on nerve axons, peripheral nerve bundles, and skeletal muscle. *J Clin Neurophysiol* 8:170-188, 1991

5

Peripheral nerves in the rat exhibit localised heterogeneity of tensile properties during limb movement

James B. Phillips¹, Xander Smit², Neil De Zoysa¹, Andrew Afoke³, Robert A. Brown¹

- 1) Tissue Repair and Engineering Centre, University College London, United Kingdom.
- 2) Department of Plastic and Reconstructive Surgery, Erasmus MC - University Medical Centre Rotterdam, The Netherlands
- 3) University of Westminster, London, United Kingdom

J Physiol. 2004 Jun 15;557(Pt 3):879-87

Abstract

Peripheral nerves in the limbs stretch to accommodate changes in length during normal movement. The aim of this study was to determine how stretch is distributed along the nerve relative to local variations in mechanical properties. Deformation (strain) in joint and non-joint regions of rat median and sciatic nerves was measured *in situ* during limb movement using optical image analysis. In each nerve the strain was significantly greater in the joint rather than the non-joint regions (2-fold in the median nerve, 5-10 fold in the sciatic). In addition, this difference in strain was conserved in the median nerve *ex vivo*, demonstrating an in built longitudinal heterogeneity of mechanical properties. Tensile testing of isolated samples of joint and non-joint regions of both nerves showed that joint regions were less stiff (more compliant) than their non-joint counterparts with joint : non-joint stiffness ratios of 0.5 ± 0.07 in the median nerve, and 0.8 ± 0.02 in the sciatic. However, no structural differences identified at the light microscope level in fascicular/non-fascicular tissue architecture between these two nerve regions could explain the observed tensile heterogeneity. This identification of localised functional heterogeneity in tensile properties is particularly important in understanding normal dynamic nerve physiology, provides clues to why peripheral nerve repair outcomes are variable, and suggests potential novel therapeutic targets.

Keywords: peripheral nerve, biomechanics, nerve stiffness

Introduction

Peripheral nerves are remarkable tissues that not only conduct electrical impulses, but also must bend and stretch to accommodate the movement of limbs. In order to achieve this they have a complex structure consisting of bundles of neurones packed into fascicles and surrounded by connective tissue layers, the perineurium and epineurium. Both neural and connective tissue elements are tethered proximally at the spinal cord and have numerous branch points allowing neurones from a single nerve trunk to synapse with various target organs. Despite some physiological connections to surrounding tissue, nerve trunks are largely free to glide along their length within their tissue bed. However, the nerve routes through the limbs tend to lie outside the plane of movement of the joints making some degree of length change inevitable during normal function. When this ability of nerves to stretch and glide freely is compromised by adhesion to surrounding tissues, for example after surgical repair, limb movement can result in localised increases in tension leading to loss of function, pain or fibrosis^{7,12}.

Numerous studies have been undertaken to define the limits to which nerves can be stretched before their function is compromised. It is known that straining nerves beyond the physiological tension range can alter their conduction properties^{14,24} and intraneural blood flow¹¹ and can result in permanent loss of function believed to be related to a breakdown in integrity of the perineurium^{9,16}.

Identifying the maximum tension which nerves can withstand and understanding the origin of their mechanical resilience is of great importance to improving the outcome of surgical nerve repairs. Their behaviour under loading is viscoelastic and is likely to be dependent upon a number of factors such as the internal fluid pressure maintained by the impermeable perineurium¹⁰, the outer-inner layer integrity²², the number and arrangement of fascicles¹⁹, and the molecular structural elements of the extracellular matrix such as collagen and elastin^{20,21}. However, the concept that nerves are mechanically homogenous may be inappropriate and misleading since the mechanical environmental loading varies at points along the limb (relating to branch point, joint, muscle, tendon and fascia location).

Since understanding the upper limit to which nerves can be stretched is such an important clinical goal, the investigation of stretch properties within normal physiological conditions has been somewhat neglected. In particular, there is scant information available on whether increased tension generated by limb movement is focussed around the articulation, or dissipated along the full length of the nerve. The transverse heterogeneity of the nerve trunk is often discussed in terms of the contribution of different concentric anatomical layers to overall mechanical behaviour, but little is known about the presence of any longitudinal variation in these structures. Variations in the number of fascicles have been observed along the length of human nerves¹⁸ and increased fasciculation has been suggested to be a protective feature of nerves crossing joints¹⁷. Such variation could cause localised sections of tissue to exhibit distinct tensile properties, yet little regard has been paid to this possibility where studies of mechanical properties are concerned.

The aim of this study was to test the hypothesis that mechanical properties of the peripheral nerve are adapted to increased local strains resulting from joint articulation.

Here we have shown that rat median and sciatic nerves undergo increased local strain in the region of articulations. This corresponds to an area of reduced stiffness relative to a region of the same nerve away from the joint. These variations in tensile properties do not correspond to variations in the distribution of fascicles or connective tissue as determined by histology, and so are likely to be due to adapted connective tissue architecture.

Materials & Methods

Two different rat nerves were selected for the experiments by virtue of the fact that they could be exposed with minimal disruption of their relationship to surrounding tissues, and contained distinct regions which ran around joints. The first was the median nerve in the rat forelimb, which runs around the inside of the elbow (joint region) then straight along the distal part of the limb (non-joint region). The second was the sciatic nerve, which runs around the outside of the hip joint (joint region) with straight (non-joint) regions proximal and distal.

OPTICAL ANALYSIS OF MEDIAN NERVE MOVEMENT; IN SITU

Male Wistar rats (Harlan, U.K.) (200 - 250 g) were sacrificed by asphyxiation and cervical dislocation according to Home Office guidelines and dissected within 30 min post-mortem. To expose the median nerve, an incision was made midway between the biceps and the cubital fossa and extended superficially to the wrist, opening the skin and fascia down to the level of the muscles. Non nerve-related connective tissue and fat were cleared from the area using microscopic dissection until the median nerve could be observed between the proximal side of the cubital fossa and the wrist. The exposed tissue was moistened continuously with phosphate buffered saline (PBS) at room temperature. The rat was pinned to a board such that the shoulder joint was immobilised in its extended position (defined as supine, shoulder abducted 90°, wrist 0° flexion/extension, elbow at 180°). Four optical location markers were spaced evenly along the exposed nerve, shown as A, B, C and D in *fig. 1a*. The markers were 0.25 mm in diameter and were created by lightly applying Bonny's Blue tissue dye with the tip of a fine blunt glass needle. The first mark was placed midway between the distal limit of the biceps and the centre of the cubital fossa, then the other marks were made distally at 2 mm intervals with the limb in its extended position.

Following marking of the nerve the forelimb was held with the elbow extended and photographed using a microscopic digital video camera (Moritex Scopeman® 504). Images were captured to a PowerMacintosh using Openlab software (Improvision) and calibrated against a millimetre scale positioned next to the nerve. The elbow was then flexed to an angle of 90° and another image was obtained. Distances between the centre points of the optical markers were measured using the digital images to give readings accurate to 50 µm. The anatomy of the joint region was such that upon flexion marker

point A remained in the same plane as the other markers, allowing an accurate comparison to be made between the markers in the two positions. In this way the local change in length (strain) was measured across the "joint" region of the median nerve (AB) and the "non-joint" region 2 mm distal (CD) in both forelimbs of 5 rats.

OPTICAL ANALYSIS OF MEDIAN NERVE MOVEMENT; EX VIVO

In order to investigate whether region-specific stretch was due to intrinsic structure or the influence of surrounding tissue, median nerves were excised under controlled conditions (below) and tested in isolation. Rats were prepared as described above and, after marking, the median nerve was carefully mobilised by microscopic dissection. Two additional marks were placed 2 mm outside the other four and denoted O and X (*fig 1a*). The distance between O and X was measured both with the limb extended and 90° flexed using a vernier calliper. With the limb held in the extended position, the nerve was clamped at points O and X in a purpose built jig which maintained the nerve at the measured *in situ* elongated length, then the nerve was excised by transection each side of the clamp (*fig 1a, inset*). Digital images of the excised nerve were recorded as before, and the clamp gauge-length was then adjusted to the previously measured 90° flexed length, simulating the shortened nerve during flexion. Digital images were captured at the shorter length and the distances AB and CD were measured for both positions to allow calculation of strain.

OPTICAL ANALYSIS OF SCIATIC NERVE MOVEMENT

Similar experiments were carried out using the rat sciatic nerve, (i) at the 'joint region' that curves around the hip and (ii) at the 'non-joint' regions each side of this. Eight Wistar rats (female, 250-400 g) were anaesthetized by inhalation of Isoflurane and a mixture of O₂/N₂O and subsequently sacrificed by cervical dislocation. The sciatic nerve was exposed between 10 mm proximal to the hip joint and the trifurcation at mid femoral level. During dissection the nerve was not mobilised from the tissue bed. To indicate different regions on the nerve, epineurial marking sutures (10/0) were placed 3 mm apart, with the hip and knee joints positioned in 90 degrees of flexion. Four regions were marked: (A) proximal to the hip joint, (B and C) at the level of the hip joint, and (D) distal to the hip joint (*fig. 1b*). The distal edge of the tendinous insertion of the external obturator muscle was used as an anatomical landmark to determine the position of the initial marking suture between regions (B) and (C).

Images of the marked nerve were captured, with the hind leg in two different positions, using a digital video camera (Sony®, model DCR-TRV240E, Sony Corp., Japan). In position 1 the hip, knee, and ankle joints were manually flexed to 90 degrees. In position 2 the hip and knee joints were manually extended to 180°, whilst the ankle was maintained at 90° flexion. To calibrate the recorded distances, a reference measuring scale was placed alongside the nerve. Images were captured to PC using Studio DV® software (Pinnacle Systems Inc, California) and length measurements were determined using Image J (NIH). The ratio of change in length after extension against original length (strain) was calculated for each of the four regions.

REGION-SPECIFIC TENSILE TESTING

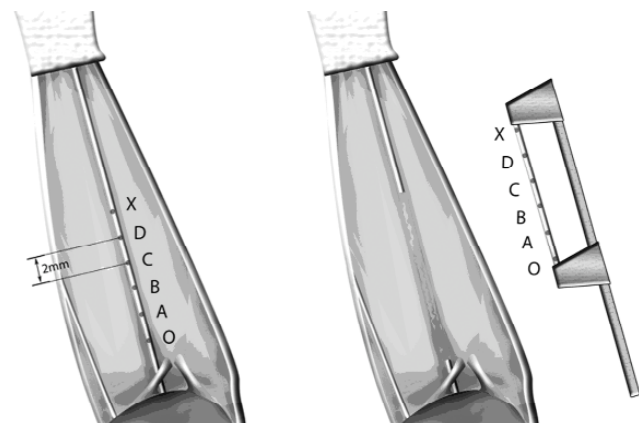


Figure 1a

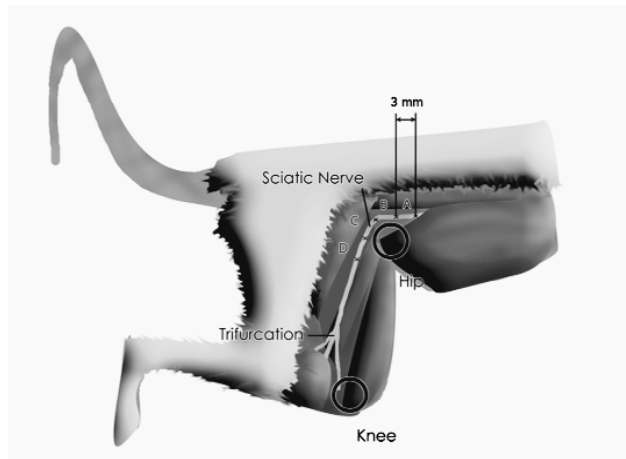


Figure 1b

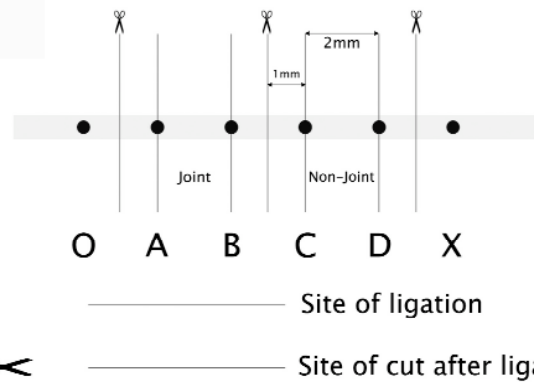


Figure 1c

Figure 1. Location of optical markings on median (A) (inset; jig for removal under native tension) and sciatic (B) nerves. (C) shows the location of ligatures and transection sites on the median nerve for tensile testing.

In addition to the optical characterisation of nerve stretch, direct tensile tests were carried out to compare the material stiffness at joint and non-joint regions of median and sciatic nerves. Three male Wistar rats were sacrificed by CO₂ inhalation followed by cervical dislocation then immediately dissected to harvest the nerves. In order to preserve the internal fluid composition of the sections of nerve, the nerves were ligated prior to transection²².

Figure 1c shows the position of the ligatures and the sites where the nerves were cut for the median nerve. The joint and non-joint sections of the nerves were carefully dissected away from the surrounding tissue and ligated using 6/0 prolene sutures (Ethicon) placed 2 mm apart (fig 1c), then excised and stored in PBS prior to tensile testing. For the sciatic nerve, the joint region was defined as a 2 mm region centred on the position defined previously for the first marking suture used in the optical analysis. The non-joint region was a 2 mm section located distally with 4 mm between the two regions. For testing, the nerve sections were clamped firmly in a jig by the regions outside the ligatures and stretched from slack to breaking point at 10 mm/min using a tensile testing machine (Testometric 220M, Testometric Co Ltd., Lancs, U.K.). Force was measured using a 10N load cell (TEDEA-Huntleigh Ltd., Cardiff, U.K.) and extension via a linear voltage differential transformer (LVDT). Force-extension signals from the transducers were digitized using an ADC-100 analogue to digital converter (Picotech Ltd., U.K.) and data were recorded on a personal computer. The data files were exported to Microsoft Excel for the production of force-extension curves. The gradient of the linear part of each force-extension curve was recorded as a measure of the stiffness of each region, and the stiffness ratio (joint stiffness/non-joint stiffness) was calculated for each nerve.

HISTOLOGICAL COMPARISON OF SITE-SPECIFIC CROSS-SECTIONAL MORPHOLOGY.

Samples of the joint and non-joint regions were harvested from fresh rat median and sciatic nerve specimens. The nerves were gently dissected out and layers of fascia connecting the nerve to surrounding tissue were trimmed away as close as possible to the outer layer of the nerve. After fixation in 4% paraformaldehyde, the sciatic nerve samples were wax embedded for routine histological sectioning and 6 µm transverse sections were stained with haematoxylin-eosin. The median nerve specimens were embedded in OCT tissue-embedding medium (Tissue-Tek®; Sakura Finetek Europe B.V., Zoeterwoude, NL) and frozen in liquid nitrogen. 8 µm cryostat sections were stained with haematoxylin-eosin. Equivalent digital micrograph images were obtained from a typical joint and non joint section of each nerve. For each section total nerve area, fascicular, and non fascicular area were determined using Adobe® PhotoShop 4.0 (Adobe Systems Inc., California) and the number of fascicles recorded. The ratio of non fascicular : total nerve area was calculated and compared between the joint and non joint region using a paired t-test.

Results

OPTICAL ANALYSIS OF DIFFERENTIAL ELONGATION

Analysis of the movement of marker points on the nerves gave an indication of how different regions responded to changes in overall length after repositioning the limbs. The change in displacement between the markers showed the strain at each nerve region. This strain is shown for the median nerve in *fig 2*. When the forelimb was moved *in situ* the nerve segment at the joint underwent more than twice the strain as the non-joint region (*fig 2a*), ($p < 0.05$). In order to establish whether this difference reflected a difference in material properties of the nerve tissue itself, or was a function of the internal limb environment, the procedure was repeated with the nerves excised (*fig 2b*). Once again the local mean deformation (strain) in the joint region was significantly greater (by a similar 2-fold factor to that *in situ*).

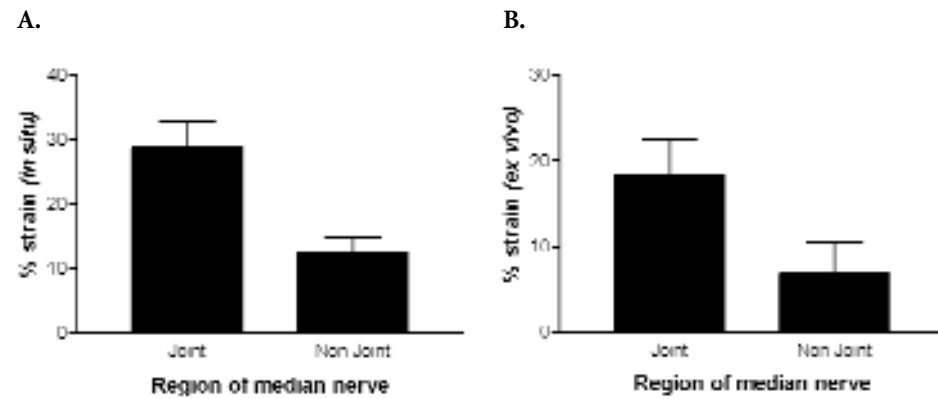


Figure 2. The joint region of the median nerve experiences more strain than the non-joint region. Median nerves were extended *in situ* by limb movement (A) or stretched after excision (B). Local strain at two regions showed the same distinctive difference both *in situ* and *ex vivo*. Data are means \pm sem, $n=5$ or 6 nerves for (A) and (B) respectively, $p = 0.02$ and 0.006 respectively (paired *t*-test).

To confirm that this site-specific difference in nerve deformation was not a special feature of the median nerve, measurements were repeated *in situ* on the sciatic nerve. In this case local anatomy made it possible to compare regions both proximal and distal to the joint region (in the median nerve the region proximal to the joint is obscured by muscle). In the sciatic nerve the joint region spanned two of the segments under test. *Fig. 3* shows that the mean strain measured over the joint was between 5 and 10 fold greater than the flanking non-joint segments. Interestingly these differences in strain between nerve segments were seen at much lower levels of total applied strain (approx 1/3 that seen in median nerve). The difference between the joint region (B) and the proximal and distal non-joint regions was significant ($p < 0.01$).

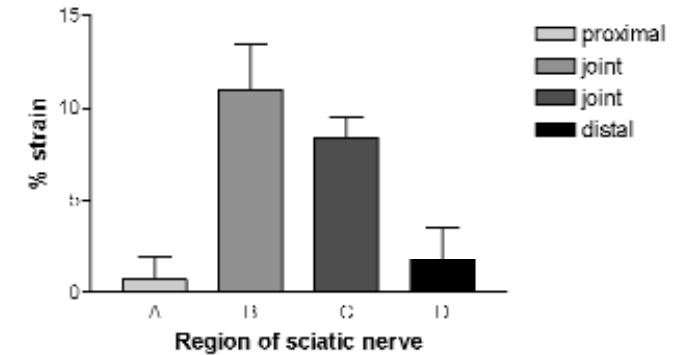
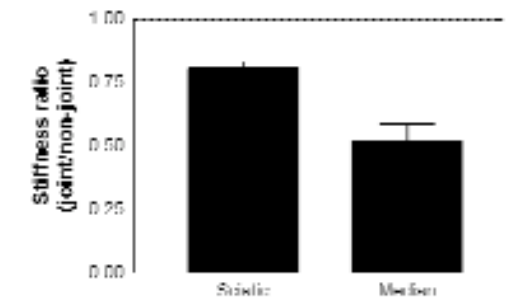


Figure 3. *In situ* strain in the sciatic nerve during flexion and extension. Four adjacent regions were monitored during flexion and extension of the rat sciatic nerve, proximal to the hip joint (A), level with the hip joint (B & C) and distal to the hip joint (D). Data shown are means \pm SEM where $n = 4$ (A,C) or 6 (B,D). One way analysis of variance (ANOVA) showed a significant difference between the means ($p < 0.01$) and Tukey's multiple comparison test showed significant differences where groups A and B or B and D were compared.

TENSILE TESTING

To compare directly the material properties of nerve tissue at joint and non-joint regions it was necessary to measure their stiffness. Force/extension curves were plotted for each region of each nerve tested, the gradient of which corresponded to the stiffness. From these data a ratio of joint : non-joint zone stiffness was obtained for each nerve (*fig 4*). In all cases the ratio was less than 1, indicating a clear trend of lower stiffness (greater compliance) in the joint segments. Mean ratio for median nerves was 0.5 ± 0.07 , and 0.8 ± 0.02 for the sciatic indicating a significantly greater stiffness at sites away from joints ($p < 0.01$, *t*-test comparing each set of experimental ratio data to null stiffness ratio of 1).

Figure 4. Stiffness ratios for joint and non-joint regions are less than 1 in both sciatic and median nerves. Stiffness ratios were calculated from the slopes of the force-extension curves obtained from stretching joint and non-joint regions of sciatic and median nerves. Data are means \pm sem, $n = 5$ (sciatic) or 6 (median). Dotted line (ratio of 1) indicates position of null stiffness ratio (i.e. no difference between regions).



HISTOLOGY

Histological examination revealed more fascicles present in the non-joint than the joint regions of the sciatic nerve, but little difference between the two regions of the median nerve (table 1). The proportion of the cross-sectional area of each nerve sample which comprised fascicular endoneurium, and that which comprised interfascicular epineurium (referred to as non-fascicular tissue) was calculated. Table 1 shows the proportion of the cross section from each nerve specimen which was made up of non-fascicular tissue compared to the total cross section (non-fascicular + fascicular tissue area). In the median nerve there was no significant difference between the proportion of non-fascicular tissue measured in the joint (0.41 ± 0.04) compared to the non-joint (0.46 ± 0.03) samples. Interestingly there was almost twice as much non-fascicular tissue in the median than the sciatic nerve by proportion. The difference between the relative areas in the sciatic nerve was significant with a mean non-fascicular tissue proportion of 0.25 ± 0.006 in the joint region and 0.36 ± 0.02 in the non-joint region ($p < 0.005$). There was no significant difference between the mean total cross sectional area at the joint and the non-joint region in either of the nerves which is consistent with the lack of branching between the regions.

Nerve	Ratio of non-fascicular area : total area		No. of fascicles joint : non-joint
	Joint region	Non-joint region	
Median nerve			
1	0.45	0.40	3 : 3
2	0.52	0.43	3 : 3
3	0.34	0.42	2 : 3
4	0.31	0.55	2 : 3
5	0.43	0.48	1 : 3
Mean (S.F.M.)	0.41 (0.04)	0.46 (0.03)	
Sciatic nerve			
1	0.24	0.29	1 : 2
2	0.23	0.30	1 : 2
3	0.26	0.37	1 : 2
4	0.23	0.40	1 : 2
5	0.27	0.36	1 : 3
6	0.24	0.43	1 : 2
Mean (S.F.M.)	0.25 (0.006)	0.36 (0.02)	

Table 1. Histological comparison of non-fascicular (connective tissue) area relative to the total nerve area in transverse sections of the joint and non-joint region of median and sciatic nerve. The difference in the mean ratio of joint vs. non joint was significant in the sciatic nerve ($p < 0.005$), but not in the median nerve using a paired *t*-test. Number of fascicles is also shown as determined for the two regions of each nerve.

Discussion

In situ experiments in both the sciatic and median nerves showed that during normal extension and flexion the joint regions underwent greater deformation than the corresponding non-joint regions. Whilst this may seem intuitive, and was suggested as likely by Sir Sydney Sunderland more than a decade ago¹⁷, it has not previously been demonstrated in an experimental system. Here we have shown quantitatively, in two different nerves in the rat, that there are regions near joints which undergo greater elongation than other areas during limb movement. However, this is not a simple function of greater loading over joints but rather reflects distinct material properties of the two zones, joint regions being inherently more compliant.

When median nerve strain was optically analysed *ex vivo*, it was found that the joint region stretched more than the non-joint region. This demonstrated that the structure of the nerve varied along its length in terms of its capacity to respond to tensile loads comparable to those generated during limb movement. This is in contrast to a previous study in which no differences could be detected in the stretch properties of different segments of median nerve harvested from human cadavers¹², although the experimental details in that study were unclear and fixation may have affected the tissue.

Here we have confirmed the presence of distinct regional heterogeneities in terms of functional tensile properties, by direct stiffness measurement in isolated tissues. This revealed that the joint regions of both nerves were more compliant than the comparator (non-joint) regions. There are a number of key differences between the sciatic and median nerve in the rat. In particular, the sciatic nerve is of greater diameter and runs around the outside of the hip joint whereas the median nerve follows the inside of the elbow joint. Also, the regions chosen for comparison in the sciatic nerve were adjacent, but more widely spaced in the median nerve. The results presented here do not seek to compare these two nerves to each other, but use each as an independent demonstration of localised heterogeneity. Since both the sciatic and the median nerve exhibit a number of branch points along their length which may influence the local mechanical environment, care was taken to ensure the regions chosen for stiffness comparison were free from branching, both by direct examination and consultation with an anatomical reference⁵.

Histological data showed that differences in stiffness cannot be explained simply by the number of fascicles present. Previous work by Sunderland and Bradley¹⁸, who used similar analyses to explore nerves in human cadavers, showed that more fascicles were present (and therefore more non-fascicular connective tissue) in regions where the nerves passed near joints, leading to the later suggestion that this was a protective feature by which vulnerable areas of nerves resisted mechanical injury¹⁷. In contrast we show here that in two regions of the rat median nerve with differences in mechanical properties there were no differences in the proportion of connective (non-fascicular) tissue between the joint and non-joint regions. In the sciatic nerve there were more fascicles (and more non-fascicular connective tissue) in the non-joint region than at the joint. This observation is opposite to that which might be predicted from Sunderland's

work on human nerves, and does not support the idea that increased fasciculation is a means by which nerves reduce strain around joints. There is no simple relationship here between morphology, connective tissue volume, and tensile properties. However, this is not unusual in biomechanics and only suggests that functional tensile testing is a more appropriate measure of the mechanical behaviour of nerves than histology.

Mechanical tension is an important issue for reconstructive surgery and nerve repair and consequently a number of studies have investigated changes in tension in human cadaveric nerves during limb movement^{1, 6, 8, 26}. Previous investigators have sought to place values on the degree to which nerves can be stretched before they become compromised through changes in conduction, blood flow, or integrity of intraneural structures^{9, 11, 13, 14, 16, 24}. These studies have failed to agree on an absolute strain-limit value, chiefly due to (i) difficulties in determining original length and disagreement on what constitutes nerve resting tension and (ii) differences in post mortem treatments (fixation, ligation, incubation etc). This study identifies a further cause in that longitudinal heterogeneity will lead to variance in tensile testing experiments unless properly controlled.

The observation that nerves exhibit longitudinal heterogeneity of material properties poses a number of intriguing questions regarding the way in which nerves are adapted to accommodate limb movement. The viscoelastic properties of nerves have been measured extensively^{3, 9, 13, 19, 23} but the key structural elements which permit this elasticity remain elusive. For many years some observers have believed nerve fibers exhibit a zigzag morphology which disappears upon stretching as the fibers straighten out. This has been related to the presence of the spiral bands of Fontana that also fade with stretching². However, the zigzag arrangement of fibers has not always been observed *in vivo*²⁵, and application of sufficient tension to straighten out the fibers *ex vivo* did not result in disappearance of the bands of Fontana, which only occurred following a further tension increase¹⁵. Earlier work by Glees⁴ identified the incisures of Schmidt-Lantermann as sites at which the myelin sheath could telescope to accommodate stretch, and proposed that this could confer stretching ability. Further investigations are required in order to investigate the properties of nerve fibers which allow them to accommodate the strain experienced by the nerve trunk. At a molecular level, elastin fibers are present throughout the tissue layers of peripheral nerves²⁰ and collagen fibers are arranged in such a way as to allow some degree of longitudinal stretch^{4, 21}. The specialised arrangement of layers of collagen fibers is likely to be the underlying structural component, in conjunction with fluid pressure, which provides the nerve with its viscoelasticity. There may also be differential movement possible between fascicle and non-fascicle elements. Further studies are planned to investigate differences in collagen architecture in different regions of a nerve which could account for the local differences in stiffness.

Another matter for consideration, which arises from these findings, is the means by which regions of differing stiffness develop. It would be interesting to examine whether reduced stiffness is an intrinsic property of nerve regions adjacent to joints or whether this property is conferred upon the nerve by movement. An understanding of this phe-

nomenon may yield important information when undertaking surgical repair of peripheral nerves. For example would movement be sufficient to decrease the stiffness of a graft at a joint region, and if not, would inappropriate local stiffness compromise the clinical outcome?

In conclusion, the results presented here demonstrate that the strain on nerves during limb movement is not equally distributed along their length, but is increased at articulations. Furthermore, the stiffness of nerve tissue varies longitudinally, with regions near joints being more compliant to tensile loading than elsewhere. However, these properties seem to result from complex tissue architecture rather than simple proportion of connective tissue or fascicular number.

Acknowledgements

The authors are grateful to Andrew McCulloch for technical assistance with the tensile testing experiments, Ellen Riem for assistance with the histology, and Professor Susan Hall for helpful comments on the manuscript. Financial support was from the EU framework 5 program in neural tissue engineering (QLK3-CT-1999-00625).

References

1. Byl C, Puttlitz C, Byl N, et al: Strain in the median and ulnar nerves during upper-extremity positioning. *J Hand Surg [Am]* 27:1032-1040, 2002
2. Clarke E, Bearn JG: The spiral nerve bands of Fontana. *Brain* 95:1-20, 1972
3. Driscoll PJ, Glasby MA, Lawson GM: An *in vivo* study of peripheral nerves in continuity: biomechanical and physiological responses to elongation. *J Orthop Res* 20:370-375, 2002
4. Glees P: Observations on the connective tissue sheaths of peripheral nerves. *J Anat* 77:153-159, 1942
5. Hebel R, Stromberg M: *Anatomy and embryology of the laboratory rat*. Wörthsee, Germany: Biomed Verlag, 1986,
6. Hicks D, Toby EB: Ulnar nerve strains at the elbow: the effect of *in situ* decompression and medial epicondylectomy. *J Hand Surg [Am]* 27:1026-1031, 2002
7. Hunter JM: Recurrent carpal tunnel syndrome, epineural fibrous fixation, and traction neuropathy. *Hand Clin* 7:491-504, 1991
8. Kleinrensink GJ, Stoeckart R, Vleeming A, et al: Mechanical tension in the median nerve. The effects of joint positions. *Clin Biomech (Bristol, Avon)* 10:240-244, 1995
9. Kwan MK, Wall EJ, Massie J, et al: Strain, stress and stretch of peripheral nerve. Rabbit experiments *in vitro* and *in vivo*. *Acta Orthop Scand* 63:267-272, 1992
10. Low P, Marchand G, Knox F, et al: Measurement of endoneurial fluid pressure with polyethylene matrix capsules. *Brain Res* 122:373-377, 1977
11. Lundborg G, Rydevik B: Effects of stretching the tibial nerve of the rabbit. A preliminary study of the intraneural circulation and the barrier function of the perineurium. *J Bone Joint Surg Br* 55:390-401, 1973

12. Millesi H, Zoch G, Rath T: *The gliding apparatus of peripheral nerve and its clinical significance. Ann Chir Main Memb Super* 9:87-97, 1990
13. Millesi H, Zoch G, Reihnsner R: *Mechanical properties of peripheral nerves. Clin Orthop Relat Res* 76-83, 1995
14. Ochs S, Pourmand R, Si K, et al: *Stretch of mammalian nerve in vitro: effect on compound action potentials. J Peripher Nerv Syst* 5:227-235, 2000
15. Pourmand R, Ochs S, Jersild RA, Jr.: *The relation of the beading of myelinated nerve fibers to the bands of Fontana. Neuroscience* 61:373-380, 1994
16. Rydevik BL, Kwan MK, Myers RR, et al: *An in vitro mechanical and histological study of acute stretching on rabbit tibial nerve. J Orthop Res* 8:694-701, 1990
17. *Sunderland: Nerve Injuries and their Repair. A Critical appraisal. London: Churchill Livingstone, 1991, pp 213-219 p*
18. Sunderland S, Bradley KC: *The cross-sectional area of peripheral nerve trunks devoted to nerve fibers. Brain* 72:428-449, 1949
19. Sunderland S, Bradley KC: *Stress-strain phenomena in human peripheral nerve trunks. Brain* 84:102-119, 1961
20. Tassler PL, Dellon AL, Canoun C: *Identification of elastic fibres in the peripheral nerve. J Hand Surg [Br]* 19:48-54, 1994
21. Ushiki T, Ide C: *Three-dimensional organization of the collagen fibrils in the rat sciatic nerve as revealed by transmission- and scanning electron microscopy. Cell Tissue Res* 260:175-184, 1990
22. Walbeehm ET, Afoke A, de Wit T, et al: *Mechanical functioning of peripheral nerves: linkage with the "mushrooming" effect. Cell Tissue Res* 316:115-121, 2004
23. Wall EJ, Kwan MK, Rydevik BL, et al: *Stress relaxation of a peripheral nerve. J Hand Surg [Am]* 16:859-863, 1991
24. Wall EJ, Massie JB, Kwan MK, et al: *Experimental stretch neuropathy. Changes in nerve conduction under tension. J Bone Joint Surg Br* 74:126-129, 1992
25. Williams PL, Hall SM: *In vivo observations on mature myelinated nerve fibres of the mouse. J Anat* 107:31-38, 1970
26. Wright TW, Glowczewskie F, Jr., Cowin D, et al: *Ulnar nerve excursion and strain at the elbow and wrist associated with upper extremity motion. J Hand Surg [Am]* 26:655-662, 2001

6

Reduction of neural adhesions by biodegradable autocrosslinked hyaluronic acid gel after injury of peripheral nerves: an experimental study

Xander Smit¹, Johan W. van Neck¹, Andrew Afoke² and Steven E.R. Hovius¹

- 1) Department of Plastic and Reconstructive Surgery, Erasmus MC - University Medical Center Rotterdam, The Netherlands
- 2) Center for Tissue Engineering Research, University of Westminster, London, UK

J Neurosurg. 2004 Oct;101(4):648-52.

Abstract

Object. Adhesion formation is a serious problem in peripheral nerve surgery, frequently causing dysfunction and pain. The authors aimed to develop an objective biomechanical method of quantifying nerve adhesions and to use this technique for the evaluation of the efficacy of an autocrosslinked hyaluronic acid (HA) gel as an antiadhesion therapy.

Methods. Thirty-three female Wistar rats underwent dissection, crush injury, or transection plus repair of the sciatic nerve. The nerves were or were not treated with the HA-gel. Six weeks after surgery, the adhesions formed were assessed by measuring the peak force required to break the adhesions over a standardized area. Results of biomechanical measurements demonstrated that the peak force significantly increased as the severity of the injury increased. After using the HA gel to treat the nerve, the peak force was significantly reduced in rats with any of the three types of injuries; peak force decreased by 26% in the animals in the dissection group, 29% in the crush injury group, and 38% in the transection and repair group, compared with the untreated animals.

Footprint analysis demonstrated an acceleration of static Toe Spread Factor (TSF) recovery after crush injury by using the gel.

Conclusions. The biomechanical method described is an objective, quantitative technique for the assessment of nerve adherence to surrounding tissue. It will be a valuable tool in future studies on antiadhesion therapies. Furthermore, HA-gel significantly reduces nerve adhesions after different types of nerve injuries and accelerates static TSF recovery after nerve crush injury.

Keywords: peripheral nerve, adhesion, hyaluronic acid, peak force, rat

Introduction

The formation of extraneural fibrosis often occurs after trauma to a peripheral nerve. The severity of the injury—varying from local tissue damage to total nerve transection—affects the migration and proliferation of fibroblasts and the deposition of extraneural collagen. Over time, collagen fibers enveloping the nerve can contract, increasing the risk of compression neuropathies that can be accompanied by dysfunction and pain. Furthermore, when a nerve adheres to its surrounding tissue, limb movement and muscle contractions may cause painful traction neuropathies^{20,30}.

The current gold standard in treating compression and traction neuropathies is surgical neurolysis, optionally followed by a local muscle flap, fat grafts, vein wrapping, or a temporarily placed silicone sheet⁶. Recently published experimental study data have revealed that different devices reduce extraneural scarring after peripheral nerve surgery^{2,17,25,26}; however, these preclinical studies have not yet led to an established antiadhesion therapy in peripheral nerve repair.

The assessment of nerve adhesions in experimental models is complicated. The staining of collagen fibers is semiquantitative at best, and the fiber architecture does not allow for quantification at all. According to the literature, the most accepted method of assessing nerve adhesions is through surgical evaluation of the wound; that is, an investigator scores the adhesions according to the difficulty experienced during nerve dissection^{17,24-26}. To our knowledge, there is currently no objective, validated method of quantifying nerve adhesions.

Hyaluronic acid is a glycosaminoglycan in the extracellular matrix in which it plays an important role in many tissue repair biological processes⁹ and has proven to have antiadhesion effects^{7,18}. Fetal wounds heal without scarring probably due to a persistently high concentration of HA in the wound, which is not the case in adults, in whom HA is rapidly degraded²².

HA-gel (Hyaloglide, Fidia Advanced Biopolymers Srl, Abano Terme, Italy) is a viscous hydrogel developed as an antiadhesion device. It is obtained through the chemical modification of HA. Crosslinking the polysaccharides of HA molecules creates a high-viscosity gel and hampers fast metabolic degradation of HA¹². The same modified HA molecules have proven to reduce adhesions in gynaecological and intra abdominal surgery, in which they are known as autocrosslinked polysaccharides (ACP series).^{4,11,12,27}

In this study we described a novel biomechanical method to quantify nerve tethering to adjacent tissue. By measuring the peak force required to break adhesions between the nerve and surrounding tissue, we examined the efficacy of HA-gel in reducing nerve adhesions in different types of injury to rat sciatic nerves. We also studied the effect of HA-gel on the recovery of function after nerve trauma.

Materials & Methods

PREPARATION OF MATERIAL

The HA-gel was obtained by an autocrosslinking reaction between the carboxyl and hydroxyl groups of the same and / or different HA molecules without insertion of a foreign molecule. Hyaluronic acid was isolated from bacteria by fermentation. The gel was prepared by hydration of the crosslinked HA molecules at a 6% concentration and steam sterilized in 2-ml glass syringes.

SURGICAL PROCEDURE

All procedures for the care and use of laboratory animals were conducted in accordance with the guidelines outlined by the Experimental Animal Committee of the Erasmus MC Rotterdam. Thirty-three female Wistar rats weighing approximately 200 g were anesthetized by inhalation of isoflurane and a mixture of O₂/N₂O. The sciatic nerve was exposed through a gluteal muscle-splitting incision.

To mimic neurolysis (dissection group, five animals), the nerve was bilaterally mobilized in the mid thigh over an area of 15 mm proximal from the trifurcation of the sciatic nerve. Two 10-0 epineural sutures (Ethylon; Ethicon, Inc., Somerville, NJ) were placed to mark a standardized 10-mm nerve segment. The right nerve was treated with HA-gel and the left nerve was not.

In the crush injury group (crush group, 14 animals), only the right nerve was mobilized in the mid thigh over an area of 15 mm proximal from the trifurcation. Two 10-0 epineural sutures were placed to mark a standardized 10-mm nerve segment. Using a surgical needle holder, crush trauma was induced by applying a standardized force (57.5 N) for 30 seconds to the middle 5 mm of the marked nerve segment. Seven experimental animals were treated with HA-gel, whereas seven control animals did not receive treatment.

In the transection group (14 rats), animals underwent total nerve transection and repair. After mobilizing the right nerve in the mid thigh over an area of 15 mm proximal from the trifurcation, two 10-0 epineural sutures were placed to mark a standardized 6-mm nerve segment. Note that the nerve segment in animals in the transection group was reduced from 10 to 6 mm to account for the weakness of the suture line in the repaired nerve vis á vis the adhesion strength. In a pilot study in untreated animals, we observed that the pull-out force due to adhesion was in some cases greater than the strength of the suture line.

The marked nerve segment was transected in the middle and immediately repaired under magnification by using four to six 10-0 epineural sutures. Seven experimental animals were treated with HA-gel, and seven control animals were not treated.

The HA-gel was applied at room temperature by using a sterile syringe and a cannula. Approximately 0.4 ml was used to envelope the 15-mm mobilized nerve area completely with a layer of gel. After the procedure, the muscle septum and skin were closed using 5-0 Vicryl (Ethicon, Inc.). Following surgery, animals were housed in pairs and had access to food and water ad libitum.

ANIMAL INSPECTION

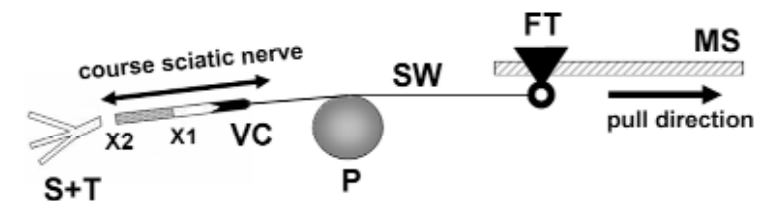
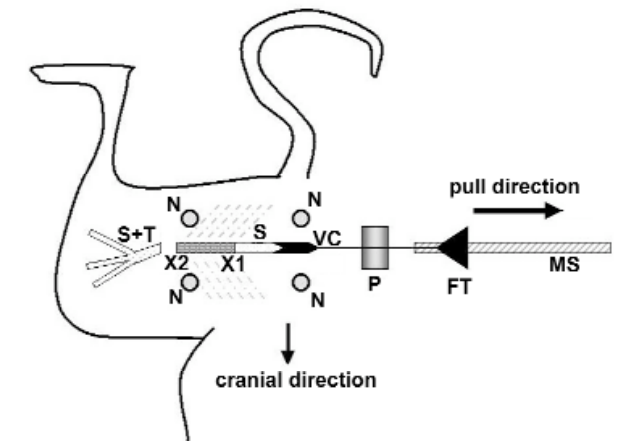
On a daily basis, all wounds were inspected and scored for wound dehiscence and infection.

PEAK PULL-OUT FORCE MEASUREMENTS

To evaluate the degree of nerve tethering to surrounding tissue, the peak force required to break adhesions between the marked nerve segment and its surrounding tissue was measured. Six weeks after surgery, the animals were anesthetized by inhalation of isoflurane as well as a mixture of O₂/N₂O and were subsequently killed by cervical

Figure 1. Schematics (upper, top view and lower, side view) and photograph (center, top view) demonstrating the experimental setup for biomechanical measurements. The shaded zone (upper) represents the standardized area over which the adhesions were broken.

FT = force transducer;
MS = motorized spiral;
N = needle; P = pulley;
S = proximal part of sciatic nerve;
S+T = distal part of sciatic nerve and trifurcation;
VC = vascular clamp;
X1 and X2 = marking sutures.



dislocation. Sciatic nerves were dissected proximally and distally from the two epineural sutures (marked previously X1 and X2 in Fig. 1). By dissecting in this way, the standardized nerve segment remained attached to its surrounding tissue. The distal nerve end was then transected at the level of the distal epineural suture initially marked (X2). The proximal nerve end was transected 10 mm proximal from the proximal epineural suture (X1).

Immobilization of the rat leg was accomplished by pinning down the upper hind portion of the leg with 19-gauge needles (Sterican; B. Braun Mesungen AG, Melsungen, Germany). The proximal nerve segment was held tightly with a stiff vascular clamp and interconnected to a force transducer by using a silver wire suture (Fig. 1 upper and center). A pulley was used to align the course of the sciatic nerve with the pull direction (Fig. 1 lower). Measurements in animals in the dissection and crush groups were obtained using a force transducer with a range of 0 to 500 g (#52-9503; Harvard Apparatus, Inc., Holliston, MA); measurements in the transection group were performed using a force transducer with a range of 0 to 2000 g (7500 series; AIKOH Engineering Co., Ltd., Nagoya, Japan). The force transducer was connected to a motorized drive with a constant extension rate of 29 mm/minute. The peak force required to pull the nerve segment out of its tissue bed was recorded.

To obtain a baseline value of the pull-out force related to the natural attachments of the sciatic nerve, peak force measurements were also obtained for the uninjured contralateral nerve in the animals in the crush group. Given that no marking sutures could be placed on these nerves, a measuring rod of 10 mm was used to determine the standardized area, which remained attached to adjacent tissue prior to the peak force measurements.

FOOTPRINT ANALYSIS

To obtain static footprints^{5,29}, a Plexiglas runway (10 x 15 x 100 cm) was used with a mirror placed under the runway at an angle of 45°. This way, a split screen provided a lateral and a plantar view of the rat. Recordings were made of the hind feet using a digital video camera (Sony®, model DCR-TRV240E, Sony Corp., Japan) on a stand positioned at 200 cm from the runway.

In the crush group footprints were obtained pre operatively and at 1, 7, 14, 17, 21, 24, 28, 35 and 42 days post operatively.

Static footprints were obtained by recording at least four occasional rest periods. Three separate images of the operated (O) and non-operated (N) foot were loaded on a personal computer using commercial software (Studio DV®, version 1.1.0.15, Pinnacle Systems Inc, California). From the digitized footprints the distance between the first and fifth toe (Toe Spread; TS) could be measured with the measure tool in Adobe® PhotoShop 4.0 (Adobe Systems Inc., California). The averaged distance of three measurements was used to calculate the following factor:

$$\text{Static Toe Spread Factor (TSF)} = (\text{OTS} - \text{NTS}) / \text{NTS}$$

Results

ANIMAL INSPECTION

No animal in any of the three injury groups displayed wound dehiscence or wound infections. None of the animals was lost during the study.

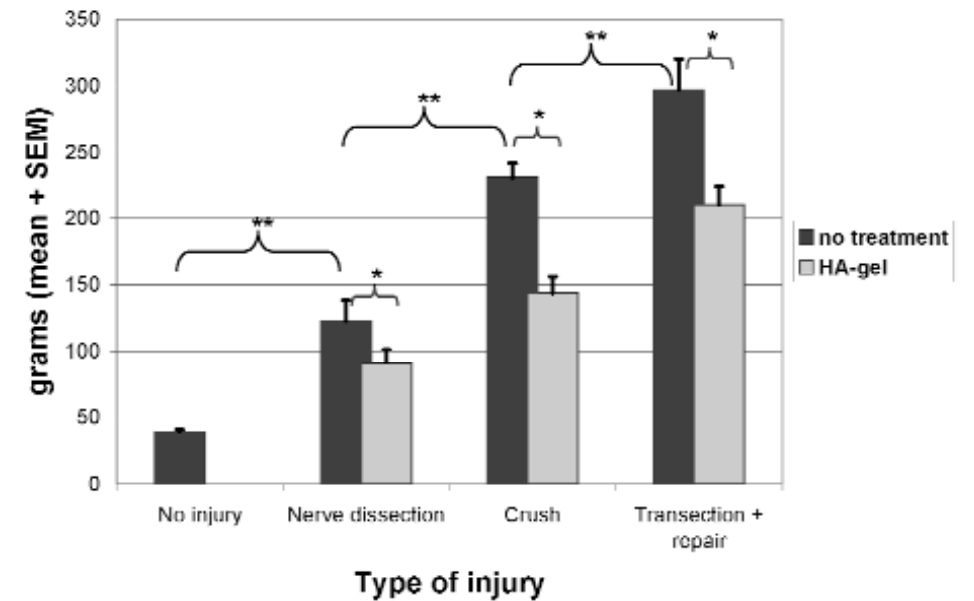


Figure 2. Bar graph illustrating the results of peak force measurements. The vertical axis represents the force required to break adhesions. Double asterisks indicate a significant difference ($p < 0.04$) between the various injury groups without treatment. In all injury groups, the single asterisk represents a significant decrease in the required pull-out force ($p < 0.02$) in gel treated animals. White bars indicate gel-treated animals; black bars represent untreated animals.

PEAK PULL-OUT FORCE MEASUREMENTS

The pull-out force required in the uninjured contralateral nerves in animals in the crush group was 38.83 ± 1.69 g (mean \pm standard error of the mean), indicating the force necessary to break the natural attachments of a nerve to its surrounding issue. This pull-out force was used as the control baseline value.

The more severe the nerve trauma, the greater the mean pull-out force required to detach the nerve (Fig. 2). The pull-out force significantly increased to 122.56 ± 15.47 g (Student t-test, $p = 0.005$) in the untreated animals in the dissection group. In animals in the crush and transection groups, the mean pull-out forces also significantly increased to 230.27 ± 11.59 g (Student t-test, $p < 0.001$) and 297.14 ± 23.06 g (Student t-test, $p = 0.03$), respectively.

When the HA-gel was applied to the nerve, a significant reduction in the pull-out

force occurred in all three injury groups (Fig. 2). In the dissection group, the pull-out force required in the gel-treated animals was reduced by 26% (122.56 ± 15.47 g in the untreated rats compared with 90.68 ± 10.24 g in the treated rats; paired t-test, $p = 0.015$). In the crush group there was a decrease of 38% (230.26 ± 11.59 g in untreated rats compared with 143.54 ± 12.50 g in the treated rats; Student t-test, $p < 0.01$), and in the transection group there was a decrease of 29% (297.14 ± 23.06 g in untreated rats compared with 210.00 ± 13.63 g in treated rats; Student t-test, $p < 0.01$). In the transection group, the pull-out force caused suture line ruptures in two of seven control animals and one of seven gel-treated animals.

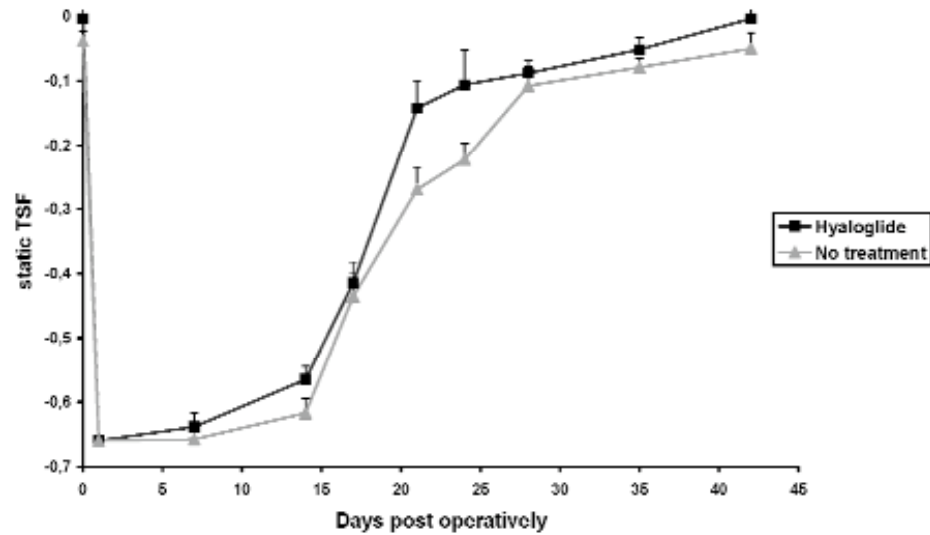


Figure 3. Functional recovery after nerve crush injury assessed by static Toe Spread Factor. The black line indicate gel treated animals; the grey line represents untreated animals.

FOOTPRINT ANALYSIS

Fig. 3 shows the static TSF over time of the crush injury group. The gel treated animals expose a higher static TSF from 7 to 42 days after surgery. At day 21 and 24 the difference in functional loss is the most distinct. Multivariate tests of repeated measures demonstrate a significant difference between the two recovery patterns ($p=0.039$).

Discussion

In this study, we described the use of a biomechanical model to quantify the degree of nerve adherence to surrounding tissue in an experimental setting. Our peak force model was used to demonstrate the antiadhesion effect of HA-gel applied following peripheral nerve trauma. Besides a reduction in nerve adhesions, an acceleration of function recovery is established using the gel.

In a non traumatized nerve, a minimal force is necessary to break the physiological attachments of the nerve to surrounding tissue elements. Sunderland³⁰ stated that trauma of increasing severity in turn affects the tissues and structures forming the bed of the nerve. Damage to the nerve through dissection, crush, or transection plus repair will cause more fibroblast activity, leading to more collagen connections between the nerve and the tissue bed. Using our method, we were able to quantify this increase in adhesions. The peak force measurements demonstrated that with an increasing severity of trauma, a greater force was required to pull the nerve out of its tissue bed.

The pull-out force provides a quantitative outcome that is related to the most rigid collagen connections. In experimental tendon research, the pull-out strength has frequently been used as a measure for tendon adhesions^{10, 19, 33}. The same biomechanical principle has been used to assess postlaminectomy adhesions in a dog study¹. To determine the effect of free fat grafts on perineural scarring after epineurectomy, the stiffness (that is, the force required to distract the nerve one unit of distance) of the rat sciatic nerve was recorded¹⁵. Because the measured stiffness is also dependent on scarring of surrounding tissue, it does not provide an absolute measure of the strength of the scar connections between nerve and surrounding tissue. In a recent study on the prevention of nerve adhesion, the force required to avulse the nerve at a 45° angle to the neural bed was measured²¹. Unfortunately, no specifics on the standardization of the nerve length were provided. In contrast to other researchers, we successfully validated our standardized method by assessing nerve adherence after various types of injury. The sensitivity of this model allowed for discrimination in the degree of nerve adhesion between not only control and gel treated animals, but also between different injury groups.

In previous studies on antiadhesion therapies in peripheral nerve surgery^{2, 17, 24-26}, adhesions were scored based on the difficulty of surgical dissection by using a numerical grading scheme introduced by Petersen, et al.²⁶. The outcome of this scoring system is not completely quantitative, and despite blinded and randomized evaluation, a numerical grading system is subjective and dependent on the investigator assigning the scores. These factors will negatively influence inter observer variability. Another method to evaluate the formation of fibrosis involves staining of collagen fibers, providing a descriptive characterization of the formed adhesions. The degree of adherence depends mainly on the architecture of the collagen fibers, which cannot be quantified by histological sections.

From our pilot study in animals that had undergone transection plus repair, it appeared that 6 weeks after surgery the strength of the adhesions over the 10-mm area was in some cases stronger than the strength of the suture line, thus causing failure

strain at the suture line. Therefore, the standardized area over which the adhesions formed would be broken was set at 6 mm in the transection group (compared with 10 mm in the other two injury groups). When analyzing the increase in the required pull-out force in relation to the injury type, the force necessary to break adhesions over a 10-mm area will be even greater in the transection group. Note that the required pull-out force for the three types of injuries could be normalized by dividing the pull-out force by the length of injury involved; however, we decided against this method because it is not known whether the pull-out force follows a linear pattern.

By using the HA-gel, a significant reduction in pull-out force was established after nerve dissection, crush injury, and transection plus repair (26, 29, and 38%, respectively). This reduction indicates that fewer (rigid) connections were formed between the nerve and its surrounding tissue bed.

During the active phase of wound repair, the reduction of adherence between different tissue layers can be approached at two levels. From a mechanical point of view, contact should be avoided between the nerve and its surrounding tissue^{3,28}. From a cellular point of view, proliferation of fibroblasts and/or the production of collagen by these fibroblasts should be diminished¹⁶. We hypothesize that HA-gel affects both mechanisms of action. The HA-gel is highly viscous and can serve as a biodegradable barrier to keep the injured nerve physically separated from adjacent tissue. Furthermore, after slow deesterification of the molecules, liberated HA may have a cellular antiadhesion effect at the injury site. Fetal wounds are known to heal without scarring, likely due to the high concentration of HA throughout the entire course of healing. In adults, however, the rich HA state exists only in the early phase of wound healing²². The slow metabolic degradation of the crosslinked HA molecules provides a sustained level of HA within the injured site. Although the adhesion-reducing effect of HA has been demonstrated at the cellular level^{7-9, 13, 18, 21, 22}, the exact mechanism of action remains unclear.

Peri operative application of HA diminished nerve adhesion after neurolysis in a rabbit model²¹. This effect was present only if the nerve and surrounding tissue were immersed in HA during the entire neurolysis procedure, however. In the present study, we demonstrated that HA-gel effectively reduces nerve adhesions after different types of injury without the need for precoating, thereby enlarging the field of application.

During the last few years, biomaterials like ADCON-T/N (a carbohydrate polymer gel)^{25,26}, human amniotic fluid²⁴, aprotinin (proteinase inhibitor)¹⁷, and HA-CMC membrane (a mixture of HA and carboxymethylcellulose)² have been studied for their antiadhesion effects in peripheral nerve surgery. Researchers in these studies have described a significant reducing effect on nerve adhesions for each of the agents studied. Partly due to differences in animal type, injury type, and time of healing, it was impossible to compare the outcomes of these investigations, however. The current study differs from others in that it offers an objective, quantitative method of measurement rather than a qualitative score obtained by histological analysis and/or graded dissection. Our biomechanical technique allows for a quantitative study to compare the efficacy of different antiadhesion therapies.

Footprint analysis in the crush group shows that the gel treated animals approach

full function recovery on an earlier time point compared to the non treated animals. No end point difference is seen between the sub groups as complete function recovery is expected six weeks after nerve crush injury^{5,14,31}. The evaluation of function does not provide an exclusive outcome measure. The results shown, do not discriminate between an increase of ingrowing axons, a faster ingrowth of axons or an improved function of the nerve due to less adhesions.

HA has histologically proven to enhance neural regeneration in combination with NGF in a gap model²³. Furthermore, slow release of HA in a gap model demonstrated to increase conduction velocity and axon counts³². This does not necessarily explain the accelerating effect of the HA based gel on function recovery after nerve crush injury.

Conclusions

We demonstrated that the peak force model described is an objective method of quantifying nerve adherence to surrounding tissue. It is a valuable tool for future studies on antiadhesion therapies in peripheral nerve surgery. Furthermore, we demonstrated a significant reducing effect on nerve adhesions when using HA-gel after different types of peripheral nerve injury. Also, acceleration in function recovery was seen after nerve crush injury. A clinical study is needed to confirm the adhesion-reducing effect and to determine the overall effect on a patient's recovery.

Acknowledgements

This research was supported by European Committee Grant No. QLK3-CT-1999-00625.

Disclaimer

None of the authors has a financial interest in Hyaloglide.

References

1. Abitbol JJ, Lincoln TL, Lind BI, et al: Preventing postlaminectomy adhesion. A new experimental model. *Spine* 19:1809-1814, 1994
2. Adanali G, Verdi M, Tuncel A, et al: Effects of hyaluronic acid-carboxymethylcellulose membrane on extra-neural adhesion formation and peripheral nerve regeneration. *J Reconstr Microsurg* 19:29-36, 2003
3. Arnold PB, Green CW, Foresman PA, et al: Evaluation of resorbable barriers for preventing surgical adhesions. *Fertil Steril* 73:157-161, 2000

4. Belluco C, Meggiolaro F, Pressato D, et al: Prevention of postsurgical adhesions with an autocrosslinked hyaluronan derivative gel. *J Surg Res* 100:217-221, 2001
5. Bervar M: Video analysis of standing—an alternative footprint analysis to assess functional loss following injury to the rat sciatic nerve. *J Neurosci Methods* 102:109-116, 2000
6. Botte MJ, von Schroeder HP, Abrams RA, et al: Recurrent carpal tunnel syndrome. *Hand Clin* 12:731-743, 1996
7. Burns JW, Skinner K, Colt J, et al: Prevention of tissue injury and postsurgical adhesions by precoating tissues with hyaluronic acid solutions. *J Surg Res* 59:644-652, 1995
8. Burns JW, Skinner K, Colt MJ, et al: A hyaluronate based gel for the prevention of postsurgical adhesions: evaluation in two animal species. *Fertil Steril* 66:814-821, 1996
9. Chen WY, Abatangelo G: Functions of hyaluronan in wound repair. *Wound Repair Regen* 7:79-89, 1999
10. Constantinescu MA, Greenwald DP, Amarante MT, et al: Effects of laser versus scalpel tenolysis in the rabbit flexor tendon. *Plast Reconstr Surg* 97:595-601, 1996
11. De Iaco PA, Muzzupapa G, Bigon E, et al: Efficacy of a hyaluronan derivative gel in postsurgical adhesion prevention in the presence of inadequate hemostasis. *Surgery* 130:60-64, 2001
12. De Iaco PA, Stefanetti M, Pressato D, et al: A novel hyaluronan-based gel in laparoscopic adhesion prevention: preclinical evaluation in an animal model. *Fertil Steril* 69:318-323, 1998
13. Deveci M, Ozturk S, Kopal C, et al: Effect of hyaluronan on adult and fetal fibroblast proliferation and collagen synthesis: in vitro study. *Eur J Plast Surg* 24:222-227, 2001
14. Dijkstra JR, Meek MF, Robinson PH, et al: Methods to evaluate functional nerve recovery in adult rats: walking track analysis, video analysis and the withdrawal reflex. *J Neurosci Methods* 96:89-96, 2000
15. Dumanian GA, McClinton MA, Brushart TM: The effects of free fat grafts on the stiffness of the rat sciatic nerve and perineural scar. *J Hand Surg [Am]* 24:30-36, 1999
16. Gomel V, Urman B, Gurgan T: Pathophysiology of adhesion formation and strategies for prevention. *J Reprod Med* 41:35-41, 1996
17. Gorgulu A, Imer M, Simek O, et al: The effect of aprotinin on extraneural scarring in peripheral nerve surgery: an experimental study. *Acta Neurochir (Wien)* 140:1303-1307, 1998
18. Hagberg L, Gerdin B: Sodium hyaluronate as an adjunct in adhesion prevention after flexor tendon surgery in rabbits. *J Hand Surg [Am]* 17:935-941, 1992
19. Hatano I, Suga T, Diao E, et al: Adhesions from flexor tendon surgery: an animal study comparing surgical techniques. *J Hand Surg [Am]* 25:252-259, 2000
20. Hunter JM: Recurrent carpal tunnel syndrome, epineural fibrous fixation, and traction neuropathy. *Hand Clin* 7:491-504, 1991
21. Ikeda K, Yamauchi D, Osamura N, et al: Hyaluronic acid prevents peripheral nerve adhesion. *Br J Plast Surg* 56:342-347, 2003
22. Longaker MT, Harrison MR, Crombleholme TM, et al: Studies in fetal wound healing: I. A factor in fetal serum that stimulates deposition of hyaluronic acid. *J Pediatr Surg* 24:789-792, 1989
23. Mohammad JA, Warnke PH, Pan YC, et al: Increased axonal regeneration through a biodegradable amniotic tube nerve conduit: effect of local delivery and incorporation of nerve growth factor/hyaluronic acid media. *Ann Plast Surg* 44:59-64, 2000
24. Ozgenel GY, Filiz G: Effects of human amniotic fluid on peripheral nerve scarring and regeneration in rats. *J Neurosurg* 98:371-377, 2003
25. Palatinsky EA, Maier KH, Touhalisky DK, et al: ADCON-T/N reduces in vivo perineural adhesions in a rat sciatic nerve reoperation model. *J Hand Surg [Br]* 22:331-335, 1997
26. Petersen J, Russell L, Andrus K, et al: Reduction of extraneural scarring by ADCON-T/N after surgical intervention. *Neurosurgery* 38:976-983; discussion 983-974, 1996
27. Pucciarelli S, Codello L, Rosato A, et al: Effect of antiadhesive agents on peritoneal carcinomatosis in an experimental model. *Br J Surg* 90:66-71, 2003
28. Saravelos HG, Li TC: Physical barriers in adhesion prevention. *J Reprod Med* 41:42-51, 1996
29. Smit X, van Neck JW, Ebeli MJ, et al: Static footprint analysis: a time-saving functional evaluation of nerve repair in rats. *Scand J Plast Reconstr Surg Hand Surg* 38:321-325, 2004
30. Sunderland: *Nerve Injuries and their Repair. A Critical appraisal.* London: Churchill Livingstone, 1991, pp 213-219 p
31. Walker JL, Evans JM, Meade P, et al: Gait-stance duration as a measure of injury and recovery in the rat sciatic nerve model. *J Neurosci Methods* 52:47-52, 1994
32. Wang KK, Nemeth IR, Seckel BR, et al: Hyaluronic acid enhances peripheral nerve regeneration in vivo. *Microsurgery* 18:270-275, 1998
33. Zhao C, Amadio PC, Momose T, et al: The effect of suture technique on adhesion formation after flexor tendon repair for partial lacerations in a canine model. *J Trauma* 51:917-921, 2001

7

RGTA, a heparan sulfate mimetic, significantly reduces neural adhesions after peripheral nerve injury in rats

H. Mischa Zuijndendorp¹, Xander Smit¹, B.S. (Stefan) de Kool^{1,2}, Joleen H. Blok², Denis Barritault³, Steven E.R. Hovius¹, Johan W. van Neck¹

- 1) Department of Plastic and Reconstructive Surgery, Erasmus MC - University Medical Center Rotterdam, The Netherlands
- 2) Department of Clinical Neurophysiology, Erasmus MC - University Medical Center, Rotterdam, The Netherlands
- 3) Laboratoire CRRET, Université Paris XII-Val de Marne, France

Abstract

Objective. Extra- and intraneural scar formation after peripheral nerve injury frequently causes tethering and compression of the nerve and inhibition of axonal regeneration. ReGeneraTing Agents (RGTA) mimic the stabilizing and protective properties of heparin sulfate towards heparin binding growth factors (HBGFs). The aim of this study was to assess the effect of RGTA on extraneural fibrosis and regeneration after crush injury in a rat sciatic nerve model.

Methods. Thirty-two female Wistar rats underwent a standardized crush injury of the sciatic nerve. The animals were randomly allocated to RGTA treatment or sham treatment in a blinded design. To score neural adhesions, the peak force required to break the adhesions between the nerve and its surrounding tissue was measured 6 weeks after nerve crush injury. To assess axonal regeneration, magnetoneurography (MNG) measurements were carried after 5 weeks. Static footprint analysis was performed pre operatively and 1, 7, 14, 17, 21, 24, 28, 35 and 42 days post operatively.

Results. MNG data show no significant difference in conduction capacity between the RGTA and the control group. Also, results of the static footprint analysis demonstrate no improved or accelerated recovery pattern. However, the mean pull out force of RGTA group (67.19 g + SEM 9.26) was significantly ($p < 0.01$) lower compared to the control group (206.96 g + SEM 13.90).

Conclusions. RGTA have a strong positive effect on nerve adherence to surrounding tissue after nerve crush injury.

Keywords: nerve injury, rat, neural adhesions, regeneration, footprint analysis, MNG

Introduction

Recovery after peripheral nerve injury is influenced by many factors, including scar formation. Scar formation consists of extra- and intraneural collagen deposits. Collagen fibers enveloping the nerve can contract, risking compression neuropathies that can be accompanied with dysfunction and pain. During limb movement and muscle contractions, nerve adherence to surrounding tissue may lead to painful traction neuropathies^{12,18,21}. Furthermore, collagen deposition at the suture line and in the distal nerve segment may interfere with axonal regeneration and subsequently lead to poor functional outcome²⁰.

The extracellular matrix (ECM) surrounding cells, in particular heparan sulfate, play important roles in the regulation of wound healing, and have critical functions as co-receptors for growth factors and matrix proteins¹. ReGeneraTing Agents (RGTA) are chemically modified dextran polymers, which mimic the stabilizing and protective properties of heparin sulfate towards heparin binding growth factors (HBGFs). RGTA are characterized by specific activity at injured sites²⁴. In various experimental animal models, i.e. bone regeneration, skin repair, colonic anastomosis and muscle regeneration, RGTA have proven to promote tissue remodelling and healing^{6,16,17,22-24,38}. In addition, in vitro studies demonstrated that RGTA enhance the bioavailability of HBGF^{25,36}. RGTA may decrease extra- and intraneural scarring after nerve injury and enhance neural regeneration by binding natural signals at the site of injury.

The objective of this study was to assess the effect of RGTA on the recovery process after peripheral nerve injury in a rat sciatic nerve crush model. A quantitative biomechanical method is used to assess the effect of RGTA on neural adhesions. Additionally, RGTA are tested for their influence on the regenerative capacity of axons using neurophysiology (magnetoneurography) and footprint analysis.

Materials & Methods

The experimental protocol was approved by the Animal Experiments Committee under the national Experiments on Animals Act and adhered to the rules laid down in this national law that serves the implementation of "Guidelines on the protection of experimental animals" by the Council of Europe (1986), Directive 86/609/EC. Animals were housed under standard conditions of light and accommodation and allowed to become accustomed to laboratory conditions for 1 week before the start of the experiment. They were fed a standard laboratory diet (Hope Farms, Woerden, The Netherlands) with food and water ad libitum.

SURGICAL PROCEDURE

A total of 32 female Wistar rats (Harlan Netherlands B.V., Horst, The Netherlands), each weighing approximately 200 g, were randomly allocated to RGTA treatment or sham treatment in a blinded design. Rats were anesthetized using isoflurane (Isofluran, Rhodia Organique Fine Limited, Bristol, UK) in a mixture of oxygen and nitrous oxide. In each animals, the right sciatic nerve was exposed through a gluteal muscle-splitting incision. Under magnification the nerve was mobilised in the mid thigh and prior to crush injury, a uniform area of 10 mm was marked by epineural sutures 10/0 Ethilon® (Ethicon Inc, Somerville). To perform a standardized nerve crush injury, 5 mm of this segment was crushed for 30 seconds using a surgical needle holder, providing a fixed pressure of 57.5N. Following local treatment with RGTA or saline, the muscle septum and skin incisions were closed with 5/0 Vicryl® (Ethicon Inc, Somerville).

RGTA

In the experimental RGTA group (RGTA type OTR4120-192, batch B104), 50 µl RGTA / sterile saline solution (0.1 mg/ml, freshly prepared) is locally administered for a period of 45 minutes post injury. At day 1, 4, 8 and 15 after surgery, a RGTA / saline solution of 1 mg/kg is injected intramuscular. The sham-treated control group received saline in an identical treatment protocol.

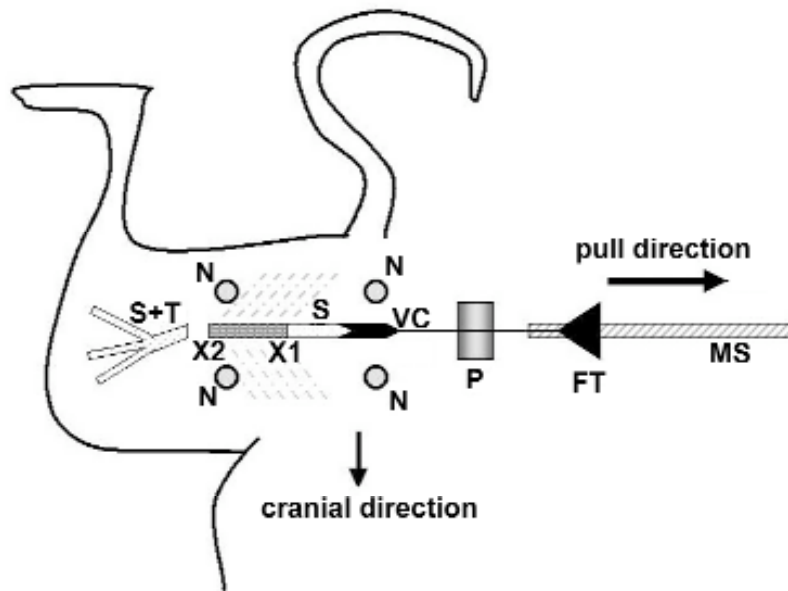


Figure 1. Schematic top view demonstrating the experimental setup for biomechanical measurements. The shaded zone represents the standardized area over which the adhesions were broken. FT = force transducer; MS = motorized spiral; N = needle; P = pulley; S = proximal part of sciatic nerve; S+T = distal part of sciatic nerve and trifurcation; VC = vascular clamp; X1 and X2 = marking sutures.

PEAK PULL-OUT FORCE MEASUREMENTS

To evaluate the degree of nerve tethering to surrounding tissue, the peak force required to break adhesions between the marked nerve segment and its surrounding tissue was measured, as described elsewhere³⁴.

Six weeks after surgery, 16 animals were anesthetized by inhalation of isoflurane as well as a mixture of O₂/N₂O and subsequently sacrificed by cervical dislocation. Sciatic nerves were dissected proximally and distally from the marked nerve segment. The distal nerve end was then transected at the level of the distal epineural suture initially marked (X2) (Figure 1). The proximal nerve end was transected 10 mm proximal from the proximal epineural suture (X1). At this point, the standardized nerve segment is only attached to its surrounding tissue.

Immobilization of the rat leg was accomplished by pinning down the upper hind portion of the leg with 19-gauge needles (Sterican; B. Braun Mesungen AG, Melsungen, Germany). The proximal nerve segment was held tightly with a stiff vascular clamp and interconnected to a force transducer with a range of 0 to 500 g (#52-9503; Harvard Apparatus, Inc., Holliston, MA) by using a silver wire suture. A pulley was used to align the course of the sciatic nerve with the pull direction. The force transducer was connected to a motorized drive with a constant extension rate of 29 mm/minute. The peak force required to pull the nerve segment out of its tissue bed was recorded.

MAGNETONEUROGRAPHY (MNG)

MNG measurements were carried out 5 weeks after nerve crush injury, according to the ex vivo MNG technique as described earlier³⁵. In short, 16 animals were anesthetized and the sciatic nerve was exposed from its origin in the lumbar spine to distal to the trifurcation at knee level, to acquire a segment of maximum length. To prevent axon leakage, the proximal part as well as the three branches of the sciatic nerve were ligated with a 6-0 suture and transected proximally and distally to the knots, respectively. The MNG recording chamber was filled with a buffer solution (Ringers Lactate containing glucose, 1 g/L) and kept at 21 ± 0.1 °C. The nerve was guided through the recording sensor coils as well as the stimulation cuff and stretched to 'in vivo' length by clamping the two sutures in the recording chamber (Figure 2). The distal nerve end was stimulated with a biphasic constant current pulse of 50 µs delivered by two isolated stimulus units (Digitimer DS3), connected in parallel. To guarantee supramaximal stimulation, the stimulator was finally set to 1.4 times the strength of the lowest current that produced a maximal signal.

Both right (operated) and left (control) sciatic nerve were measured. In the recording setting of the right nerve, the stimulation cuff cathode was positioned 10 mm distal to the marking suture placed prior to the crush lesion. Sensor 1 and sensor 2 were positioned 4 mm and 14 mm proximal to the marking suture, respectively. By applying distal stimulation and proximal recording, only axons with fibres regenerating across the lesion were stimulated and recorded. For the contralateral (unoperated) nerve similar recording settings were used, and an imaginary suture line was created at the same distance from the distal nerve end as present in the crushed nerve.

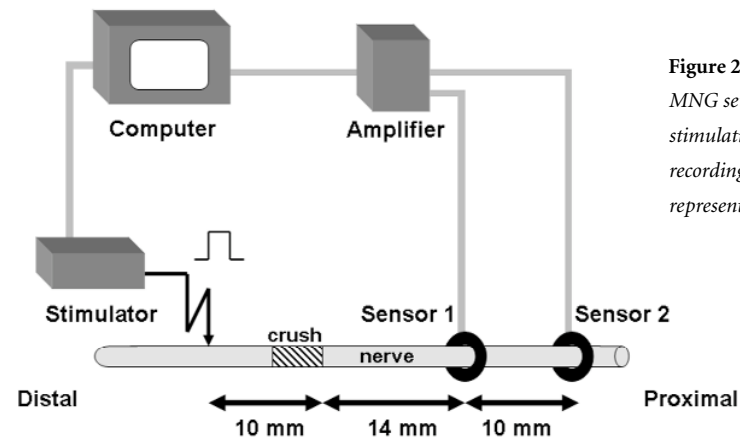


Figure 2. Schematic view of MNG setup demonstrating distal stimulation and proximal recording. The dark shaded area represents the crush lesion.

Each signal was calibrated by means of an accompanying 1 μ A calibration signal, which was recorded prior to every stimulus. Next, CNACs were analyzed on a personal computer using custom-made software (DataCorr3 written in VBA for MS Excel). In each recording setup, 4 consecutive batches of 256 CNACs were recorded and averaged. Further analyses were performed using MatLab (The MathWorks, Natick, MA), after which the following variables were calculated from the signal: (1) 1st peak amplitude (1PA), (2) peak-peak amplitude (PPA), (3) area (A) and (4) conduction velocity (CV). The biphasic character of the signal derived from sensor 1 enabled calculation of all of these variables. Because of the generally monophasic character of the signal recorded with sensor 2, only the 1PA and the CV were calculated for this sensor. Different neurophysiological variables are expressed as right – left ratios.

FOOTPRINT ANALYSIS

Static footprint analysis was performed pre operatively and at 1, 7, 14, 17, 21, 24, 28, 35 and 42 days post operatively, following the procedure described elsewhere³⁵. From the digitized footprints the distance between the first and fifth toe (Toe Spread; TS) was measured. The averaged distances of three measurements were used to calculate the static Toe Spread Factor (TSF) = (OTS – NTS) / NTS (O=operated/right; N=normal/left). A value of –0.66 was allocated to the static TSF, in case no footprints were measurable due to total impairment³⁵.

The animals were meticulously examined for signs of autotomy and contracture. All animals with absence of a part of the foot and/or showing contracture were excluded from footprint analysis.

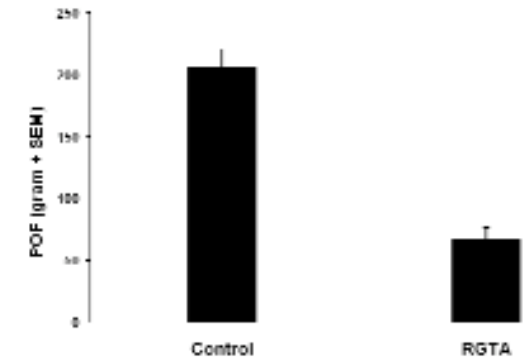
STATISTICAL ANALYSIS

The data were analysed using the Statistical Package for the Social Sciences version 10 (SPSS, Chicago, IL) software. Statistical significance was accepted at $p < 0.05$. Individual statistical tests are mentioned where used.

Results

No animals in any of the group displayed wound dehiscence or wound infections. One animal died preoperatively. One animal was excluded from MNG and SFA evaluation because of automutilation.

Figure 3. Bar graph illustrating the results of peak force measurements. The vertical axis represents the force required to break adhesions.



PULL OUT FORCE

In Figure 3 the effect of RGTA on the POF is demonstrated. The unpaired Student's t-test demonstrates a significant reduction in the RGTA group ($p < 0.01$). The mean POF in the control group was 206.96 g (SEM 13.90) and reduced by 67% to 67.19 g (SEM 9.26) in the RGTA group.

MAGNETONEUROGRAPHY

Table 1 shows the results of the neurophysiological examination after 5 weeks. All six MNG outcome variables do not significantly differ between RGTA and control group (unpaired Student's t-test).

Table 1. MNG outcome variables in means (SEM) of control animals and RGTA treated animals: conduction velocity (CV) of sensor 1 & 2; 1st peak amplitude (1PA) of sensor 1 & 2; peak-peak amplitude (PPA); and area (A) of sensor 1. P values of the unpaired Student's t-test are given.

	Group	Mean (SEM)	p-value
1PA sensor 1	control	0,445 (0,0305)	0,53
	RGTA	0,477 (0,0331)	
PPA sensor 1	control	0,513 (0,0331)	0,51
	RGTA	0,543 (0,0280)	
CV sensor 1	control	0,476 (0,0896)	0,39
	RGTA	0,552 (0,0507)	
A sensor 1	control	0,670 (0,0381)	0,98
	RGTA	0,671 (0,0485)	
1PA sensor 2	control	0,644 (0,1328)	0,25
	RGTA	0,507 (0,0368)	
CV sensor 2	control	0,688 (0,0848)	0,77
	RGTA	0,715 (0,0494)	

FOOTPRINT ANALYSIS

The recovery patterns of static TSF over time after crush injury of RGTA and control group show similarity and no distinct difference in functional loss is visualized (Figure 4). In concordance, multivariate tests of repeated measures demonstrate no significant difference between the two recovery patterns ($p=0.698$).

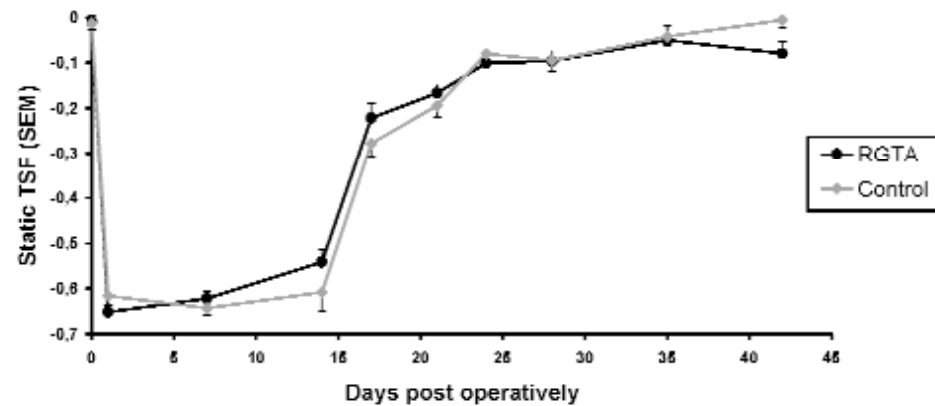


Figure 4. Mean static TSF (SEM) as a function of time after surgery of RGTA group (black circles) and control group (grey diamonds).

Discussion

Our results demonstrate that RGTAs significantly reduce adhesions after peripheral nerve crush injury. Neurophysiological data show no enhanced regeneration in RGTA treated animals. Nevertheless, RGTAs do not impede axonal regeneration or functional recovery.

Heparan sulfate is a natural component of the extracellular matrix. Heparan sulfate plays an important role in cellular processes by binding secreted growth factors and cytokines. Heparan Sulphate controls the activity of these molecules by protection from chemical and physiological degradation, thereby providing a reservoir for delayed release¹.

After injury, heparin sulphates will become degraded by activated heparinase³. RGTAs were engineered to replace the degraded heparan sulfate at the site of injury in order to protect the natural signals without preventing these signals from operating their natural stimulatory functions. Specific activity at injured sites was demonstrated in a model of ischemic muscle healing using labeled RGTAs intravenously injected. RGTAs in a non-injured rat were readily eliminated, whereas in animals after crushing muscle, RGTAs remained solely localized in the damaged muscle until regeneration was completed²⁴. Previous studies demonstrated that RGTAs enhance the bioavailability of

HBGF^{25,36}. In various experimental animal models, RGTAs promote tissue remodelling and healing, i.e. bone regeneration, skin repair, colonic anastomosis and muscle regeneration^{6,16,17,22-24,38}.

EXTRANEURAL SCARRING

This study revealed that nerve adherence to surrounding tissue is reduced by RGTAs. In most studies on prevention of extraneural scarring in peripheral nerve surgery, adhesions were evaluated by a description of histological findings or scored based on the difficulties of surgical dissection using a numerical grading scheme introduced by Peterson et al³⁰. To assess the anti adhesion effect of RGTAs after nerve injury, we used a biomechanical method previously described by Smit et al³⁴. The measured pull out force provides a quantitative outcome, strictly related to the connections between nerve and its surrounding tissue. In slightly different experimental set ups, the pull out force has been used in two other studies to score neural adhesions^{13,27}.

Many strategies have been used in an attempt to reduce extraneural scarring. Several surgical techniques have been developed to create an autologous barrier, such as wrapping the nerve with vein, dermo-fascial fat grafts or muscle flaps^{9,15,31,32}. Foreign materials providing a physical barrier, like silicone cuffing, have been studied as well¹⁰. However, these devices may induce foreign body reaction or migrate. ADCON-T/N (a carbohydrate polymer gel) and viscous injectable pure alginate sol can provide a biodegradable barrier^{27,30}. Agents, which may exert a pharmacological effect on adhesion formation, include mitomycin C (chemotherapeutic agent), human amniotic fluid, aprotinin (proteinase inhibitor), and anti-TGF-beta^{8,11,14,26,28,29}. Hyaluronic acid gel, as well as HA-CMC membrane (a mixture of hyaluronic acid and carboxymethylcellulose), may affect adhesion formation at a cellular and mechanical level^{7,13,28}.

The diminishing effect of RGTAs on extraneural scarring has not been reported earlier. In vitro, RGTAs induce a decrease of collagen III production by different cultured cells^{5,25}. Biopsies of human intestinal tissue from Crohn's disease patients ex vivo exposed to RGTAs show direct diminution of collagen III².

AXONAL REGENERATION AND FUNCTIONAL RECOVERY

Neurophysiological measurements were performed using magnetoneurography. MNG has proven to be a valuable tool to quantify peripheral nerve regeneration in rabbit and rat models^{33,37}. MNG data show no significant difference in conduction capacity between the RGTA and the control group. This indicates no enhancement of axonal regeneration, nor a negative effect of RGTAs in a crush model. Over the years, several experimental strategies have proven to promote nerve regeneration and functional recovery, including the use of electrical stimulation and the application of hyaluronic acid, FK506, steroids and anti-TGF-beta^{4,8,19,26,29}. The effect of RGTAs on nerve regeneration has not been reported. We hypothesized that RGTAs enhance regeneration through a reduction of intraneural fibrosis. Furthermore, RGTAs might affect regeneration through binding and protecting preexisting and newly synthesized HBGFs. We did not disclose improvement of conduction capacity five weeks after injury. Also, no

improved or accelerated recovery pattern of static TSF was demonstrated during the six weeks following injury. Our results might be explained by the type of injury we applied in our model. The crush model is a widely used model for studies on injuries of rat sciatic nerves. Nevertheless, a disadvantage is that functional recovery measured by footprint analysis following crush injury in rats is excellent. In the present study, the static TSF was practically normalized at six weeks. Therefore, any effect on axonal regeneration might not be observed. When the severity of the injury is increased, i.e. in a nerve repair model, acceleration and improvement of regeneration might be demonstrated. We emphasize the need for further studies to investigate the effect of RGTAs on peripheral nerve regeneration in a nerve transaction model.

In summary, we have proven the effectiveness of RGTAs in reducing the pull out force after nerve crush injury. The results of this study do not reveal positive or negative influence of RGTAs on axonal regeneration. We conclude that local and systemic application of RGTAs after peripheral nerve trauma has a therapeutic effect on neural adhesions and should further be investigated.

Acknowledgements

The authors are grateful to Ineke Hekking and Mariken Zbinden for surgical assistance.

References

1. Alberts B, Bray D, Lewis J, et al: *Molecular biology of the cell*. Garland Publishing, Inc., 1994,
2. Alexakis C, Caruelle JP, Sezeur A, et al: Reversal of abnormal collagen production in Crohn's disease intestinal biopsies treated with regenerating agents. *Gut* 53:85-90, 2004
3. Bame KJ: Heparanases: endoglycosidases that degrade heparan sulfate proteoglycans. *Glycobiology* 11:91R-98R, 2001
4. Bansberg SF, McCaffrey TV: The effect of systemic triamcinolone acetonide on nerve repair. *Otolaryngol Head Neck Surg* 96:158-164, 1987
5. Benazzoug Y, Logeart D, Labat-Robert J, et al: Derivatized dextrans modulate collagen synthesis in aortic smooth muscle cells. *Biochem Pharmacol* 49:847-853, 1995
6. Benoit J, Meddahi A, Ayoub N, et al: New healing agent for colonic anastomosis. *Int J Colorectal Dis* 13:78-81, 1998
7. Dam-Hieu P, Lacroix C, Said G, et al: Reduction of postoperative perineural adhesions by Hyaloglide gel: an experimental study in the rat sciatic nerve. *Neurosurgery* 56:425-433; discussion 425-433, 2005
8. Davison SP, McCaffrey TV, Porter MN, et al: Improved nerve regeneration with neutralization of transforming growth factor-beta1. *Laryngoscope* 109:631-635, 1999
9. Dumanian GA, McClinton MA, Brushart TM: The effects of free fat grafts on the stiffness of the rat sciatic nerve and perineural scar. *J Hand Surg [Am]* 24:30-36, 1999
10. Finsterbush A, Porat S, Rouso M, et al: Prevention of peripheral nerve entrapment following extensive soft

tissue injury, using silicone cuffing: an experimental study. *Clin Orthop Relat Res* 276-281, 1982

11. Gorgulu A, Imer M, Simsek O, et al: The effect of aprotinin on extraneural scarring in peripheral nerve surgery: an experimental study. *Acta Neurochir (Wien)* 140:1303-1307, 1998
12. Hunter JM: Recurrent carpal tunnel syndrome, epineural fibrous fixation, and traction neuropathy. *Hand Clin* 7:491-504, 1991
13. Ikeda K, Yamauchi D, Osamura N, et al: Hyaluronic acid prevents peripheral nerve adhesion. *Br J Plast Surg* 56:342-347, 2003
14. Ilbay K, Etus V, Yildiz K, et al: Topical application of mitomycin C prevents epineural scar formation in rats. *Neurosurg Rev* 28:148-153, 2005
15. Jones NF, Shaw WW, Katz RG, et al: Circumferential wrapping of a flap around a scarred peripheral nerve for salvage of end-stage traction neuritis. *J Hand Surg [Am]* 22:527-535, 1997
16. Lafont J, Baroukh B, Berdal A, et al: RGT11, a new healing agent, triggers developmental events during healing of craniotomy defects in adult rats. *Growth Factors* 16:23-38, 1998
17. Lafont J, Blanquaert F, Colombier ML, et al: Kinetic study of early regenerative effects of RGT11, a heparan sulfate mimetic, in rat craniotomy defects. *Calcif Tissue Int* 75:517-525, 2004
18. Lundborg G: *Nerve injury and repair*. Churchill Livingstone, 1988,
19. Maggi SP, Lowe JB, 3rd, Mackinnon SE: Pathophysiology of nerve injury. *Clin Plast Surg* 30:109-126, 2003
20. Mathur A, Merrell JC, Russell RC, et al: A scanning electron microscopy evaluation of peripheral nerve regeneration. *Scan Electron Microsc* 975-981, 1983
21. McCall TD, Grant GA, Britz GW, et al: Treatment of recurrent peripheral nerve entrapment problems: role of scar formation and its possible treatment. *Neurosurg Clin N Am* 12:329-339, 2001
22. Meddahi A, Alexakis C, Papy D, et al: Heparin-like polymer improved healing of gastric and colic ulceration. *J Biomed Mater Res* 60:497-501, 2002
23. Meddahi A, Benoit J, Ayoub N, et al: Heparin-like polymers derived from dextran enhance colonic anastomosis resistance to leakage. *J Biomed Mater Res* 31:293-297, 1996
24. Meddahi A, Bree F, Papy-Garcia D, et al: Pharmacological studies of RGT(11), a heparan sulfate mimetic polymer, efficient on muscle regeneration. *J Biomed Mater Res* 62:525-531, 2002
25. Mestries P, Borchiellini C, Barbaud C, et al: Chemically modified dextrans modulate expression of collagen phenotype by cultured smooth muscle cells in relation to the degree of carboxymethyl, benzylamide, and sulfation substitutions. *J Biomed Mater Res* 42:286-294, 1998
26. Nath RK, Kwon B, Mackinnon SE, et al: Antibody to transforming growth factor beta reduces collagen production in injured peripheral nerve. *Plast Reconstr Surg* 102:1100-1106; discussion 1107-1108, 1998
27. Ohsumi H, Hirata H, Nagakura T, et al: Enhancement of perineurial repair and inhibition of nerve adhesion by viscous injectable pure alginate sol. *Plast Reconstr Surg* 116:823-830, 2005
28. Ozgenel GY, Filiz G: Combined application of human amniotic membrane wrapping and hyaluronic acid injection in epineurectomized rat sciatic nerve. *J Reconstr Microsurg* 20:153-157, 2004
29. Ozgenel GY, Filiz G: Effects of human amniotic fluid on peripheral nerve scarring and regeneration in rats. *J Neurosurg* 98:371-377, 2003
30. Petersen J, Russell L, Andrus K, et al: Reduction of extraneural scarring by ADCON-T/N after surgical intervention. *Neurosurgery* 38:976-983; discussion 983-974, 1996
31. Rose EH, Norris MS, Kowalski TA, et al: Palmaris brevis turnover flap as an adjunct to internal neurolysis of the chronically scarred median nerve in recurrent carpal tunnel syndrome. *J Hand Surg [Am]* 16:191-201, 1991

32. Ruch DS, Spinner RM, Koman LA, et al: The histological effect of barrier vein wrapping of peripheral nerves. *J Reconstr Microsurg* 12:291-295, 1996
33. Smit X, Stefan de Kool B, Walbeehm ET, et al: Magnetoneurography: recording biomagnetic fields for quantitative evaluation of isolated rat sciatic nerves. *J Neurosci Methods* 125:59-63, 2003
34. Smit X, van Neck JW, Afoke A, et al: Reduction of neural adhesions by biodegradable autocrosslinked hyaluronic acid gel after injury of peripheral nerves: an experimental study. *J Neurosurg* 101:648-652, 2004
35. Smit X, van Neck JW, Ebeli MJ, et al: Static footprint analysis: a time-saving functional evaluation of nerve repair in rats. *Scand J Plast Reconstr Surg Hand Surg* 38:321-325, 2004
36. Tardieu M, Gamby C, Avramoglou T, et al: Derivatized dextrans mimic heparin as stabilizers, potentiators, and protectors of acidic or basic FGF. *J Cell Physiol* 150:194-203, 1992
37. Walbeehm ET, Dudok van Heel EB, Kuypers PD, et al: Nerve compound action current (NCAC) measurements and morphometric analysis in the proximal segment after nerve transection and repair in a rabbit model. *J Peripher Nerv Syst* 8:108-115, 2003
38. Zimowska M, Constantin B, Papy-Garcia D, et al: Novel glycosaminoglycan mimetic (RGTA, RGD120) contributes to enhance skeletal muscle satellite cell fusion by increasing intracellular Ca²⁺ and calpain activity. *J Cell Physiol* 205:237-245, 2005

General Discussion, Conclusions and Research Perspectives

General Discussion

To improve recovery after peripheral nerve injury, surgeon and patient have to win the struggle at the site of nerve injury. This thesis is initiated to elucidate different problems and quantify different processes related to the site of peripheral nerve injury. These problems and processes cannot be addressed to in randomized clinical outcome studies. Patient and injury related variables influencing outcome after nerve injury are heterogeneous⁴⁴, consequently leading to statistical problems. Therefore, well-designed experimental research in the field nerve injury is of great value.

In **chapter 1**, experimental assessment techniques of peripheral nerve injury are reviewed and discussed for their (dis)advantages. Furthermore, physiology and pathophysiology of the peripheral nervous system are described with a focus on fundamental problems related to the site of injury.

In this thesis, experimental evaluation techniques of function of target organs (footprint analysis), and axon regeneration (conduction capacity) are investigated for their relation and value. Furthermore, peripheral nerves are studied for physiological biomechanical properties. Tensile forces are of paramount importance for nerve repair, especially when bridging nerve gaps. Biomechanical evaluation is also used to quantify neural adhesions after nerve injury and to test the effect of antiadhesion strategies.

The study in **chapter 2** was designed to evaluate and validate different techniques of functional evaluation, i.e. footprint analysis, after sciatic nerve injury in rats. The most commonly used method of functional assessment after nerve repair in the rat is walking track analysis, resulting in the Sciatic Function Index (SFI). Traditional and new video techniques of walking track analysis are both known to be labour-intensive¹³. In this chapter, we demonstrate an excellent correlation between the laborious SFI and the time efficient static footprint analysis used to assess functional recovery after repair of the rat sciatic nerve. In 2000, Bervar introduced a new method that enabled reliable and fast alternative footprint analysis, resulting in the Static Sciatic Index (SSI)⁴. The main benefits of this digitized static video recording technique are ease and speed with which the essential footprints could be collected and analysed. In this study, we confirm the time effectiveness and moreover, we conclude that the use of the static Toe Spread Factor (static TSF) is preferable, as the supplementary value of SSI over static TSF is not proven and calculation of static TSF is easier than calculation of SSI.

Over the years, the use of video analysis has been expanded by determining other parameters of functional recovery, like stance phase of a gait cycle, stance duration and ankle angle^{32, 53, 54}. Such extensive, but labour-intensive, functional gait analyses indeed have been proven to give an accurate reflection of the nerve's target organ function. However, the power to discriminate between experimental groups has not been confirmed in literature yet. As mentioned in chapter 1, the function of target organs is only of relative value when studying fundamental problems at the site of injury. Recovery of target organ function, for example measured by static footprint analysis, is dependent on too many factors not related to the site of injury.

In conclusion, footprint analysis should only serve as additional evaluation method of nerve injury, providing indirect evidence of the recovery process of the nerve at the site of injury. Static footprint analysis is comparable to the traditional walking track analysis but easier and more time efficient.

The aim in **chapter 3** was to develop and validate a set up enabling accurate quantification of the conduction capacity of a rat sciatic nerve. In vivo neurophysiological measurements are heavily prone to errors, i.e. recording distances and temperature, especially in small sized animals. In this chapter, a setup is described, developed to accurately make ex vivo MNG measurements on rat sciatic nerves. Biphasic stimulation with optimized grounding reduced the stimulus artifact. The mean variability (<5%) of MNG signals demonstrated that the design of the recording chamber allows for a precise and reproducible setup. An inherent side effect of ex vivo measurements is a decrease in nerve viability over time. However, ex vivo nerve viability was assured for at least 2 hours after dissection, which is sufficient to perform multiple measurements. Recent studies showed that ex vivo nerve measurements, enabling high reproducibility and signal quantification, can be performed with ENG in (compartmental) bath solutions^{15, 16, 33, 34, 40, 57}. Multiple chambers allow for evaluation of local drug influence on the nerve's conduction capacity. However, the advantage of magnetically recording neurophysiological signals (MNG) over electrically recording neurophysiological signals (ENG) is that magnetic fields are less influenced by the impedance of biological tissue surrounding the nerve, and by the position of the nerve in relation to the sensor^{27, 60-62}.

The general conclusion of this chapter is that ex vivo MNG can reliably quantify the nerve's conduction capacity (signal amplitude and conduction velocity). Irrespective of the type of recording (electrical or magnetic), we emphasize the advantages of an ex vivo set up for neurophysiological studies on the nerve's conduction capacity of small sized animals. This allows for better control of confounding factors of the measurements.

The study described in **chapter 4** reports on the recovery pattern of neurophysiological features, and function of target organs after rat sciatic nerve transection followed by direct repair. Previous investigations studying electrophysiology of nerve regeneration and its relation to other outcome measures used conventional EMG or ENG, accompanied by the disadvantages mentioned earlier^{14, 26, 48}. Using ex vivo MNG, more profound conclusions can be drawn on the neurophysiological outcome after nerve injury and its relation to function of target organs as measured by static TSF and muscle weight (MW).

Neurophysiological experiments of nerve regeneration are known to require long term study end points. This study, however, demonstrated that 8 weeks after nerve repair, neurophysiological features like 1st peak amplitude (1PA), peak peak amplitude (PPA), area (A) and conduction velocity (CV) have already reached approximately two thirds of the values measured 24 weeks postoperatively. Thus, recovery of neurophysiological signals is primarily established within the early weeks of regeneration.

Electrophysiological changes in aging animals have been reported extensively^{47, 55, 56, 59}. The need of right - left ratios in longitudinal studies is therefore of outmost importance. Our finding, that up to an age of 35 weeks, conduction capacity enhances, agrees with literature.

The moderate correlations found between static TSF (function) and MNG variables (conduction capacity) can be explained by the difference in recovery pattern as measured by static TSF and MNG. After approximately 10 weeks, static TSF recovery levels off, whereas in case of MNG, neurophysiological variables still increase significantly after this period. This plateau phase has been described in previous studies using the sciatic function index^{21, 31}, however not compared to the recovery pattern of neurophysiological features. From this chapter it becomes clear that the process of axon regeneration continues, even though improvement of function appears to stagnate. It might be concluded that maturation of axons does not have consequences for final function. This would probably be true if static TSF was an adequate measure of final nerve function. However, it is more likely that spreading of the toes already can be established by ingrowth of relatively few or immature axons. Footprint analysis does not allow for quantification of refined movements or strength of various muscles as possible in a human setting. Thus, when studying axon growth after nerve injury, the function of target organs, as measured by footprint analysis is only of relative value.

A widely discussed drawback of footprint analysis is the loss of animals due to autotomy and contracture of the rat's hind paw^{7, 31, 50}. No relation exists between autotomy and / or contracture and poor conduction capacity. A possible bias in footprint analysis caused by exclusion of autotomy / contracture animals is therefore confuted.

Reinnervation of the muscle after sciatic nerve repair causes a significant increase in MW up to at least 24 weeks after surgery. Regression analysis demonstrated that an increase in number and / or maturation of regenerated nerve fibers is strongly related to the weight of the muscle. There was no significant relation between static TSF and MW. Apparently, both indirect measures are totally different derivatives of the regeneration process. For experimental rat studies of nerve fiber regeneration after injury, we recommend the use of a more direct derivative of the regeneration process, such as MNG.

The discrepancy between neurophysiology and function of target organs also exists in a clinical setting⁵². In contrast to the rat model in which recovery of function stagnates in the early phase after injury, in humans functional improvement is seen up to 5-6 years after surgery^{17, 44}. From literature, there is no consensus on the neurophysiological recovery after nerve repair in humans. In conceptual models a recovery period of 18 months is suggested⁴³. It should be noted that a major difference exists between clinical and experimental evaluation of (1) neurophysiology and (2) function of target organs after nerve injury. The disadvantages of assessment of function of target organs in an animal model are extensive and have been discussed earlier, whereas the possibilities of functional evaluation after nerve repair in a clinical setting are extensive and precise²⁵. Conversely, in human, neurophysiological assessment is restricted to (most often) non invasive techniques where animal models allow invasive and accurate neurophysiological measurements.

The study in **chapter 5** describes how stretch is distributed along the nerve relative to articulations. During normal extension and flexion the joint regions underwent greater deformation than the corresponding non-joint regions. Tensile testing of isolated samples of both regions of both nerves showed that joint regions were less stiff (more compliant) than their non-joint counterparts. Thus, is not a simple function of greater loading over joints but rather reflects distinct material properties of the two zones, joint regions being inherently more compliant. This could not be explained by structural differences identified by fascicular/non-fascicular tissue architecture, as suggested by Sunderland⁵¹. From this study and from literature, it is unclear by which means regions of differing stiffness develop. The point to which nerves reach their physiological The tension range of peripheral nerves at which the neural function is compromised has been subject of many investigations^{28, 30, 35, 45, 58}.

When repairing a nerve defect, the surgeon has to decide whether to use a nerve graft (or interponate) or an end-to-end repair under tension. In literature, there is disagreement about this decision point and attempts have been made to express the significant level of nerve gap in centimeters or percentage of dissected nerve²². From our study, we conclude that during decision making to treat nerve defects, indications cannot be expressed in length of gap or as a percentage of the dissected nerve segment in situ as great variation exists along the length of the nerve.

Chapter 6 compromises a study on neural scarring. Adhesion formation is a serious problem in peripheral nerve surgery, frequently causing dysfunction and pain^{23, 51}. The assessment of nerve adhesions in experimental models is complicated. Histology and surgical evaluation of the wound are widely accepted methods of assessing nerve adhesions^{18, 19, 37-39, 41}, but critically reviewed in this chapter. Adhesion formation between nerve and surrounding tissue (extraneural scarring) was assessed and validated in a newly developed biomechanical model by measuring the peak force required to break the adhesions. With an increasing severity of trauma, adhesions increased significantly. We emphasize that a simple nerve dissection (= neurolysis) can cause substantial extraneural scarring. Having proven that neural adhesions can be accurately quantified using the described model, the role of other evaluation methods should be reconsidered. Although histology is only semi quantitative it may have an additional role in investigations on strategies to prevent neural scarring. Staining of collagen can help to understand the working mechanism of antiadhesion therapies. Furthermore, intraneural scarring cannot be assessed by a biomechanical model and requires histology.

Hyaluronic acid (HA) a glycosaminoglycan in the extracellular matrix, where it plays an important role in many tissue repair biological processes⁸ and has proven to have antiadhesion effects^{5, 20}. Hyaloglide (Fidia Advanced Biopolymers Srl, Abano Terme, Italy) is a viscous hydrogel, developed as an antiadhesion device. In gynaecological and intra-abdominal surgery (ACP-gel), it has proven to reduce adhesions^{3, 10, 11, 42}. The study in this chapter demonstrates a significant reducing effect on nerve adhesions, when using Hyaloglide after different types of peripheral nerve injury. The working mechanism of Hyaloglide is not revealed from this study. This autocrosslinked HA based

gel is highly viscous and can serve as a biodegradable barrier to physically keep the injured nerve separated from the adjacent tissue^{2,46}. Furthermore, after slow deesterification of the molecules, liberated HA may have a cellular antiadhesion effect at the injured site^{5,6,8,12,20,24,29}.

Various strategies have proven to effectuate an antiadhesion effect after nerve injury^{1,18,19,24,36-39,41,49}. Due to different experimental models and evaluation methods it is not possible to compare these strategies and up to now, these strategies have not been weighed against each other in one quantitative study. To our knowledge, these experimental studies have not yet resulted in randomized clinical trials concerning neural adhesion following peripheral nerve injury. The feasibility of such trials is disputable as quantitative evaluation of neural adhesions is almost impossible in human. Nevertheless, a device like Hyaloglide^{9,49} is currently used in a clinical setting.

The aim of **chapter 7** was to assess the effect of RGTAs on extraneural fibrosis and regeneration after crush injury in a rat sciatic nerve model. ReGeneraTing Agents (RGTAs) mimic the stabilizing and protective properties of heparin sulfate towards heparin binding growth factors (HBGFs). RGTAs have proven to promote tissue remodelling and healing in various experimental animal models, i.e. bone regeneration, skin repair, colonic anastomosis and muscle regeneration.

Using the biomechanical model (chapter 6) we demonstrated that RGTAs are effective in reducing the pull out force, i.e. neural adhesions, after nerve crush injury. Regulation of HBGF activity by RGTAs effectuates a reduction of extraneural scar formation, in particular regulation of TGF-beta, which promotes collagen deposition and fibrosis.

The results of this study do not reveal positive or negative influence of RGTAs on axonal regeneration as measured by magnetoneurography (chapter 3 & 4). Also, no improved or accelerated recovery pattern of static TSF (chapter 2) was demonstrated during the six weeks following injury. A lack of improved conduction capacity using RGTAs may be explained by the type of injury. Following crush injury (axontmesis), axonal regeneration is complete and relatively fast compared to total transection of a nerve (neurontmesis). It is possible that the positive effect of RGTAs, i.e. reduction of intraneural fibrosis, is not relevant in this type of injury in the rat model. When severity of injury is increased, for example in a nerve repair model, acceleration and improvement of regeneration by the use of RGTAs may be demonstrated.

When comparing pull out force (POF) results of chapter 6 and chapter 7, there is no significant difference between crush injury control groups six weeks after crush injury. Mean POF (+ SEM) of control HA-gel study is 230.26 (+ 11.59 g) and mean POF (+ SEM) of control RGTA study is 206.96 g (+ SEM 13.90). The small difference may be caused by the fact that these studies were performed by different investigators at different time points. Yet, a striking difference is noted between the antiadhesion effect of HA-gel and RGTAs. HA-gel effectuates a decrease of 29% in peak force, whereas RGTAs accomplish a decrease of 67% in peak force after nerve crush injury. To demonstrate a significant difference between both antiadhesion therapies both strategies should be

investigated in one study. Then, a possible synergy of RGTAs and HA-gel can also be studied.

Main conclusions of this thesis

From the studies performed in our experimental rat model, the following conclusions can be drawn:

- Static TSF derived from digitized static footprint analysis reveals identical information on function of target organs as SFI derived from the more time consuming (digitized) walking track analysis.
- MNG of rat sciatic nerve in an ex vivo recording chamber can reliably quantify the nerve's conduction capacity, from early on in the regeneration process.
- Despite isolation of the nerve, (ex vivo) viability is assured for at least 2 hours after dissection using the described recording chamber.
- After sciatic nerve injury recovery patterns as assessed by MNG (direct measure of axon regeneration) and by MW and static TSF (indirect measures of axon regeneration) vary significantly.
- The process of regeneration does not stop when functional recovery, as measured by footprint analysis becomes stagnant.
- When studying axon growth after nerve injury, the function of target organs, as measured by footprint analysis, is only of relative value.
- No relation exists between poor conduction capacity, and autotomy and contractures.
- For studies of nerve fiber regeneration after injury, the use of a direct measure, i.e. conduction capacity, of the regeneration process is recommended over indirect measures, i.e. muscle weight and footprint analysis.
- At articulations, peripheral nerves exhibit increased strain during limb movement and decreased stiffness.
- The localised heterogeneity of tensile properties is not related to fascicular/non-fascicular tissue architecture.
- Biomechanical assessment enables a quantitative and objective measure of neural adhesions and is to be preferred over surgical evaluation of the wound.
- Hyaloglides and RGTA are both effective in reducing neural adhesions after nerve injury
- Hyaloglides effectuates a faster recovery process of the static TSF after nerve injury
- After nerve injury, RGTA does not have an effect on the recovery of static TSF and on the recovery of conduction capacity.
- The struggle at the site of nerve injury can well be studied in a rat sciatic nerve model

Research Perspectives

The general aim of this thesis was to quantify physiological and pathophysiological processes, associated with the site of a possible nerve injury, in the rat sciatic nerve model. Validated experimental methods providing quantifiable outcome data can provide solid evidence for potential beneficial strategies to promote recovery after peripheral nerve injury. It is not feasible to review all future possibilities in this field of research. However, a few research perspectives can be summarized, which are directly related to this thesis:

- In future experimental studies on promotion of recovery after nerve injury, the type of assessment technique should carefully be considered. A quantifiable measure is preferred, which is directly related to the hypothesis of the experiment.
- Experimental research using Magnetoneurography requires an investment in technical knowledge. The financial aspects of the recording set up are comparable to other conventional neurophysiological methods. When deciding to perform neurophysiological measurements as an assessment method, ex vivo measurements are preferable over conventional electrophysiology.
- Proving beneficial effect of antiadhesion therapies in randomized clinical trials is rarely feasible. Negative side effects of antiadhesion strategies should be avoided and disclosed. Then, when experimental evidence of antiadhesion strategies is clear, one should consider clinical use without testing in randomized clinical trials.
- The localised heterogeneity of tensile properties is not related to fascicular/non-fascicular tissue architecture. Further studies should be planned to investigate differences in collagen architecture in different regions of a nerve which could account for the local differences in tensile properties.
- After nerve injury, Hyaloglides has an antiadhesion effect and accelerates recovery of static TSF. The working mechanisms of the findings remain unrevealed in this thesis. The exact antiadhesion working mechanism of Hyaloglides should be further investigated. Furthermore, it is interesting to know whether the acceleration of recovery of static TSF is due to increased conduction capacity or due to better gliding properties of the nerve.
- After nerve injury, RGTA has an antiadhesion effect but no effect on the recovery of conduction capacity. We emphasize that the study on RGTA includes only one time point and one type of trauma (crush). The effect of RGTA on recovery of conduction capacity after different types of injury and the effect on intra neural scarring should further be investigated.
- Hyaloglides is locally applied to the injured nerve. Therefore, its effect will be accomplished within early days after nerve injury. RGTA can be applied locally and systemically. RGTA may have a longer time range in which its antiadhesion effect is successful. This possible synergy of Hyaloglides and RGTA should be further investigated.

References

1. Adanali G, Verdi M, Tuncel A, et al: Effects of hyaluronic acid-carboxymethylcellulose membrane on extra-neural adhesion formation and peripheral nerve regeneration. *J Reconstr Microsurg* 19:29-36, 2003
2. Arnold PB, Green CW, Foresman PA, et al: Evaluation of resorbable barriers for preventing surgical adhesions. *Fertil Steril* 73:157-161, 2000
3. Belluco C, Meggiolaro F, Pressato D, et al: Prevention of postsurgical adhesions with an autocrosslinked hyaluronan derivative gel. *J Surg Res* 100:217-221, 2001
4. Bervar M: Video analysis of standing—an alternative footprint analysis to assess functional loss following injury to the rat sciatic nerve. *J Neurosci Methods* 102:109-116, 2000
5. Burns JW, Skinner K, Colt J, et al: Prevention of tissue injury and postsurgical adhesions by precoating tissues with hyaluronic acid solutions. *J Surg Res* 59:644-652, 1995
6. Burns JW, Skinner K, Colt MJ, et al: A hyaluronate based gel for the prevention of postsurgical adhesions: evaluation in two animal species. *Fertil Steril* 66:814-821, 1996
7. Carr MM, Best TJ, Mackinnon SE, et al: Strain differences in autotomy in rats undergoing sciatic nerve transection or repair. *Ann Plast Surg* 28:538-544, 1992
8. Chen WY, Abatangelo G: Functions of hyaluronan in wound repair. *Wound Repair Regen* 7:79-89, 1999
9. Dam-Hieu P, Lacroix C, Said G, et al: Reduction of postoperative perineural adhesions by Hyaloglidge gel: an experimental study in the rat sciatic nerve. *Neurosurgery* 56:425-433; discussion 425-433, 2005
10. De Iaco PA, Muzzupapa G, Bigon E, et al: Efficacy of a hyaluronan derivative gel in postsurgical adhesion prevention in the presence of inadequate hemostasis. *Surgery* 130:60-64, 2001
11. De Iaco PA, Stefanetti M, Pressato D, et al: A novel hyaluronan-based gel in laparoscopic adhesion prevention: preclinical evaluation in an animal model. *Fertil Steril* 69:318-323, 1998
12. Deveci M, Ozturk S, Kopal C, et al: Effect of hyaluronan on adult and fetal fibroblast proliferation and collagen synthesis: in vitro study. *Eur J Plast Surg* 24:222-227, 2001
13. Dijkstra JR, Meek MF, Robinson PH, et al: Methods to evaluate functional nerve recovery in adult rats: walking track analysis, video analysis and the withdrawal reflex. *J Neurosci Methods* 96:89-96, 2000
14. Frykman GK, McMillan PJ, Yegge S: A review of experimental methods measuring peripheral nerve regeneration in animals. *Orthopedic Clinics of North America* 19:209-219, 1988
15. Fukuoka Y, Komori H, Kawabata S, et al: Visualization of incomplete conduction block by neuromagnetic recording. *Clin Neurophysiol* 115:2113-2122, 2004
16. Fukuoka Y, Komori H, Kawabata S, et al: Imaging of neural conduction block by neuromagnetic recording. *Clin Neurophysiol* 113:1985-1992, 2002
17. Gaul JS, Jr.: Intrinsic motor recovery—a long-term study of ulnar nerve repair. *J Hand Surg [Am]* 7:502-508, 1982
18. Gorgulu A, Imer M, SimYek O, et al: The effect of aprotinin on extraneural scarring in peripheral nerve surgery: an experimental study. *Acta Neurochir (Wien)* 140:1303-1307, 1998
19. Gorgulu A, Uzal C, Doganay L, et al: The effect of low-dose external beam radiation on extraneural scarring after peripheral nerve surgery in rats. *Neurosurgery* 53:1389-1395; discussion 1395-1386, 2003
20. Hagberg L, Gerdin B: Sodium hyaluronate as an adjunct in adhesion prevention after flexor tendon surgery in rabbits. *J Hand Surg [Am]* 17:935-941, 1992
21. Hare GM, Evans PJ, Mackinnon SE, et al: Walking track analysis: a long-term assessment of peripheral nerve recovery. *Plast Reconstr Surg* 89:251-258, 1992
22. Hentz VR, Rosen JM, Xiao SJ, et al: The nerve gap dilemma: a comparison of nerves repaired end to end under tension with nerve grafts in a primate model. *J Hand Surg [Am]* 18:417-425, 1993
23. Hunter JM: Recurrent carpal tunnel syndrome, epineural fibrous fixation, and traction neuropathy. *Hand Clin* 7:491-504, 1991
24. Ikeda K, Yamauchi D, Osamura N, et al: Hyaluronic acid prevents peripheral nerve adhesion. *Br J Plast Surg* 56:342-347, 2003
25. Jaquet JB. *Median and Ulnar Nerve Injuries: Prognosis and Predictors for Clinical Outcome*. Rotterdam: ErasmusMC Rotterdam; 2004.
26. Kanaya F, Firrell JC, Breidenbach WC: Sciatic function index, nerve conduction tests, muscle contraction, and axon morphometry as indicators of regeneration. *Plast Reconstr Surg* 98:1264-1274, 1996
27. Kuypers PD, Gielen FL, Wai RT, et al: A comparison of electric and magnetic compound action signals as quantitative assays of peripheral nerve regeneration. *Muscle Nerve* 16:634-641, 1993
28. Kwan MK, Wall EJ, Massie J, et al: Strain, stress and stretch of peripheral nerve. Rabbit experiments in vitro and in vivo. *Acta Orthop Scand* 63:267-272, 1992
29. Longaker MT, Harrison MR, Crombleholme TM, et al: Studies in fetal wound healing: I. A factor in fetal serum that stimulates deposition of hyaluronic acid. *J Pediatr Surg* 24:789-792, 1989
30. Lundborg G, Rydevik B: Effects of stretching the tibial nerve of the rabbit. A preliminary study of the intraneural circulation and the barrier function of the perineurium. *J Bone Joint Surg Br* 55:390-401, 1973
31. Meek MF, Den Dunnen WF, Schakenraad JM, et al: Long-term evaluation of functional nerve recovery after reconstruction with a thin-walled biodegradable poly (DL-lactide-epsilon-caprolactone) nerve guide, using walking track analysis and electrostimulation tests. *Microsurgery* 19:247-253, 1999
32. Meek MF, Van Der Werff JF, Nicolai JP, et al: Biodegradable p(DLLA-epsilon-CL) nerve guides versus autologous nerve grafts: electromyographic and video analysis. *Muscle Nerve* 24:753-759, 2001
33. Mert T, Gunes Y, Guven M, et al: Comparison of nerve conduction blocks by an opioid and a local anesthetic. *Eur J Pharmacol* 439:77-81, 2002
34. Mert T, Gunes Y, Guven M, et al: Effects of calcium and magnesium on peripheral nerve conduction. *Pol J Pharmacol* 55:25-30, 2003
35. Ochs S, Pourmand R, Si K, et al: Stretch of mammalian nerve in vitro: effect on compound action potentials. *J Peripher Nerv Syst* 5:227-235, 2000
36. Ohsumi H, Hirata H, Nagakura T, et al: Enhancement of perineurial repair and inhibition of nerve adhesion by viscous injectable pure alginate sol. *Plast Reconstr Surg* 116:823-830, 2005
37. Ozgenel GY: Effects of hyaluronic acid on peripheral nerve scarring and regeneration in rats. *Microsurgery* 23:575-581, 2003
38. Ozgenel GY, Filiz G: Effects of human amniotic fluid on peripheral nerve scarring and regeneration in rats. *J Neurosurg* 98:371-377, 2003
39. Palatinsky EA, Maier KH, Touhalisky DK, et al: ADCON-T/N reduces in vivo perineural adhesions in a rat sciatic nerve reoperation model. *J Hand Surg [Br]* 22:331-335, 1997
40. Paparounas K, O'Hanlon GM, O'Leary CP, et al: Anti-ganglioside antibodies can bind peripheral nerve nodes of Ranvier and activate the complement cascade without inducing acute conduction block in vitro. *Brain* 122 (Pt 5):807-816, 1999
41. Petersen J, Russell L, Andrus K, et al: Reduction of extraneural scarring by ADCON-T/N after surgical intervention. *Neurosurgery* 38:976-983; discussion 983-974, 1996
42. Pucciarelli S, Codello L, Rosato A, et al: Effect of antiadhesive agents on peritoneal carcinomatosis in an

experimental model. *Br J Surg* 90:66-71, 2003

43. Robinson LR: Traumatic injury to peripheral nerves. *Muscle Nerve* 23:863-873, 2000
44. Ruijs AC, Jaquet JB, Kalmijn S, et al: Median and ulnar nerve injuries: a meta-analysis of predictors of motor and sensory recovery after modern microsurgical nerve repair. *Plast Reconstr Surg* 116:484-494; discussion 495-486, 2005
45. Rydevik BL, Kwan MK, Myers RR, et al: An in vitro mechanical and histological study of acute stretching on rabbit tibial nerve. *J Orthop Res* 8:694-701, 1990
46. Saravelos HG, Li TC: Physical barriers in adhesion prevention. *J Reprod Med* 41:42-51, 1996
47. Schmelzer JD, Low PA: Electrophysiological studies on the effect of age on caudal nerve of the rat. *Exp Neurol* 96:612-620, 1987
48. Shen N, Zhu J: Application of sciatic functional index in nerve functional assessment. *Microsurgery* 16:552-555, 1995
49. Smit X, van Neck JW, Afoke A, et al: Reduction of neural adhesions by biodegradable autocrosslinked hyaluronic acid gel after injury of peripheral nerves: an experimental study. *J Neurosurg* 101:648-652, 2004
50. Sporel Ozakat RE, Edwards PM, Hepgul KT, et al: A simple method for reducing autotomy in rats after peripheral nerve lesions. *J Neurosci Methods* 36:263-265, 1991
51. Sunderland: *Nerve Injuries and their Repair. A Critical appraisal.* London: Churchill Livingstone, 1991, pp 213-219 p
52. Van de Kar HJ, Jaquet JB, Meulste J, et al: Clinical value of electrodiagnostic testing following repair of peripheral nerve lesions: a prospective study. *J Hand Surg [Br]* 27:345-349, 2002
53. Varejao AS, Cabrita AM, Meek MF, et al: Motion of the foot and ankle during the stance phase in rats. *Muscle Nerve* 26:630-635, 2002
54. Varejao AS, Cabrita AM, Patricio JA, et al: Functional assessment of peripheral nerve recovery in the rat: gait kinematics. *Microsurgery* 21:383-388, 2001
55. Verdu E, Buti M, Navarro X: The effect of aging on efferent nerve fibers regeneration in mice. *Brain Res* 696:76-82, 1995
56. Verdu E, Ceballos D, Vilches JJ, et al: Influence of aging on peripheral nerve function and regeneration. *J Peripher Nerv Syst* 5:191-208, 2000
57. Vleggeert-Lankamp CL, van den Berg RJ, Feirabend HK, et al: Electrophysiology and morphometry of the Aalpha- and Abeta-fiber populations in the normal and regenerating rat sciatic nerve. *Exp Neurol* 187:337-349, 2004
58. Wall EJ, Kwan MK, Rydevik BL, et al: Stress relaxation of a peripheral nerve. *J Hand Surg [Am]* 16:859-863, 1991
59. Wheeler SJ: Effect of age on sensory nerve conduction velocity in the horse. *Res Vet Sci* 48:141-144, 1990
60. Wijesinghe RS, Gielen FL, Wikswo JP: A model for compound action potentials and currents in a nerve bundle. I: The forward calculation. *Annals of Biomedical Engineering* 19:43-72, 1991
61. Wijesinghe RS, Gielen FL, Wikswo JP: A model for compound action potentials and currents in a nerve bundle. III: A comparison of the conduction velocity distributions calculated from compound action currents and potentials. *Annals of Biomedical Engineering* 19:97-121, 1991
62. Wijesinghe RS, Wikswo JP: A model for compound action potentials and currents in a nerve bundle. II: A sensitivity analysis of model parameters for the forward and inverse calculations. *Annals of Biomedical Engineering* 19:73-96, 1991

Nederlandse samenvatting

Om het klinische herstel na letsel van een perifere zenuw te verbeteren, moet zowel patiënt als chirurg de strijd winnen ter plaatse van het zenuwletsel. Dit promotieonderzoek is opgezet met als doelstelling (patho)fysiologische processen, die zich afspelen op de plek van het letsel, in kaart te brengen en in maat en getal uit te kunnen drukken. Een groeiende kennis op het gebied van de (patho)fysiologie van de neurobiologie heeft zich de afgelopen decennia maar deels vertaald in een klinisch functionele verbetering na perifere zenuwletsel. Het proefdiermodel speelt een cruciale rol in deze vertaalslag. Klinisch onderzoek op het gebied zenuwletsel wordt bemoeilijkt door heterogeniteit van letsels en patiëntenpopulatie. Gerichte en kwantitatieve evaluatietechnieken van perifere zenuwletsel in een proefdiermodel maken de uiteindelijke vertaalslag naar de kliniek kleiner en/of makkelijker.

In **hoofdstuk 1** wordt de fysiologie en pathofysiologie van het perifere zenuwstelsel besproken, waarbij speciale aandacht uitgaat naar fundamentele problemen gerelateerd aan de plaats van het zenuwletsel. De nervus ischiadicus van de rat is een veel gebruikt experimenteel model voor het evalueren van perifere zenuwletsel. Dit hoofdstuk omvat een kritisch overzicht van experimentele technieken die beschikbaar zijn voor de evaluatie van perifere zenuwletsel in het rattenmodel. Grofweg worden de evaluatietechnieken onderverdeeld naar histologie, neurofysiologie, functie van eindorganen en biomechanica.

In dit proefschrift vindt een vergelijking plaats tussen evaluatietechnieken van functioneel herstel van eindorganen (zoals voetafdruk analyse), en axonregeneratie (zoals geleidingscapaciteit). Daarnaast worden de biomechanische eigenschappen onderzocht van perifere zenuwen onder fysiologische omstandigheden. De rekeigenschappen van een zenuw zijn van groot belang bij het chirurgisch herstel van zenuwletsel, in het bijzonder indien er een defect bestaat tussen twee zenuwuiteinden. De biomechanica wordt ook gebruikt bij het ontwikkelen van een model waarin neurale verklevingen kunnen worden gekwantificeerd voor het testen van anti-verkleefing strategieën.

De studie in **hoofdstuk 2** is opgezet met als doelstelling het evalueren en valideren van verschillende methoden van functie analyse na zenuwletsel gebruikmakend van voetafdrukken. Het looppatroon van de rat geldt al jaren als functionele maat voor herstel van de zenuw in een rattenmodel. De meest gangbare techniek van voetafdruk analyse is 'Walking Track Analysis'. Hierbij worden middels verf, inkt of (digitale) video opnames diverse voetafdruk parameters vastgelegd van een lopende rat, uiteindelijk resulterend in de 'Sciatic Function Index' (SFI). Een nadeel van deze methode is o.a. het tijdrovende aspect. Een vereenvoudigde methode van deze functie analyse is de statische voetzool analyse. De studie in dit hoofdstuk laat een uitstekende correlatie zien tussen de tijdrovende SFI en de meer tijd efficiënte statische voetzool analyse ter evaluatie van functieherstel na letsel van de nervus ischiadicus van de rat. In 2000 introduceerde Bervar een nieuw, betrouwbaar en statisch alternatief voor 'Walking Track Analysis', resulterend in de 'Static Sciatic Index' (SSI). De winst van deze digitale statische video

techniek wordt behaald door het gemak en snelheid waarmee de benodigde voetafdrukken kunnen worden verzameld. Deze studie bevestigt de efficiëntie van de statische techniek en laat bovendien zien dat de 'static Toe Spread Factor' (static TSF) de voorkeur heeft boven de uitkomst van de SSI. De aanvullende waarde van de SSI boven de 'static TSF' kan namelijk niet worden bewezen en de berekening van de 'static TSF' is gemakkelijker dan die van de SSI.

In de introductie is reeds beschreven dat de functie van het eindorgaan, zoals bepaald met bijvoorbeeld voetafdruk analyse, slechts van relatieve waarde is bij experimentele studies naar fundamentele problematiek ter plaatse van het zenuwletsel. Het herstel van eindorgaan functie is namelijk afhankelijk van te veel factoren die niet gerelateerd zijn aan de plaats van het zenuwletsel.

Wij concluderen dat voetzool analyse alleen als supplementaire evaluatie techniek van perifere zenuwletsel gebruikt moet worden, daar het slechts een indirecte uitkomstmaat geeft van het herstelproces ter plaatse van het trauma. Statische voetzool analyse is vergelijkbaar met de traditionele 'Walking Track Analysis', maar is te prefereren daar het minder tijd in beslag neemt.

De doelstelling van **hoofdstuk 3** is het ontwikkelen en valideren van een opstelling waarin de geleidingscapaciteit van de rattenzenuw gekwantificeerd kan worden. Neurofysiologische metingen in kleine proefdieren die in vivo verricht worden zijn ernstig onderhevig aan artefacten, o.a. veroorzaakt door korte en variërende geleidingsafstanden en temperatuurwisselingen. In deze studie wordt een opstelling ontwikkeld waarbij, in een ex vivo setting, in een meetkamer zeer accurate magenetoneurografische metingen (MNG) kunnen worden verricht op de nervus ischiadicus van de rat. Bifasische stimulatie en optimale aarding zorgen voor een forse reductie van het stimulus artefact. De lage variabiliteit (<5%) van de MNG signalen bewijst dat het ontwerp van de meetkamer zorg draagt voor precieze en reproduceerbare metingen. Een inherent effect van neurofysiologische ex vivo metingen is de uitdoving van het signaal in de tijd. Deze studie laat zien dat de gepresenteerde opstelling een overlevingstijd van de MNG signalen waarborgt van minimaal twee uur, hetgeen genoeg tijd is voor meerdere MNG metingen.

Ook electroneurografische metingen (ENG) kunnen in een ex vivo bad worden verricht. Het voordeel van MNG boven ENG metingen is dat magnetische velden nauwelijks worden beïnvloed door de weerstand van vocht en of weefsel tussen de sensor en de zenuw. Dit leidt tot een verhoogde reproduceerbaarheid van de MNG signalen.

De conclusie van dit hoofdstuk is dat ex vivo MNG metingen betrouwbaar de geleidingscapaciteit van de zenuw kunnen kwantificeren. Ongeacht het type meting (elektrisch of magnetisch) benadrukken wij de voordelen van neurofysiologische ex vivo metingen boven in vivo metingen in kleinere proefdiermodellen.

Hoofdstuk 4 beschrijft het herstelpatroon in de tijd na doorsnijding en herstel van de nervus ischiadicus van de rat, weergegeven in neurofysiologische kenmerken en weergegeven in functie van eindorganen. In eerdere onderzoeken naar de relatie tussen

neurofysiologie en andere experimentele evaluatietechnieken van perifeer zenuwletsel, is altijd gebruik gemaakt van conventionele electroneurografie (ENG) en / of electromyografie. Met de ex vivo MNG techniek uit hoofdstuk 2 kunnen krachtigere conclusies worden getrokken over de relatie tussen neurofysiologie en de functie van eindorganen, zoals static TSF en spiergewicht (MW).

Deze studie laat zien dat het herstel van neurofysiologische parameters als 1^e piek amplitude (1PA), piek piek amplitude (PPA), oppervlakte van het signaal (A) en geleidingssnelheid (CV) voor een groot deel plaats vindt in de eerste weken van het regeneratieproces. Neurofysiologische eigenschappen van een zenuw veranderen met de leeftijd, hetgeen ook wordt aangetoond in dit hoofdstuk. Wij benadrukken daarom de noodzaak voor rechts - links vergelijkingen in longitudinale neurofysiologische studies, waardoor de invloed van het leeftijdsaspect wordt meegenomen in de evaluatie.

Er bestaat slechts een matige correlatie tussen functie (static TSF) en geleidingscapaciteit (MNG). Dit kan worden verklaard door het verschil in herstelpatronen in de tijd, welke worden uitgedrukt in static TSF en de verschillende MNG parameters. Het is duidelijk dat het herstelproces van static TSF na 10 weken stagneert, terwijl na deze periode de MNG parameters nog wel een significante toename laat zien. Het regeneratieproces gaat dus door op het moment dat functieherstel gemeten door static TSF stagneert. Het lijkt waarschijnlijk dat het spreiden van de tenen door de rat al kan worden bereikt, bij ingroei van relatief weinig of matig ontwikkelde axonen. De functie van eindorganen, zoals gemeten met de static TSF is slechts van geringe waarde bij de evaluatie van axongroei na zenuwletsel.

Een groot en bekend nadeel van voetzool analyse (statisch of dynamisch) is de uitval van proefdieren door contracturen en / of automutilatie. Deze studie laat geen relatie zien tussen uitval door contracturen en / of automutilatie, en verminderde geleidingscapaciteit. Een mogelijke bias, als gevolg van exclusie van proefdieren, wordt daarom uitgesloten.

Er bestaat een duidelijke en significante relatie tussen spiergewicht, welke samenhangt met reïnnervatie van de spier, en de geleidingscapaciteit van een zenuw. Desalniettemin, bestaat er geen significante relatie tussen spiergewicht en static TSF. Blijkbaar zijn deze twee indirecte uitkomstmaten totaal verschillende afgeleiden van het regeneratieproces. Onze aanbeveling is dat bij experimentele studies naar axonregeneratie na zenuwletsel, beter een direct afgeleide van het regeneratieproces gebruikt kan worden, zoals bijvoorbeeld MNG.

De studie in **hoofdstuk 5** beschrijft de verdeling van rek over het verloop van een zenuw en met betrekking tot de gewrichten. Tijdens fysiologische bewegingen (flexie en extensie) ondergaat een zenuwsegment ter plaatse van een gewricht (gewrichtsregio) meer verandering in lengte, dan een zenuwsegment lopend in een niet-gewricht regio. Rektesten van geïsoleerde stukken zenuw uit beide regio's tonen aan dat de zenuw minder stijf is in een gewrichtsregio. Bovengenoemde bevindingen bewijzen dat er niet slechts een grotere belasting bestaat op het zenuwsegment ter plaatse van een gewricht; er moet echter ook een verschil bestaan in biomechanische eigenschappen van de

zenuwsegmenten in beide regio's. Dit resulteert in een grotere compliantie van de zenuw in een gewrichtsregio. Histologie laat zien dat dit verschil niet kan worden verklaard door structurele verschillen in de fascikel / niet fascikel weefselverdeling.

In de kliniek zijn de rekeigenschappen van een zenuw van groot belang bij het chirurgisch herstel van een zenuw, in het bijzonder als er een defect ('nerve gap') bestaat wat overbrugd moet worden. Het kritieke punt, waarop besloten moet worden dit zenuwdefect 'end to end' te herstellen, of juist met een interponaat te overbruggen, is discutabel. Gezien de resultaten van deze studie is het duidelijk dat de besluitvorming hierover niet uitgedrukt kan worden in centimeters zenuwdefect of in percentage van het vrij geprepareerde zenuwsegment.

In **hoofdstuk 6** is een experimentele studie verricht naar neurale verklevingen. De vorming van adhesies is een groot probleem op het gebied van perifeer zenuwletsel, zich klinisch uitend in functieverlies en ernstige pijnsyndromen. Het scoren van zenuwverklevingen in een experimentele setting is niet eenvoudig. Histologie en chirurgische beoordeling van het wondgebied worden veel gebruikt in de literatuur, maar hebben grote tekortkomingen zoals beschreven in de introductie van dit proefschrift. Voor deze studie is een biomechanisch model ontworpen waarin verklevingen tussen zenuw en omliggend weefselbed (extraneurale littekenvorming) worden gekwantificeerd aan de hand van de kracht die nodig is om de verkleving te breken. Er wordt aangetoond dat bij een toename in de ernst van het trauma, er significant meer kracht nodig is om de ontstane verklevingen te breken. Met het beschreven biomechanische model kunnen dus objectief en kwantitatief zenuwverklevingen worden gescoord. Het chirurgisch beoordelen van de wond ter evaluatie van extraneurale littekenvorming moet worden beschouwd als een inferieure techniek.

Hyaluronzuur (HA) is een glycosaminoglycaan in de extracellulaire matrix. HA speelt een belangrijke rol in diverse biologische processen van weefselherstel en heeft reeds aangetoond een anti-adhesieve werking te hebben op andere chirurgische gebieden. HA-gel (Hyaloglide, Fidia Advanced Biopolymers Srl, Abano Terme, Italy) is een viskeuze gel op basis van water en HA, en is ontwikkeld als een anti-verkleving strategie. Het ontwikkelde biomechanische model toont aan dat er een significant verlagend effect op de neurale verklevingen optreedt, indien HA-gel wordt gebruikt na verschillende soorten trauma van de perifere zenuw. In de literatuur worden meerdere experimentele strategieën beschreven die een anti-adhesief effect hebben na perifeer zenuwletsel. Dit heeft echter nog niet geleid tot een klinisch gerandomiseerde studie waarin dit effect wordt bewezen. De haalbaarheid van een goed opgezette klinische studie naar zenuwverklevingen is ook discutabel. De klinische implementatie van anti-adhesieve strategieën zou al overwogen moeten worden op het moment dat toxiciteit en andere neveneffecten zijn uitgesloten en er goede experimentele studies aan ten grondslag liggen.

Het doel van **hoofdstuk 7** was het bestuderen van het effect van RGTAs op extraneurale verklevingen en op de regeneratie van axonen na crush trauma van de perifere zenuw. ReGeneraTing Agents (RGTAs) bevatten de stabiliserende en beschermende

eigenschappen van heparine sulfaat op heparine bindende groeifactoren (HBGFs). In eerdere experimentele studies o.a. op het gebied van bot regeneratie, huidgenezing, darmnaden en spierregeneratie hebben RGTAs bewezen een positief effect te hebben op weefselherstel.

Met behulp van het biomechanische model uit hoofdstuk 6 wordt aangetoond dat RGTAs een significant reducerend effect hebben op neurale verklevingen na crush trauma van de perifere zenuw. De resultaten van deze studie tonen noch een positieve noch een negatieve werking aan op het herstel van geleidingscapaciteit van de zenuw, welke werd bepaald met MNG metingen (hoofdstuk 3 & 4). Ook werd er geen verschil gezien in het herstelpatroon van de static TSF (hoofdstuk 2) in de zes weken na het trauma. Een voorzichtige vergelijking van de resultaten uit hoofdstuk 6 & 7 laat zien dat na crush trauma van de perifere zenuw het gebruik van HA-gel een reductie in breekkracht bewerkstelligt van 29% en het gebruik van RGTAs een reductie in breekkracht bewerkstelligt van 67%. Een mogelijke synergetische werking van beide strategieën zou nader onderzocht moeten worden.

In **hoofdstuk 8** worden na de discussie de belangrijkste conclusies uiteengezet. Tevens wordt een voorzet gegeven voor toekomstig experimenteel onderzoek naar perifere zenuwletsels.

List of publications

M. Ghazvini, W. Mandemakers, M. Jaegle, M. Piirsoo, S. Driegen, M. Koutsourakis, **X. Smit**, F. Grosveld, D. Meijer. A cell type-specific allele of the POU gene Oct-6 reveals Schwann cell autonomous function in nerve development and regeneration. *EMBO J*. 2002 Sep 2;21(17):4612-20.

X. Smit, B.S. de Kool, E.T. Walbeehm, E.B.M. Dudok van Heel, J.W. van Neck, S.E.R. Hovius. Magnetoneurography: Recording biomagnetic fields for quantitative evaluation of isolated rat sciatic nerves. *J Neurosci Methods*, 2003: 125; 59-63

X. Smit, J.W. van Neck, A. Afoke, S.E.R. Hovius. Een bio-afbreekbare hyluronzuurgel ter vermindering van neurale verklevingen. *Abstract Ned. Tijdschr Geneesk* 2004 29 mei;148(22) p.1123

M. Giacomini, F. Raffo, **X. Smit**, B.S. de Kool, J.W. van Neck, S.E.R. Hovius, C. Ruggiero. Evaluating neural tissue regeneration by ANN based classification of MNG signals". *WSEAS Transactions on Computers*, 2004; 5(3):1625-1628

J.B. Phillips, **X. Smit**, N. De Zoysa, A. Afoke, R.A. Brown. Peripheral nerves in the rat exhibit localized heterogeneity of tensile properties during limb movement. *J Physiol*. 2004 Jun 15;557(Pt 3):879-87.

X. Smit, J.W. van Neck, A. Afoke, S.E.R. Hovius. Reduction of neural adhesions by biodegradable autocrosslinked hyaluronic acid gel after injury of peripheral nerves: an experimental study. *J Neurosurg*. 2004 Oct;101(4):648-52

X. Smit, J.W. van Neck, M.J. Ebeli, S.E.R. Hovius. Static footprint analysis: a time-saving functional evaluation of nerve repair in rats. *Scand J Plast Reconstr Surg Hand Surg*. 2004;38(6):321-5.

S.O. Hofer, N.A. Posch, **X. Smit**. The facial artery perforator flap for reconstruction of perioral defects. *Plast Reconstr Surg*. 2005 Apr;115(4):996-1003; discussion 1004-5.

X. Smit, B.S. de Kool, J.H. Blok, G.H. Visser, S.E.R. Hovius, J.W. van Neck. Recovery of neurophysiological features with time after rat sciatic nerve repair: a magneto-neurographic study. *J Peripher Nerv Syst*. In press

Dankwoord

Professor Hovius, beste prof, het is ruim tien jaar geleden dat ik begon met laser doppler metingen op de afdeling. Een opleiding of promotie lagen voor mij in die periode nog volledig buiten beschouwing. Ik had er een goed gevoel bij! In de jaren hierop volgend heeft u mij altijd de mogelijkheid gegeven mijn gevoel te volgen en mij gesteund daar waar nodig was. Dit heeft onder andere geleid tot dit proefschrift. Ik ben u hiervoor erg dankbaar.

Han van Neck, beste Han, ik betwijfel ernstig of ik hier (nu al) had gestaan, als jij niet was aangetrokken voor het NeuroTE project. Beiden niet geremd door enige kennis van de neurobiologie ontstond er een plan, kwam er overzicht, werden er studies gestart en produceerden we papers. Ik ben blij jou als copromotor te mogen hebben. Ik dank je voor de afgelopen jaren.

De gehele promotiecommissie wil ik bedanken:

Professor de Zeeuw, beste Chris, op de 12^e verdieping begon mijn promotie-onderzoek. Enkele jaren én een tussentijdse verhuizing naar de 15^e later, was jij zonder enige twijfel bereid om mijn manuscript te beoordelen. Dank hiervoor. Ik kan de manier waarop jij de 12^e verdieping onderzoek laat ademen, zeer waarderen.

Beste *professor Snijders*, beste *professor Thomeer*, ik was zeer verrast door het enthousiasme waarmee jullie hebben gereageerd op het verzoek mijn manuscript te beoordelen. Veel dank voor jullie tijd en interesse voor mijn onderzoek en voor het plaatsnemen in mijn promotiecommissie.

Beste *professor Stegeman*, beste *professor Ritt*, dank voor het plaatsnemen in mijn promotiecommissie. Het was prettig met enthousiasme ontvangen te worden om over mijn onderzoek te praten.

Gerhard Visser, beste Gerhard, vanaf het begin van het onderzoek ben jij op de achtergrond aanwezig geweest. Tijdens gezamenlijke meetings is mij opgevallen dat jij, ondanks de betrokkenheid op de achtergrond, vaak het juiste punt van discussie naar voren haalde. Ik dank je voor je hulp de afgelopen jaren.

Erik Walbeehm, beste Erik, jouw gedrevenheid heeft mij warm gemaakt voor London, voor de anatomie van de hand, voor het experimentele onderzoek en voor de plastische chirurgie in het algemeen. Ik ben je hiervoor erg dankbaar.

Joleen Blok, beste Joleen, jij bent te hulp geschoten bij het al lopende MNG experiment. Ik ben je dankbaar voor de manier waarop je zonder enige weerstand bent gaan meedenken en zodoende deze studie naar een hoger niveau hebt geholpen.

Stefan de Kool, beste Stefan, jij bent het genie achter het bakje. (Te) vaak hebben we zitten turen in dat bakje. Het werd het uiteindelijk allemaal waard toen de resultaten kwamen. Dank voor onze prettige samenwerking.

Michiel Dudok van Heel, beste Michiel, jij kon als geen ander op een duidelijke manier helderheid verschaffen bij, voor mij, lastige neurofysiologische vraagstukken. Het heeft allemaal veel te kort geduurd.

Robert Brown, dear Robert, the connection with London will not stop here. Over the years, I have learned so much from the way you approach research. I am grateful for the many pleasant years working with you.

Vivek Mudera, dear Vivek, you introduced me to the world of research. I thank you for that. I will always remember the many nice moments in London.

Andrew Afoke, dear Andrew, after secondary school education I did not think that physics would continue to play an important role in my life. You have taught me that the role of biomechanics in research should not be underestimated. I am grateful to have had the opportunity to work with you.

James Philips, dear James, I enjoyed the many NeuroTE meetings, your visits in Rotterdam and my visits in London, the paper we wrote together and the pub discussions we had. I still owe you a pint!

Beste *Rob de Widt sr.*, *Rob de Widt jr.* en *Tony Vierling*, het oog wil ook wat en daar hebben jullie voor gezorgd! Veel dank daarvoor.

Ineke Hekking, beste Ineke, altijd was jij bereid te helpen met het verbeteren en uitvoeren van experimenten in wéér een nieuwe opstelling, uitgesteld in het lab. Ik dank je hiervoor en voor de gezellige uren en uren achter de microscoop.

Carin Oostdijk, beste C, het is ongelooflijk hoe jij de boel draaiende houdt. Ik dank je voor het kopje thee voor m'n sollicitatie, het briefje hier, de email daar, de afspraak dan en de kletspraatjes tussendoor. Tnx!

Irene Mathijssen, beste Irene, aan een half woord heb jij genoeg. Dank voor je steun en het vele plezier.

De maatschap heelkunde uit het Ikazia Ziekenhuis, beste bazen, jullie hebben mij opgeleid tot dokter. De compacte sfeer in het Ikazia is óngelooflijk waardevol. Dank voor deze mooie periode.

Beste *Teun Luysterburg*, *Chantal Moues*, *Thijs de Wit*, *Michiel Zuidam*, *Mischa Zuijgendorp*, *Sanne Moolenburgh* en *Sarah Versnel*, korte of langere tijd hebben wij samen op de onderzoeksafdeling gewerkt. Allemaal zaten we in hetzelfde schuitje. Dat gaf een goed gevoel!

Beste *vrienden*, het gebeurt niet vaak dat je bewust nadenkt over de vrienden om je heen. Ik besef me dat jullie mijn leven een stuk rijker maken!

Hinne Rakhorst, beste Hinne, wellicht heeft het met 5 april 1974 te maken, maar dat kan het niet alleen zijn. In relatief korte tijd ben jij een goed maatje geworden. Ik bewonder de spirit waarmee jij zaken weet aan te pakken. Ik kijk uit naar de komende jaren en ben er trots op dat jij op deze dag aan mijn zijde staat.

Jean Bart Jaquet, beste Sjaak, de afgelopen jaren is er tussen ons een band ontstaan die niet zomaar te beschrijven valt. Dat doe ik dus ook niet. Het gebeurt dus dat collega's vrienden worden. Ik denk dat de zaken bij ons omgekeerd liggen. Jij bent een goede vriend die collega is geworden. Ik ben hier ongelooflijk trots op.

Rob en Lies, lieve broer en zus, meer dan begrijpelijk was mijn onderzoek een compleet mysterie voor jullie. Daarentegen begrepen jullie volledig dat dit onderzoek veel voor mij betekende en dat ik er veel energie in stak. Dat gaf mij een erg goed gevoel. Ik ben enorm blij jullie als broer en zus te hebben!

Lieve *papa en mama*, het is moeilijk uit te drukken hoe fijn het is om jullie om mij heen te hebben. Jullie stralen liefde en vertrouwen uit en dat geeft mij steun in alles wat ik doe. Ik dank jullie daarvoor.

Lieve *Niki*, jij bent mijn meisje. We horen bij elkaar en daar zijn geen woorden voor nodig. Ik houd van je!

Curriculum Vitae

Xander Smit werd op 5 april 1974 geboren in Eindhoven. In 1992 werd het VWO diploma behaald aan het Sint-Laurenscollege te Rotterdam. In het zelfde jaar startte hij met de studie geneeskunde aan de Erasmus Universiteit in Rotterdam. Gedurende zijn studie werkte hij als “Forgeron” op de afdeling spoedeisende hulp van het Ikazia Ziekenhuis te Rotterdam. Hiernaast werkte hij mee aan laser doppler metingen, tijdens en na microvasculaire ingrepen op de afdeling Plastische en Reconstructieve Chirurgie van het huidige Erasmus MC Rotterdam. Zijn afstudeerproject werd verricht aan “the Tissue Repair Unit of the University College of London” (dr. R.A. Brown and prof.dr. D.A. McGrouther). De samenwerking en contacten met London werden de onderzoeksjaren hierop volgend voortgezet. Na het behalen van het artsexamen in 1999, werd gestart met promotie-onderzoek naar perifere zenuwletsels aan de afdeling Plastische en Reconstructieve Chirurgie van het Erasmus MC Rotterdam, hetgeen uiteindelijk heeft geresulteerd in dit proefschrift. Na een tussentijdse AGNIO periode in 2002 op dezelfde afdeling, werd de opleiding tot plastisch chirurg in het vooruitzicht gesteld. In een vertrouwde omgeving volgde hij vanaf 1 april 2004 de tweejarige vooropleiding algemene chirurgie in het Ikazia Ziekenhuis te Rotterdam (opleider dr. W.F. Weidema). De periode tussen vooropleiding en opleiding werd overbrugd door een fellowship in het Grootte Schuur Ziekenhuis te Kaapstad (dr. M. Solomons) waar ervaring werd opgedaan in trauma gerelateerde handchirurgie. Per 1 september 2006 is hij gestart met de opleiding tot plastisch chirurg aan de afdeling Plastische en Reconstructieve Chirurgie van het Erasmus MC Rotterdam (opleider prof.dr. S.E.R. Hovius).